©[2007]

JUN TAE KIM

STATIC AND DYNAMIC ADSORPTION OF β-LACTOGLOBULIN ON

POLYMERIC MEMBRANE SURFACE AND DEVELOPMENT OF NOVEL

MEMBRANES BY SURFACE MODIFICATION

by

JUN TAE KIM

A Dissertation submitted to the

Graduate School-New Brunswick

Rutgers, The State University of New Jersey

in partial fulfillment of the requirements

for the degree of

Doctor of Philosophy

Graduate Program in Food Science

written under the direction of

Professor Sean X. Liu

and approved by

_____

_____

_____

_____

New Brunswick, New Jersey

[Oct, 2007]

ABSTRACT OF THE DISSERTATION

STATIC AND DYNAMIC ADSORPTION OF β-LACTOGLOBULIN ON

POLYMERIC MEMBRANE SURFACE AND DEVELOPMENT OF NOVEL

MEMBRANES BY SURFACE MODIFICATION

By JUN TAE KIM

Dissertation Director:
Professor Sean X. Liu

The protein adsorption on polymeric membrane surface is the major factor to cause the membrane fouling in ultrafiltration (UF) processing to concentrate, fractionate, and separate whey proteins from liquid whey which is byproduct of cheese manufacturing process. Membrane fouling, which is defined as the decrease of the filtration performances such as permeation flux, efficiency, and selectivity is still one of the major problems encountered in many food industries employing membrane separation processing. In order to better understand fouling mechanism, to optimize the process condition to minimize fouling, and to develop the novel membranes to reduce fouling, the protein adsorption on the polymeric membrane surface was studied by static adsorption and dynamic adsorption experiments.

From the static adsorption experiment, the adsorption capacity and the surface heterogeneity of β-lactoglobulin were determined at various conditions of the protein solution by an adsorption isotherm. Dynamic adsorption process was studied by QCM-D,

which allows monitoring of the protein adsorption process in real time by simultaneously measuring of frequency shift (Δf) and dissipation shift (ΔD).

To develop the novel membranes to reduce the protein adsorption and fouling, two surface modification methods were developed by hydrophilic polymers grafting using UV/Ozone treatment and thin film composite (TFC) through interfacial polymerization. The hydrophilic polymer grafted membranes might reduce the hydrophobic interactions between protein and membrane surface by improve the hydrophilicity of the polymeric membrane. UV/Ozone is one of the powerful techniques to initiate and activate the polymeric membrane surface to graft the hydrophilic polymers. Interfacial polymerization has been a well established way to prepare the thin active layer by a polycondensation reaction in two immiscible phases (organic solvent and water phase). Dense and thin polyamide layer can be formed on the polymeric membrane surface. The hydrophilic polymers such as PVA, PEG, and chitosan were modified on the polyamide thin layer to improve the hydrophilicity of the modified membranes. Some surface properties of modified PES membranes were characterized by contact angle, FT-IR, XPS, and AFM. These results proved that PES membranes were modified successfully with hydrophilic polymers and showed more hydrophilic property and lower protein adsorption.

ACKNOWLEDGEMENT

DEDICATION

To my Mom and Dad, Mrs. Boo-Youn Park and Mr. Tae-Rang Kim,

my parents in law, Mrs. Hong-Ja Park and Mr. Myeong-Tae Shin,

my wife, Gye-Hwa Shin.

TABLE OF CONTENTS

LISTS OF TABLES

LIST OF ILLUSTRATIONS

NOMENCLATURES

A	Amplitude
C	Mass sensitivity constant (=17.7 ngcm-2Hz-1 at f=5 MHz)
C_e	Equilibrium concentration of solute in liquid phase (mol/L)
D	The sum of all energy dissipated
ΔD	Dissipation shift
E_b	Binding energy
E_k	Kinetic energy
$E_{dissipated}$	Dissipated energy
E_{stored}	Stored energy
f	Resonance frequency
Δf	Frequency shift
K	Equilibrium constant
K_F	Equilibrium constant for the Freundlich isotherm
n	Overtone numbers (n=3, 5, and 7)
$1/n$	Adsorption intensity or surface heterogeneity
Δm	Adsorbed mass per unit surface
q_e	Equilibrium adsorbate concentration on adsorbent (mol/g)
q_{max}	Maximum adsorbate concentration on adsorbent (mol/g)
R	Surface or adsorbent
S	Solute
S_F	Free binding sites

S_O	Occupied sites
S_T	Total binding sites
SR	The adsorbed state of solute on the surface
t	Time
θ	Contact angle
τ	Decay time
φ	Phase angle
ρ	Density
η	Viscosity
μ	Shear elasticity
h	Thickness
δ	Viscous penetration depth
ω	Angular frequency of the oscillation
γ_{SG}	The solid-gas interfacial energy
γ_{SL}	The solid-liquid interfacial energy
γ_{LG}	The liquid-gas interfacial energy

CHAPTER I. INTRODUCTION

1.1. Background

The uses of whey protein and whey derivatives such as whey protein isolate (WPI) and whey protein concentrate (WPC) in food industry have grown steadily worldwide because of their excellent functional properties and nutritional quality (de la Fuente et al., 2002). Whey is an important by-product of cheese manufacturing process. Effective utilization of whey proteins depend on the purification of whey proteins and high solid content. To concentrate, fractionate, and purify whey proteins and whey derivatives, membrane separation technologies have been commonly used in the food industry because membrane filtration is capable of separating the native proteins from aqueous mixtures. It is very difficult to maintain the native properties using thermal treatment techniques such as drying and evaporation (Atra et al., 2005). Membrane fouling, defined as decrease in permeation flux over the filtration time and the formation of a solute fouled layer on the membrane surface and/or inside the pore surfaces, however, is a persistent problem in the food industry employing membrane separation processing (Marshall et al., 1993; Chan and Chen, 2004). The decrease in the filtration performance such as permeation flux and selectivity over a process cycle by fouling has caused a higher capital expense to restore the filtration performance by using powerful cleaning agents that may reduce the life span of membranes.

Since most proteins have a heterogeneous surface and amphiphilic (both hydrophilic and hydrophobic) properties, they can interact easily with a hydrophobic polymeric surface by different types of interactions such as electrostatic interactions, van

der Waals forces, hydrophobic interaction, hydrogen bond, and so on. Although fouling phenomenon always exists in almost all membrane processes by the various interactions between protein and the membrane surface and between proteins themselves, the fouling by the protein adsorption on polymeric membranes is particularly acute and irreversible due mainly to the strong interactions such as hydrophobic interaction and electrostatic attraction between protein and the polymeric membrane surface (Babu and Gaikar, 2001; Sun et al., 2003).

Protein adsorption on polymeric surface is affected by various factors such as protein size and shape, pH and charge of protein solution, topology and charge of polymeric surface, intermolecular forces between protein molecules, and chemistry of the polymeric surface (Andrade and Hlady, 1986; Sadana, 1992). Although many factors can affect protein adsorption and membrane fouling, this study was focused on the protein-membrane interaction and the surface chemistry of polymeric membrane because membrane fouling is strongly influenced by the physicochemical properties of the membrane and protein.

1.2. Rationale and Significance

Although most thermal treatment methods such as drying and evaporation can concentrate whey protein and whey derivatives from the liquid whey, they are incapable of fractionate and purify the pure components. Membrane filtration is safe and economical technique to purify and concentrate whey proteins from the liquid whey. It is also the most suitable way to obtain the native product without any phase changes such as protein denaturation compare to other processing techniques using heat treatment. Because the

functional properties of proteins depend on their structure, it is pivotal to maintain their native structure during the processing. Membrane fouling, however, is an inevitable problem in the most membrane applications and should be reduced to improve the product yield and save the processing cost. In order to better understand the fouling mechanism of milk proteins on polymeric membranes and optimize the process condition to minimize the fouling, it is necessary to study the protein adsorption process onto the polymeric membrane surface and viscoelastic properties of the adsorbed protein layer.

In fluid feed stream, the ideal membrane to minimize membrane fouling is the hydrophilic membrane because the hydrophobic interaction between membrane and protein is the main factor to cause the permanent membrane fouling. However, most commercial membrane materials are relatively hydrophobic because the hydrophilic membranes are some drawback in their mechanical strength and thermal and chemical stability. Surface modification of polymeric membrane plays an important role in membrane performance such as permeation flux and selectivity. By surface modification of polymeric membrane, two distinct layers can be formed: thin surface layer can dominate the selectivity, flux, and adsorption properties while the thick substrate layer provides mechanical strength and chemical stability.

1.3. Research Objectives

The main goal of this research was the understanding of the interactions between protein and membrane surface and the development of a novel membrane by surface modification methods to reduce the protein adsorption on the membrane surface. Surface modification methods were developed to improve the protein adsorption resistance while

the membranes properties such as the mechanical property and thermal and chemical resistance were maintained. To achieve this goal, the dissertation involves various specific objectives as follows:

(1) To investigate the protein adsorption process on polymeric membrane surface by static and dynamic adsorption experiments.

(2) To fit the adsorption isotherm and determine the model parameters to predict the adsorption capacity from static adsorption process.

(3) To monitor the dynamic adsorption process and determine the viscoelastic properties of the protein adsorbed layer on the polymeric membrane surface using QCM-D technique.

(4) To investigate the conformation and surface coverage of the protein adsorbed layer on the polymer membrane surface using atomic force microscopy (AFM).

(5) To modify the membrane surface using hydrophilic polymers grafting using UV/Ozone and interfacial polymerization methods.

(6) To characterize the modified membrane surface using contact angle, FTIR, XPS, and AFM.

(7) To compare the protein adsorption on the unmodified and modified membrane surfaces from static adsorption experiment.

CHAPTER II. LITERATURE REVIEW

2.1. Whey Protein

2.1.1. Composition of Whey

Whey protein and whey derivatives such as whey protein isolates (WPI) and whey protein concentrates (WPC) have a high level of essential amino acids, an excellent functional properties, and desirable sensory characteristics. These amenable properties of whey protein and whey derivatives have increased the use of them as a food additive in food product applications such as meats, beverages, dairy products, baked goods, infant formula, dietetic foods, and health promoting foods (De Wit, 1998; de la Fuente et al., 2002).

As an important by-product of a cheese manufacturing process, whey is defined as the fraction of milk remaining after the precipitation of casein micelles. Typically, 100 kg of milk yields 10 kg of cheese and 90 kg of the liquid whey. There are two principal types of whey by the processing conditions. Sweet whey is produced during the manufacturing of rennet type hard cheese like cheddar or Swiss cheese. Acid whey is obtained during the manufacturing of acid type cheese like cottage cheese (Rattray and Jelen, 1996). Even if the composition is little different with the types of whey, whey generally consists of protein (0.75 ~ 0.80%), fat (0.04 ~ 0.50%), lactose (4.85 ~ 4.90 %), minerals (0.50 ~ 0.80%), and water (93.5 ~ 93.7%) as shown in Table 2.1. Total solid content in liquid whey is only 6.5% and water content is about 93.5%.

Table 2.1. Composition of whey depending on the types: fluid sweet, fluid acid, dried sweet, and dried acid whey.

	Composition of Whey (%)			
	Fluid Sweet Whey	Fluid Acid Whey	Dried Sweet Whey	Dried Acid Whey
Total Solid	6.35	6.50	96.5	96.0
Moisture	93.70	93.50	3.5	4.0
Fat	0.50	0.04	0.8	0.6
Protein	0.80	0.75	13.1	12.5
Lactose	4.85	4.90	75.0	67.4
Ash	0.50	0.80	7.3	11.8
Lactic Acid	0.05	0.40	0.2	4.2

(Source: http://*www.albalagh.net/halal/col4.shtml)

Whey proteins in milk consist of four types of proteins: α-lactalbumin, β-lactoglobulin, proteose-peptones, and blood proteins such as serum albumin and immunoglobulins. The compositions of whey proteins in milk and in total milk protein were shown in Table 2.2. The total whey protein content was only 6.4 g/kg milk or about 20% of total milk protein. The individual whey proteins have their own unique functional, nutritional, and biological characteristics that are not in whey protein concentrates. For example, α-lactalbumin has been used especially in infant formula and in various biological areas as a nutraceutical because of its high tryptophan content (4 tryptophan residues per molecule) (Pearce, 1992; Maubois and Ollivier, 1997). β-Lactoglobulin has been used as a food stabilizer in many food processing. Bovine serum albumin (BSA) is one of the most intensively used proteins in many food and therapeutic applications. Bovine immunoglobulins (Ig) can enhance the immunological properties of infant formula and they can be used therapeutically in the treatment of animal neonates.

As a by-product in cheese manufacturing process, the liquid whey had caused serious environmental problems in its disposal methods such as discharging into ocean and fields (Smithers et al., 1996) as well as laid a financial burden on the processors. Since the environmental regulations have been enforced and many beneficial functions of whey protein have been known worldwide, however, various technologies to separate and fractionate the pure whey protein and whey derivatives have been developed to use them in the food industry (Zydney, 1998).

Table 2.2. Whey protein composition in milk and in milk protein (Walstra et al., 1999).

Whey Proteins	Concentration (g/kg milk)	Composition (g/100g milk protein)
β-lactoglobulin	3.2	9.8
α-lactalbumin	1.2	3.7
Proteose-peptone	0.8	2.4
Bovine serum albumin	0.4	1.2
Immunoglobulins	0.8	2.4
IgG1, IgG2	0.65	1.8
IgA	0.14	0.4
IgM	0.05	0.2

2.1.2. β-Lactoglobulin

As a globular type protein, β-lactoglobulin is very soluble in aqueous solution and fold into compact units which have roughly spherical shape. According to some literature reviews, β-lactoglobulin is the most abundant (over 50 % of total whey protein) whey protein in bovine milk and the principal component in fouling deposits on the membrane surface and inside the pores (Fennema, 1996; Murray and Deshaires, 2000; Elofsson et al., 1996). Generally, β-lactoglobulin consists of the mixture of variants A and B. At room temperature and at neutral pH, β-lactoglobulin exists mainly as a dimer structure in which two monomeric units are noncovalently linked. The dimer structure of β-lactoglobulin can be dissociated into monomer structure in acidic (below pH 3.5) and alkaline (above pH 7.5) conditions. The monomeric unit of β-lactoglobulin consists of 162 amino acid residues, has a molecular mass of about 18.3 kDa, and has two disulfide bonds (C106-C119 and C66-C160) and one free cysteine (C121) (Hoffmann and van Mill, 1999; Verheul et al., 1999). The isoelectric point of β-lactoglobulin is pH 5.2. Although the biological function of β-lactoglobulin has not been demonstrated yet, the sulfhydryl (-SH) group of β-lactoglobulin has been used as a stabilizer in many food products such as emulsion (Euston et al., 1999; Christiansena et al., 2004) and confections (Cayot and Lorient, 1997). Some selected properties of β-lactoglobulin are summarized in Table 2.3.

Table 2.3. Selected properties of β-lactoglobulin (Walstra et al., 1999).

Properties	Value
Molar mass	18,300
Amino acid residues/molecule	162
Cysteine (res./mol.)	5
-S-S- linkages/mole.	2
Hydrophobicity (kJ/res.)	5.1
Isoelectric point (pI)	5.2

2.2. Membrane Filtration

2.2.1. Definitions and Classification

Membrane filtration is defined as the separation of two or more components from a fluid stream based on the size differences of the components. The primary role of the membrane is to act as a selective barrier. It can permit passage of certain small components and retain other large components from a mixture (Cheryan, 1998). The use of membrane filtration has been increased in the separation of macromolecules such as proteins because membrane filtration has a lot of advantages such as low energy consumption, no additive requirements, high purity, and no phase change of products. Since the nutritional and functional characteristics of whey protein and whey derivatives are related to the structure and biological functions of these proteins, it is pivotal to maintain their native conditions during the concentration and fractionation process; membrane filtration accomplishes fractionation and concentration without denaturing proteins.

Based on the pore size of the membrane or the molecular weight of the solute molecules that the membrane can separate, membrane filtration can be classified in four categories: Microfiltration (MF), Ultrafiltration (UF), Nanofiltration (NF), and Reverse Osmosis (RO). These filtrations are the application of hydraulic pressure to speed up the transport process but the nature of the membrane itself can control which components are permeated and which are retained as shown in Figure 2.1. Microfiltration has the largest pore size (0.05 to 20 microns) in membrane filtration processes. It is designed to retain particles in the micron range including inorganic particles and microorganisms. Ultrafiltration is the second largest in pore size (0.002 to 0.2 microns) as it can separate and concentrate macromolecules like proteins and colloids. UF is commonly used in

pharmaceutical production, biotechnology, and pre-treatment for ultra-pure water production as well as food and beverage processing. As a relatively new process, nanofiltration uses charged membranes and the pore size is less than 2 nm. This pore size is too small to allow permeation of many organic compounds such as sugars, divalent ions, and dissociated forms of a compound. Reverse Osmosis is widely used in drinking water and wastewater purification because RO can retain almost all components except pure water molecules. Ultrafiltration and microfiltration systems require less energy in their operation because they are operated at low pressures compared to either nanofiltration or reverse osmosis. The low pressures can also extend the life span of a membrane.
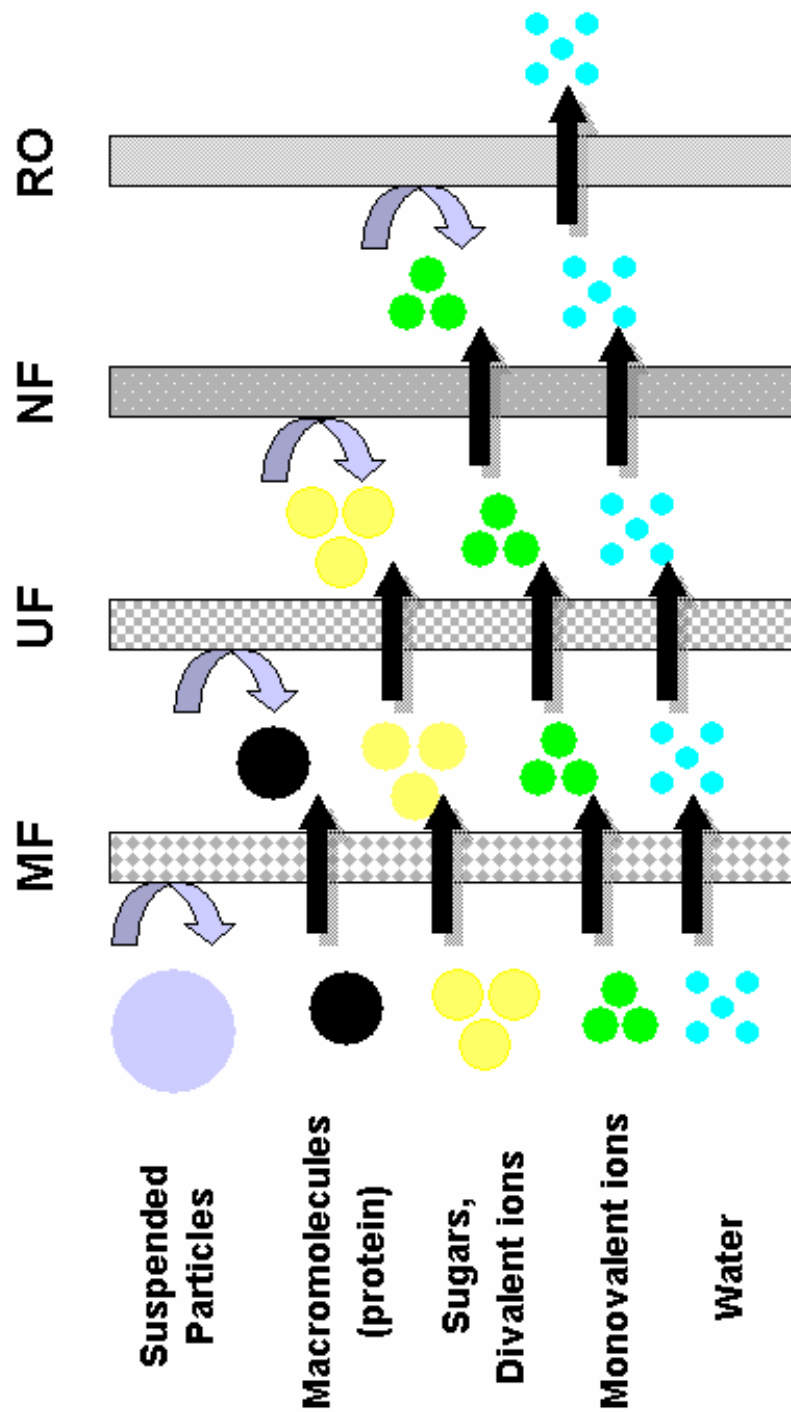
Figure 2.1. Membrane filtrations and their separation characteristics: MF (microfiltration), UF (ultrafiltration), NF (nanofiltration), and RO (reverse osmosis).

2.2.2. Membrane Materials Used in Ultrafiltraiton

2.2.2.1. Cellulose Acetate (CA)

Cellulose acetate (CA) is the classic membrane material used in membrane industries to create skinned membranes and one of the first polymer membranes that have been used for aqueous based separation. CA is prepared from cellulose by reaction with acetic anhydride, acetic acid, and sulfuric acid. The advantages of CA membrane are as follows; a) hydrophilicity which is very important in reducing the membrane fouling, b) wide range of pore size can be manufactured, and c) low cost. Cellulose acetate membrane , however, has also many drawbacks; a) a narrow temperature range: maximum temperature is 30℃ which may cause a problem in sanitation, b) a narrow pH range: the polymer hydrolyzes easily under acidic conditions since acid tends to attack the β-glucosidic links in the cellulose backbone, c) poor resistance to chlorine which is a universal sanitizer in the process industries: chlorine oxidizes cellulose acetate and weakens the membrane, and d) highly biodegradable: it is highly susceptible to microbial attack.

2.2.2.2. Polysulfone (PS) and Polyethersulfone (PES)

The family of polysulfone membranes is one of the most favorable membrane materials in microfiltration (MF) and ultrafiltration (UF). Polysulfone (PS) and polyethersulfone (PES) have diphenylene sulfone repeating units in their structure as shown in Figure 2.2. The $-SO_2$ group in the polymeric sulfone is very stable due to the electronic attraction of resonating electrons between adjacent aromatic groups. Polyethersulfone is particularly favorable as a membrane polymer in MF and UF applications due to the following favorable characteristics: a) wide temperature limits

(from -100℃ to 150℃) which is an advantage in fermentation and sterilization, b) wide pH

tolerances (from pH 1 to pH 13) which is definitely an advantage for cleaning purposes, c)

good chemical resistance in various chemical agents including chlorine, and d) easy to

fabricate membranes in a wide variety of configurations and modules. The main

disadvantage of PS and PES, however, is their hydrophobicity which makes them prone to

fouling in comparison to the more hydrophilic polymers.

2.2.2.3. Polyvinylidene Fluoride (PVDF)

Polyvinylidene fluoride is a very popular material for MF and UF due to its good

strength and resistance to high temperature, common solvents, acids, and bases. PVDF is

especially popular for fruit juice clarification because of its resistance to limonene. But

PVDF is very expensive compare to other membrane polymers. Figure 2.2 shows the

structure of the membrane polymers which are popularly used in ultrafiltration system.
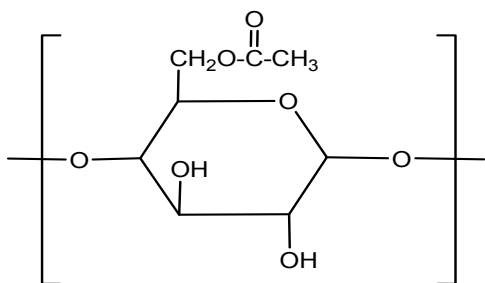
(A) Cellulose Acetate (CA)
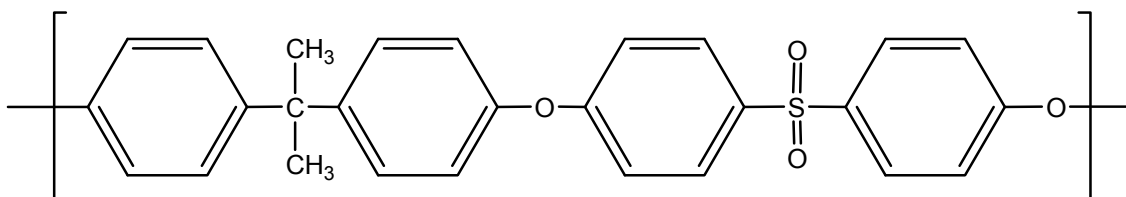
(B) Polysulfone (PS, Trade name is UDEL)
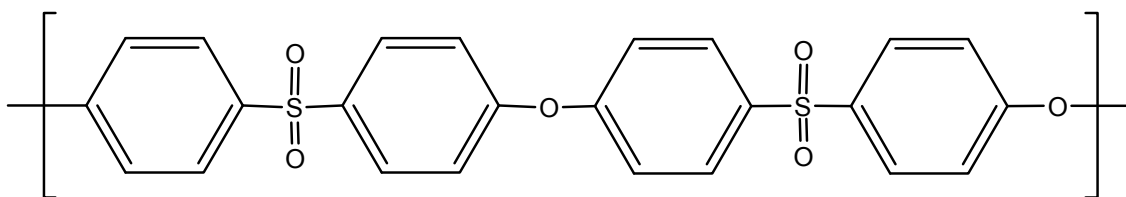
(C) Polyethersulfone (PES, Trade name is RADEL)
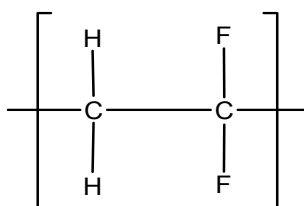
(D) Polyvinylidene Fluoride (PVDF)

Figure 2.2. Structure of the widely used membrane polymers in ultrafiltration system: (A) cellulose acetate (CA), (B) polysulfone (PS), (C) polyethersulfone (PES), and (D) polyvinylidene fluoride (PVDF).

2.2.3. Membrane Fouling

Although membrane filtration is an important technology in the food processing and has many advantages, the major limitation of its applications is the membrane fouling, which is defined as a decrease in permeation flux over processing time by the accumulation of solute and/or the formation of fouled layer onto the membrane surface and inside pores. Membrane fouling occurred in the filtration of protein solutions can result in significant loss of filtration performance such as selectivity and permeation flux thus could have a serious impact on the efficiency and economics of the whey protein recovery process. The adsorption of protein molecules onto the membrane surface and the entrapment of protein and protein aggregates inside the pores are known as the major factor to induce membrane fouling. The fouling mechanism has been investigated in order to improve permeation flux and reduce membrane fouling (Jim et al., 1992; Jonsson et al., 1996; Costa et al., 2006). Based on many previous researches, hydrophobic interactions and electrostatic interactions have been identified to interpret the fouling mechanisms (Mcdonogh et al., 1990; Nystrom et al., 1994; Kelly and Zydney, 1995; Ricq et al., 1999). These interactions are generally affected by the membrane properties such as hydrophilicity, surface topography, roughness, pore size, and pore distribution and solution properties such as solute type, concentration, pH, and ionic strength.

Although it is possible to delay the onset and reduce the amount of fouling by the control the processing conditions and/or the modification of membrane surface, fouling is inevitable problem in membrane filtration process. In order to maintain the permeation flux and selectivity of membrane processes, various cleaning methods are commonly used in the food industry (Bartlett et al., 1995; Muthukumaran et al., 2005). For example, in the

dairy industry employing the membrane filtration system, membranes are daily cleaned in an empirical way until the final flux is better than 90% of the initial one (Delaunaya et al., 2006). Membrane cleaning usually performs in three forms: physical, chemical, and biological methods (Trägårdh, 1989). As a physical cleaning method, ultrasonic technique has been widely used to remove the foulants of ultrafiltration and microfiltration membranes (Muthukumarana et al., 2004; Simon et al., 2000; Li et al., 2002; Kobayashi et al., 2002). Chemical cleaning is the most common method to clean membranes. Alkaline solutions, acids, metal chelating agents, and surfactants have been used as the cleaning agents (Liikanen et al, 2002; Madaeni et al., 2001; Sadhwani and Veza, 2001). However, the physical and chemical cleaning methods may significantly reduce the lifetime of the membrane which in turn increases the replacement cost.

2.3. Protein Adsorption

Adsorption is a physical-chemical process of the solute accumulation from the fluid phase to the condensed layer on a solid or liquid surface. The term of adsorption is used not only to stand for the process of interfacial accumulation but also to refer to the amount of accumulated molecules on the interface. The solutes adsorbed on the surface are called the adsorbate, while the substance which provides the surface is called the adsorbent. Adsorption processes are frequently categorized as two processes: chemisorption and physisorption. Chemisorption is the process where a chemical binding like covalent binding is dominant between the adsorbate and the adsorbent. On the other hand, physisorption is the process where van der Walls force, ionic bonding, and polar

interactions are dominant instead of any chemical bond (Masel, 1996). The stability of protein structure itself relies on the interactions that differ in their relative strengths and frequency in proteins. These interactions affect the protein adsorption on the polymeric surface as well as the protein conformation. These are the major interactions occurred in the protein molecules dissolved in surrounding water.

i) *van der Waals interactions*. van der Waals interactions are particular class of intermolecular forces. There are attractive and repulsive van der Waals forces that control the interactions between atoms and are very important in protein structure. Their origin is an interaction of the fields that arise from the movement of electrons around the positive charged atomic nucleus. Even if van der Waals interactions are relatively weak, they are still important for entities consisting of many atoms like solid surfaces or proteins.

ii) *Coulomb interactions*. As an inter-molecular interaction, the Coulomb interaction takes place between molecules that have a net charge. In aqueous system, an ion is always surrounded by several other ions of opposite and equal which have a screening effect on the Coulomb interaction. Coulomb interaction is much weaker in water than in the interior of a protein.

iii) *Hydrophobic interaction*: Hydrophobic interaction occurs exclusively in an aqueous environment because of the dehydration of two non-polar parts of protein molecules. This interaction becomes an attraction mainly driven by entropy changes. The contribution from hydrophobic interaction often dominates over those from other types of

physical interaction. Since the side chains of many amino acid residues are hydrophobic, the hydrophobic effect may contribute significantly to intra-molecular interactions in proteins.

iv) *Hydrogen bond*. Hydrogen bond is a special type of attractive interaction that exists between certain chemical groups of opposite polarity. It also contributes significantly to the stability of α-helices and to the interaction of β strands to form parallel or anti-parallel β sheets of proteins. In aqueous media the contribution of hydrogen bonding to the adsorption affinity is often minor because of the compensation of adsorbate-adsorbent and water-water contributions. Although it is stronger than van der Waals forces, the hydrogen bond is much weaker than other bonds like ionic bond and covalent bond.

Adsorption equilibrium is the fundamental property of the solute-surface interaction because the adsorption process will be continued until the thermodynamic equilibrium of the solute concentration is reached. The equilibrium at a given temperature is usually presented with an isotherm which is the plot of the amount of the adsorbed solute as a function of the solute concentration. The adsorption isotherm is useful for selecting the most appropriate adsorbent and also for predicting the performance of adsorption systems. For example, the adsorption capacity of a surface is needed to be reduced such as protein adsorption and fouling.

Figure 2.3 shows the typical adsorption isotherms: linear isotherm, Langmuir isotherm, and Freundlich isotherm. These isotherm models are currently used to fit the adsorption isotherms in bioseparations (Cussler, 1997; Ribeiro et al., 2001). The linear isotherm is given by the following equation:

$$q_e = KC_e \qquad\qquad (2\text{-}1)$$

where q_e is the equilibrium concentration of adsorbate, C_e is the equilibrium concentration of the solute in the fluid phase, and K is the equilibrium constant. Even if it is frequently assumed for the adsorption process, the simple linear isotherm rarely occurs. Both Langmuir and Freundlich isotherms have been generally used to describe the protein adsorption on the surface.
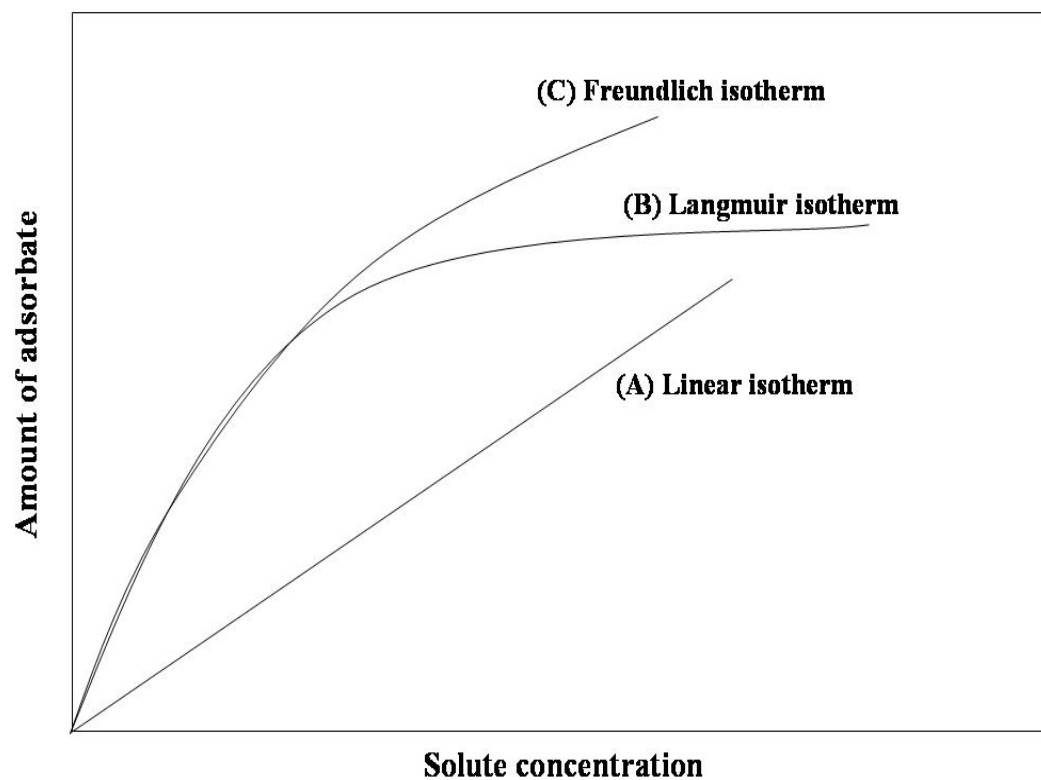
Figure 2.3. Typical adsorption isotherms: (A) linear isotherm, (B) Langmuir isotherm, and (C) Freundlich isotherm.

2.3.1. Langmuir Isotherm

As one of the simplest isotherms to describe the monolayer adsorption, Langmuir isotherm was developed by Irving Langmuir to describe the adsorption of gases onto the plane surfaces at a fixed temperature (Langmuir, 1918). Langmuir isotherm assumes that (1) the adsorbed layer should be monolayer, (2) there are finite numbers of identical adsorption sites on the surface, and (3) the adsorption ability of a solute to the each of these sites is independent of the occupation of neighboring sites (Adamson, 1982; Masel, 1996). The Langmuir isotherm might be derived by the following equilibrium:

$$S + R \quad \Leftrightarrow \quad SR \tag{2-2}$$

where S is the solutes in solution, R is the surface or adsorbent, SR represents the adsorbed state of solute on the surface. The equilibrium constant of this reaction can be written:

$$K = \frac{[SR]}{[S][R]} \tag{2-3}$$

Suppose that the surface carries binding sites per unit weight, S_T, of which S_O are occupied and S_F are free binding sites.

$$S_T = S_O + S_F \tag{2-4}$$

If $[R]$ is proportional to the number of the vacant sites, S_F/S_T, and $[SR]$ is proportional to the surface coverage of the adsorbed molecules, S_O/S_T, we may write:

$$[R] = \alpha \cdot \frac{S_F}{S_T} \qquad \text{and} \qquad [SR] = \alpha \cdot \frac{S_O}{S_T} \tag{2-5}$$

$$K = \frac{[SR]}{[S][R]} = \frac{\alpha \cdot \frac{S_O}{S_T}}{[S] \cdot \alpha \cdot \frac{S_F}{S_T}} = \frac{1}{[S]} \cdot \frac{S_O}{S_F}$$

$$= \frac{1}{[S]} \cdot \frac{S_O}{S_T - S_O} = \frac{1}{[S]} \cdot \frac{\frac{S_O}{S_T}}{1 - \frac{S_O}{S_T}} \tag{2-6}$$

$$\frac{S_O}{S_T} = \frac{K \cdot [S]}{1 + K \cdot [S]} \tag{2-7}$$

S_O/S_T is called the fractional coverage or the occupied fraction of the total number of sites. This is denoted q:

$$q = \frac{K \cdot [S]}{1 + K \cdot [S]} = \frac{[S]}{1/K + [S]} \tag{2-8}$$

As S_T represents the total number of adsorption sites per mass solid, it may be denoted q_{max} and the Langmuir equation takes the following form:

$$q_e = q_{max} \cdot \frac{K \cdot [S]}{1 + K \cdot [S]} \qquad (2\text{-}9)$$

[S] is proportional to the concentration (C) of the solute.

$$q_e = \frac{q_{max} K C_e}{1 + K C_e} \qquad (2\text{-}10)$$

and the linear form of the equation is

$$\frac{C_e}{q_e} = \frac{1}{q_{max} K} + \frac{1}{q_{max}} C_e \qquad (2\text{-}11)$$

where C_e is the equilibrium solute concentrations in solution (mol/L), q_e is equilibrium concentration of adsorbate on the surface (mol/g or mol/cm^2), K is a direct measure for the intensity of the adsorption process, and q_{max} is maximum concentration of adsorbate, reflecting the adsorption capacity. Langmuir constants, K and q_{max} can be determined from its slope and intercept of the linear equation.

2.3.2. Freundlich Isotherm

In Langmuir isotherm, it was assumed that finite number of binding sites existed on the surface and the reaction of the adsorbate to each of these sites was thermodynamically identical. It means that the same equilibrium constant could describe the adsorption process throughout the entire concentration range of the adsorbate. In many cases, however, the adsorbate could modify the surface properties and thus the equilibrium constant in the Langmuir isotherm can be changed. In this situation, Freundlich isotherm is more useful as an empirical equation. The Freundlich equation is commonly given by

$$q_e = K_F C_e^{1/n} \qquad (2\text{-}12)$$

with the linear form,

$$\ln q_e = \ln K_F + \frac{1}{n} \ln C_e \qquad (2\text{-}13)$$

where K_F is a constant for the Freundlich system, related to the bonding energy. K_F can be defined as the adsorption or distribution coefficient and represents the quantity of the adsorbate on the surface for a unit equilibrium concentration ($C_e = 1$ mol/L). The slope $1/n$, ranging between 0 and 1, is a measure of adsorption intensity or surface heterogeneity, becoming more heterogeneous as its value gets closer to zero. A plot of $ln\ q_e$ versus $ln\ C_e$ enables the empirical constants K_F and $1/n$ to be determined from the intercept and slope by the linear regression.

2.4. Quartz Crystal Microbalance with Dissipation Monitoring (QCM-D)

2.4.1. QCM Technique

QCM technique is centered on a thin quartz crystal with metal electrodes deposited on its both sides (O'Sullivan and Guilbault, 1999). Gold is usually used as an electrode. Since the quartz is the piezoelectric crystalline form of SiO_2, it shows the piezoelectric effect: when an alternating electric field (AC voltage) is applied over the electrodes, the quartz crystal will be oscillated periodically at its fundamental resonance frequency. The oscillation depends on the cutting angle of the quartz crystal. The quartz crystal commonly used for QCM application is AT-cut which is cut at an angle of 35° from the crystallographic ZX-plane as shown in Figure 2.4 (O'Sullivan and Guilbault, 1999; Marx, 2003). AT-cut quartz crystal provides a stable oscillation with almost no temperature fluctuation in frequency at room temperature.
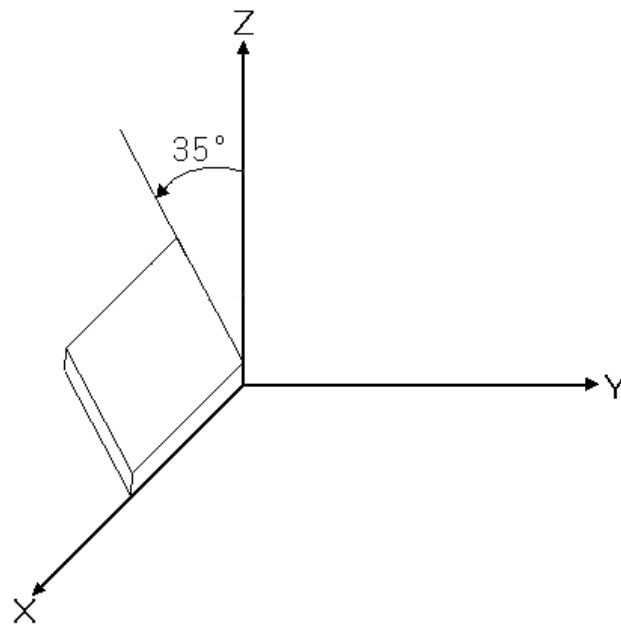
Figure 2.4. AT-cut quartz crystal.

The principle of the QCM is as follows: when the quartz crystal is immersed in aqueous solution, it is excited to oscillate at a fundamental resonant frequency (5 MHz). When the substrate is adsorbed on the crystal surface the resonant frequency decreases with the increase in the amount of mass adsorbed on the crystal. If the adsorbed mass is evenly distributed, sufficiently rigid to have no energy dissipation, thin to have negligible internal friction, and small compared to the mass of the crystal, the frequency shift (Δf) is proportional to the adsorbed mass per unit surface (Δm) under Sauerbrey equation:

$$\Delta m = -\frac{C \cdot \Delta f}{n} \qquad\qquad (2\text{-}14)$$

where C is the mass sensitivity constant ($=17.7$ ng·cm^{-2}·Hz^{-1} at $f = 5$ MHz) and n is the overtone number (in the present case $n = 3$, 5, and 7). However, if the adsorbed layer does not follow the oscillation rigidly, the energy dissipation in the oscillation will be changed. Because most protein layers adsorbed at the interface are hydrated and highly viscoelastic, they are not completely rigid and can cause the energy dissipation significantly. In such case, Sauerbrey equation is not valid anymore. In order to obtain more accurate mass change and viscoelastic properties of the adsorbed protein layer, energy dissipation should be considered. QCM-D can measure the frequency shit (Δf) and dissipation shift (ΔD) simultaneously at three different overtones (n= 3rd (15 MHz), n= 5th (25 MHz), and n= 7th (35 MHz)). These multiple Δf and ΔD data obtained at several overtones were used to calculate the viscoelastic properties of the adsorbed protein layer based on the Voigt based viscoelastic model system (Voinova et al., 1999).

2.4.2. Dissipation Factor

Dissipation factor describes the energy loss of an oscillatory system during one period of oscillation. Dissipation factor can be defined as follows:

$$D = \frac{E_{dissipated}}{2\pi E_{stored}}$$ (2-15)

where $E_{dissipated}$ is the dissipated energy and E_{stored} is the energy stored in the oscillating system. D is the sum of all energy dissipated in the oscillatory system. In 1966, Spencer and Smith found that the amplitude of a quartz crystal decays as an exponential sinusoidal when the driving power to a piezoelectric crystal oscillator is switched off. The relationship between amplitude and decay time is described by the general form as follows:

$$A(t) = A_0 e^{t/\tau} \sin(2\pi f t + \varphi)$$ (2-16)

where A is the amplitude, t is the time, τ is the decay time, f is the resonant frequency, and φ is the phase angle. The QCM-D system can determine the decay time (τ) as well as the resonance frequency (f) of the exponentially damped sinusoidal voltage signal over the crystal caused by switching of the voltage applied to the piezoelectric oscillator. The dissipation factor, D, is inversely proportional to the decay time, τ, as follows:

$$D = \frac{1}{\pi f \tau} = \frac{2}{\omega \tau}$$ (2-17)

where f is the resonant frequency and τ is the decay time. By recording the voltage during the decay and numerically fitting to equation (2-17), both the resonance frequency and the dissipation factor of the crystal can be achieved simultaneously as shown in Figure 2.5.

In this study, the viscoelastic representation based on the viscoelastic model (Voinova, et al., 1999) has been used to simulate the QCM-D response such as density, viscocity, elasticity, and thickness of adsorbed protein layer using Q-Tool software. Figure 2.6 shows the schematic illustration of the geometry and the parameters used to simulate the response of a quartz crystal upon mass load in contact with bulk liquid. According to the research of Voinova, et al., the relationship between QCM-D response and viscoelastic properties of the adsorbed layer was explained with the equations as follows:

$$\Delta f \approx -\frac{1}{2\pi\rho_0 h_0}\left\{\frac{\eta_3}{\delta_3} + h_1\rho_1\omega - 2h_1\left(\frac{\eta_3}{\delta_3}\right)^2 \frac{\eta_1\omega^2}{\mu_1^2 + \omega^2\eta_1^2}\right\} \tag{2-18}$$

$$\Delta D \approx \frac{1}{\pi f\rho_0 h_0}\left\{\frac{\eta_3}{\delta_3} + 2h_1\left(\frac{\eta_3}{\delta_3}\right)^2 \frac{\eta_1\omega}{\mu_1^2 + \omega^2\eta_1^2}\right\} \tag{2-19}$$

where ρ_0 and h_0 are the density and thickness of the crystal. η_3 is the viscosity of the bulk liquid and δ_3 is the viscous penetration depth of the shear wave in the bulk liquid and ρ_3 is the density of liquid. ω is the angular frequency of the oscillation. In this model, the protein adlayer is represented by four parameters: density (ρ_1), viscosity (η_1), shear elasticity (μ_1), and thickness (h_1). Among them, the thickness of the protein layer was obtained by

dividing the total mass by the density, which was assumed to be 1,200 kg/m^3 for the protein layer with trapped water (Rodahl, et al., 1997). We also assumed that the polymer-coated quartz crystal was purely elastic, and the surrounding solution was purely viscous and Newtonian.
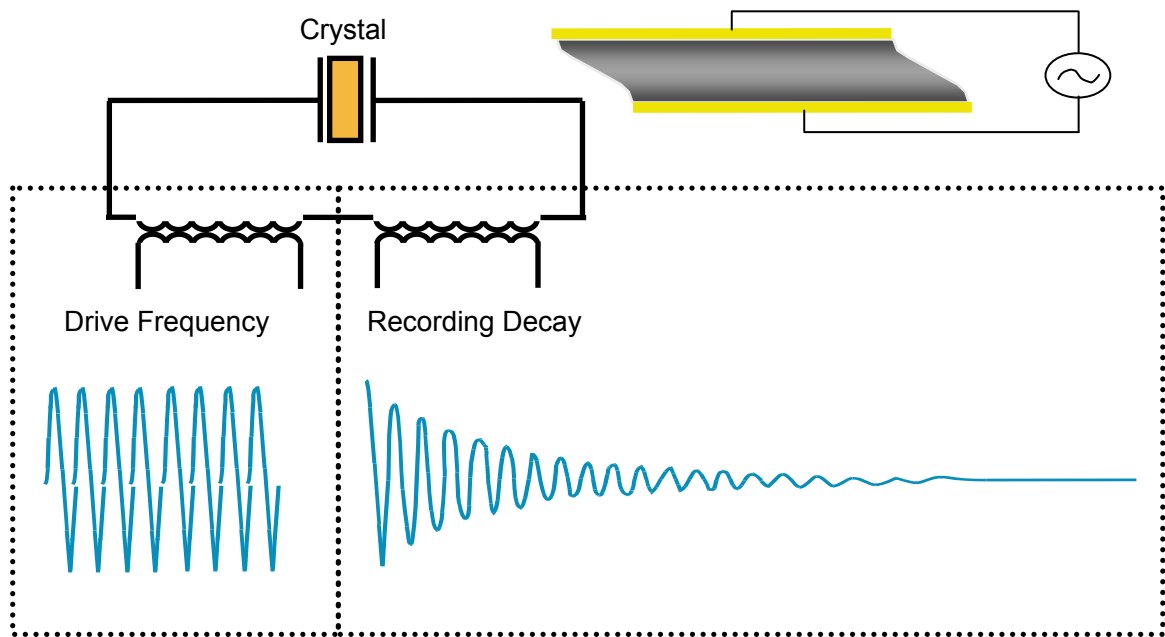
Figure 2.5. Measurement principle of frequency and dissipation (Q-Sense).
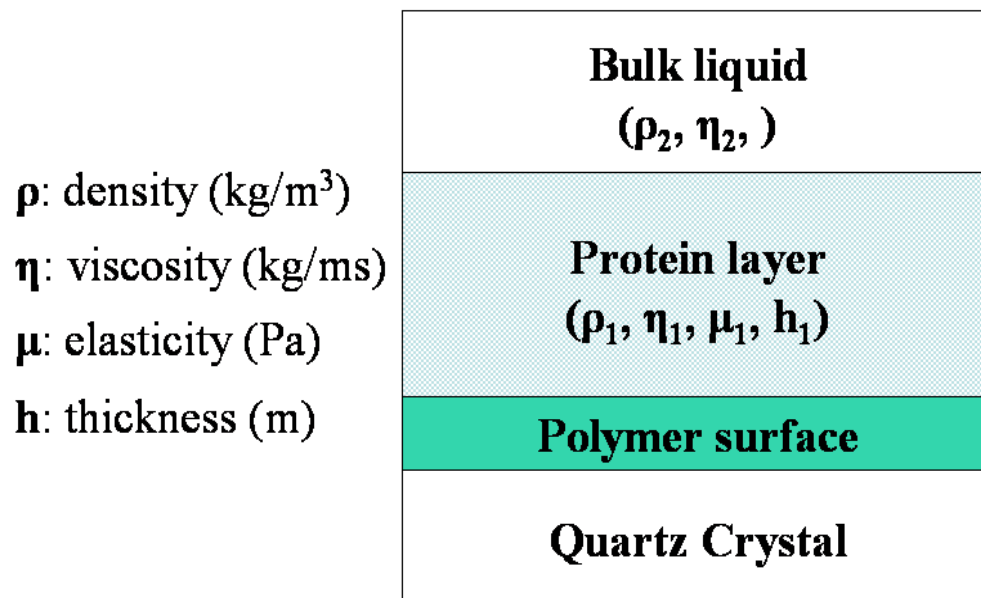
Figure 2.6. The layered structure of PES-coated quartz crystal, which is first modified with PES film, followed by the adsorption of β-lactoglobulin molecules. β-Lactoglobulin thin adlayer can be described by density (ρ_1), viscosity (η_1), shear elasticity (μ_1), and thickness (h_1).

2.5. Surface Modification of Membrane

Generally, it has been known that membrane fouling on hydrophobic polymer surfaces is mainly a result of the hydrophobic interaction between the protein and the hydrophobic polymeric membrane surface. To reduce this fouling, it is therefore logic to use the hydrophilic polymeric membranes instead of the hydrophobic membrane. Among commercial membranes, cellulose acetate is a widely used hydrophilic membrane. Many hydrophilic membranes such as cellulose acetate and biopolymer based membranes, however, have several drawbacks such as weak mechanical strength, thermal and chemical resistance, and microbial attack. Hydrophilic surface modification of the existing membrane material is the most practical solution to reduce membrane fouling while maintaining its mechanical and resistant properties (Wavhal and Fisher, 2002; Reddy et al., 2003) because the hydrophobic nature of polymer backbones can maintain its properties, while the hydrophilic thin skin can reduce the protein adsorption.

Surface modification of membrane can be classified into two main categories; physical modification and chemical modification. Physical modifications involve exposure to radiation (Inchinose and Kawabushi, 1996; Hollander and Behnish, 1998), plasma (Gerenser, 1987; France and Short, 1998; Song et al., 2000; Kim et al., 2002), and ion beams (Dong and Bell, 1999). But one of the major drawbacks of these physical modifications is that the physicochemical characteristics of the modified surfaces can be time dependent which means the surface reactivity can be gradually deteriorated (Wavhal and Fisher, 2003). On the other hand, chemical modification is not time dependent because the membrane surface reacts directly with chemical agents. Higuchi et al. (2004) introduced aspartic acid onto the polysulfone membranes and revealed that the protein

adsorption was reduced on the modified membrane surface. Yang and Lin (2003) improved the hydrophilicity of polysulfone membrane by immobilization with chitosan and heparin and then showed the reduction of the protein adsorption on the chitosan and heparin immobilized polysulfone membranes. Taniguchi et al. (2003) investigated that the low protein adsorption and low irreversible membrane fouling was exhibited by UV-assisted graft polymerization of *N*-vinyl-2-pyrrolidine (NVP) onto PES membrane.

Thin film composite (TFC) polyamide (PA) membranes have become the main type of membranes used for reverse osmosis and nanofiltration due to their excellent membrane performance and favorable economics (Zhzng et al., 2006). Interfacial polymerization (IP) has been a well-established method to prepare the thin active layer for thin film composite membranes. This technique is based on the polycondensation reaction between two immiscible solvents including dissolved monomers such as polyacyl chlorides in organic solvent and polyamine in water phase. Very thin active layer is quickly formed at the interface and remains attached to the substrate (Petersen, 1993; Freger, 2003).

CHAPTER III. STATIC AND DYNAMIC ADSORPTION OF

β-LACTOGLOBULIN ON POLYETHERSULFONE MEMBRANE SURFACE

3.1. Introduction

Most proteins have propensity to spontaneously and irreversibly adsorb at the solid-liquid interfaces because proteins have amphiphilic (both hydrophilic and hydrophobic) properties. They are generally soluble in aqueous solutions and several interactions such as van der Waals interactions, hydrogen bonds, hydrophobic interaction, and electrostatic interactions occur when they are dissolved in aqueous solutions. Protein adsorption phenomenon at interfaces is also an important issue in many research areas such as biotechnology, pharmaceutics, and biosensors (Norde, 1992 and 2003; Haynes and Norde, 1994). The adsorption of proteins involved in the above-mentioned areas, however, does not always play a positive role in these processes. For example, although the increase in protein concentration at interfaces is usually an advantage in biosensor applications, it is undesirable in causing fouling in the medical device (Werner et al., 1999) and in the food industry using stainless steel or plastic containers/pipings and employing membrane separations for food processing (Visser and Jeurnink, 1997; Murray and Deshaires, 2000). In this study, the protein adsorption on the polymeric membrane surface at various solution conditions such as protein concentration, pH, and salt concentration was investigated by static adsorption experiment and dynamic adsorption experiment.

3.2. Experimental Rationale and Design

In order to better understand the fouling mechanism of whey proteins on the polymeric membrane surface and develop new strategies and/or optimize the process conditions to minimize the membrane fouling, it is necessary to study the protein adsorption process and viscoelastic properties of the protein layer adsorbed on the polymeric membrane surface. The adsorption capacity of the surface, which depends on adsorption conditions such as the concentrations and the pHs of the protein solution, was investigated through the adsorption isotherm models in the static adsorption study. QCM-D technique was also used for the dynamic adsorption study. Quartz crystal microbalance with dissipation monitoring (QCM-D) technique can provide the unique and quantitative information on the viscoelastic properties of the adsorbed protein layer as well as monitor the protein adsorption process in real time by the simultaneous measuring of frequency shifts (Δf) and dissipation shifts (ΔD). In order to study protein adsorption on polymeric membrane surface, polyethersulfone (PES) and β-lactoglobulin were used as a membrane polymer and as a standard protein, respectively. β-Lactoglobulin is the most abundant whey protein (over 50% of total whey proteins) in milk and the principal component in fouling deposits on the membrane surface and inside the pores (Fennema, 1996; Murray and Deshaires, 2000; Elofsson et al., 1996). PES is the most common and lesser prone to protein fouling in ultrafilatration of protein solutions; it also has excellent mechanical properties and resistant properties to high temperature, a wide range of pH, and various chemical agents (Cheryan, 1998).

3.3 Materials and Methods

3.3.1. Materials

Polyethersulfone (PES) polymer was kindly provided by Solvay Advanced Polymers, L.L.C. (Alpharetta, GA) under the trade name of RADEL[RM] H-2000P NT. Flat sheet PES membrane was purchased from Sterlitech (Kent, WA). MWCO of flat sheet PES membrane is 20,000. Bovine milk β-lactoglobulin, which is a mixture of A and B variants crystallized and lyophilized three times (Lot No. 033K7003), phosphate-buffered saline (PBS), and *N, N*-dimethylformamide (DMF) were purchased from Sigma-Aldrich (St. Louis, MO). Deionized water was obtained from a Millipore Milli-Q filtration system (Millipore Corporation, MA, USA) with a resistivity of 18.2 MΩ cm.

3.3.2. Experimental Procedure

3.3.2.1. Static Adsorption Experiments

Static adsorption experiments of β-lactoglobulin on virgin PES membranes and modified PES membranes were carried out by shaking 2 x 2 cm^2 pieces of membrane with 50 ml aqueous solution of β-lactoglobulin of desired concentrations (0.5 to 2.5 mg/ml) and pHs (pH 3.0, 5.2, 7.0, and 9.0) at room temperature for 24 hr to reach the equilibrium state. At the end of the adsorption period, the concentration of the residual protein solutions was determined with a UV-Vis spectrophotometer (UV-1700, Shimadzu) via the absorbance at 280 nm. By comparing the initial and final concentrations, the adsorption amounts can be calculated. The calibration curves and equations of absorbance versus β-lactoglobulin

concentrations from 0.5 mg/ml to 2.5 mg/ml in working condition were obtained by linear

regression.

3.3.2.2. Dynamic Adsorption Experiments

Dynamic adsorption experiments were carried out with a quartz crystal

microbalance with dissipation monitoring (QCM-D). 1% (w/v) solution of PES was

prepared by blending 1g of PES with 99ml of DMF. After PES was completely dissolved,

this solution was filtrated with a 0.45μm syringe filter to remove the impurities.

β-Lactoglobulin solutions were prepared as stock solution of 10% (w/v) concentration, and

stored in a freezer until their uses. Protein-free PBS buffer was used to obtain the baseline

and in the rinsing steps to wash out the reversible proteins after the protein adsorption

processes occurred.

QCM-D measurements were performed with the Q-Sense D 300 system (Q-Sense,

Goeteborg, Sweden) equipped with a QAFC 302 axial flow chamber (Figure 3.1). Since

this chamber has a heating/cooling system and a control valve, the experimental

temperature and flow rate could be maintained constantly. Quartz crystals with a

fundamental resonant frequency of 5 MHz, 0.3mm thickness, and 14 mm diameter

(QSX301; Q-Sense) were spin-coated with a spin coater (Headway Research Inc., Garland,

TX) using 1% (w/v) PES solutions in DMF and evaporated at the room temperature for at

least 24 hrs. The polymer-coated crystal was inserted into the QCM-D chamber. Frequency

and dissipation shifts versus time curves induced by the addition of β-lactoglobulin

solutions were recorded. The QCM-D chamber was stabilized at temperature of 24.75 ±

0.1℃. When frequency and dissipation shift were at equilibrium state, protein-free PBS

buffer was injected to remove the reversible protein. Four times of rinsing step were

accomplished for each experiment. All experiments were duplicated at least three times

and normalized to the fundamental resonant frequency of the quartz crystal (5 MHz). Data

were modeled using the software, Q-Tools, (Q-Sense, Goeteborg, Sweden) and

quantitative information on the viscoelastic properties of the adsorbed protein layer was

obtained. To clean the used crystals, the used crystals were immersed in the solvent for 48

hrs, sonicated for 5 mins, rinsed with deionized water, and dried with nitrogen. The crystals

dried by nitrogen were immersed in a 1:1:5 mixture of H_2O_2 (30%), NH_3OH (25%), and

deionized water at 80℃ for 15 mins. After rinsing with deionized water and drying with

nitrogen, the crystals were exposed to UV/Ozone for 10 mins by a UVO cleaner (Jelight

Company, Irvine, CA).
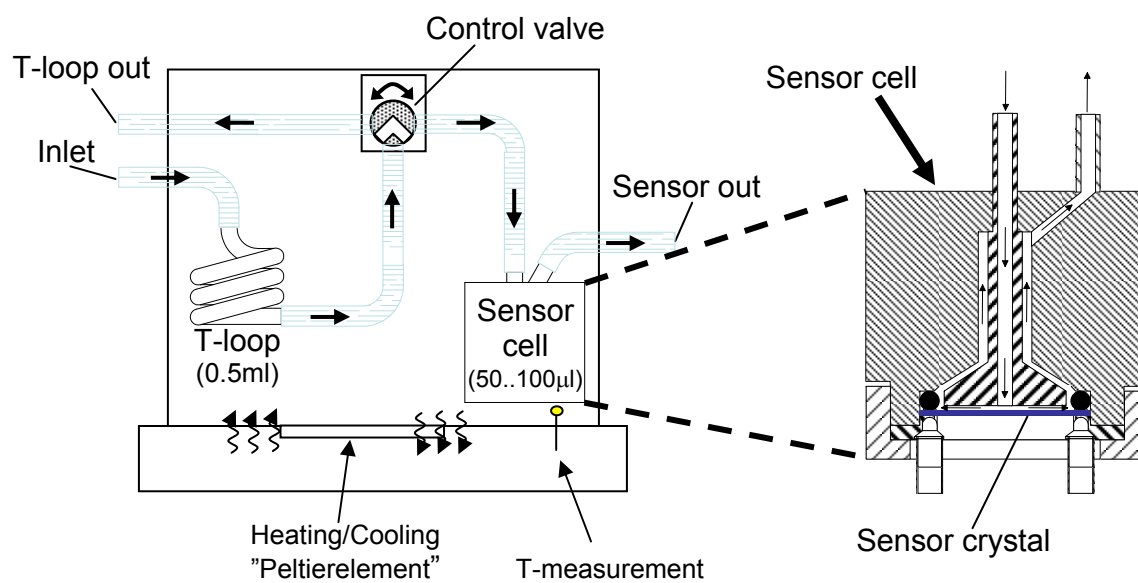
Figure 3.1. The schematic of QCM-D chamber, QAFC 302 axial flow chamber (Q-Sense).

3.3.2.3. Contact Angle Measurement

The measurement of contact angle between water and a membrane surface is the easiest and the most commonly used method to characterize the hydrophilicity of a membrane surface because contact angel is determined by the interaction between water and the outermost atomic layers of a membrane surface. When a drop of liquid is placed on a solid surface, the triple interface formed between solid, liquid, and gas will move in response to the forces arising from the three interfacial tensions until equilibrium is reached. The situation is illustrated in Figure 3.2 which shows a drop of liquid (L) on a flat solid surface (S) with air (G) as the third phase. A hydrophobic surface allows high contact angle due to the low free energy, whereas a hydrophilic surface allows low contact angle as following the Young's equation;

$$\gamma_{SG} = \gamma_{SL} + \gamma_{LG} \cdot \cos\theta \qquad\qquad (3\text{-}1)$$

where γ_{SG} is the solid-gas interfacial energy, γ_{SL} is the solid-liquid interfacial energy, γ_{LG} is the liquid-gas energy, and θ is contact angle of the surface.

The contact angles of the PES modified and unmodified quartz crystal, and commercial flat sheet PES membrane were measured using the sessile drop method on a VCA Optima surface analysis system. A 28 gauge blunt-tip needle was attached to a VCA Optima mechanically controlled micrometer for dispensing a 2 µL deionized water droplet onto the surface of a sample. Five measurements were made for each sample and used to determine the average and standard deviation for the data.
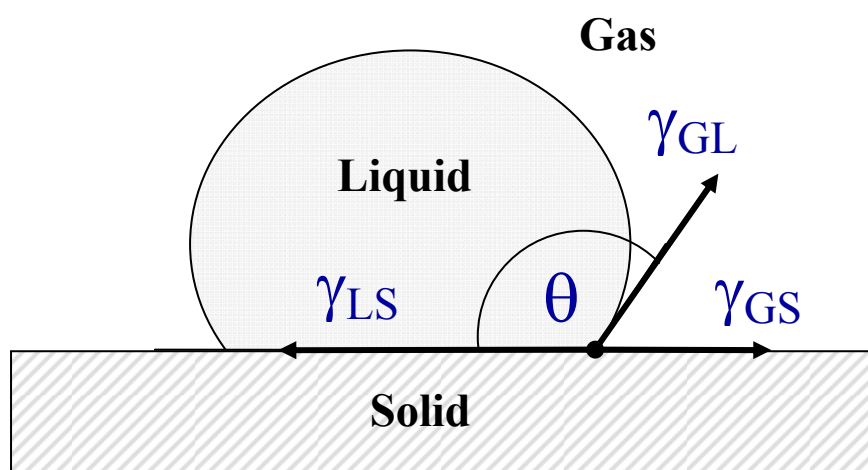
Figure 3.2. The contact angle at the triple interface for a drop of liquid on a solid surface.

3.3.2.4. ATR/FTIR Measurements

Attenuated total reflectance-Fourier transform infrared (ATR/FTIR) spectroscopy is a useful tool for studying protein adsorption because it is a non-invasive surface-sensitive technique that provides a lot of information (Fontyn et al., 1991). Principle of FTIR measurement is that the gas to be analyzed is led through a cuvette with an infra red (IR) light source at one end that is sending out scattered IR light, and a modulator that "cuts" the infra red light into different wave lengths. At the other end of the cuvette a detector is measuring principle it is the absorption of light at different wave lengths that is an expression of the concentration of gasses to be analyzed. Fourier Transformation mathematics is used as a data processing to turn the measured absorption values into gas concentrations for the analyzed gasses.

In fact, in ATR-FTIR spectroscopy, the varying parameters such as the beam incidence angle, allow the analysis of the surface layer only. For the ATR-FTIR spectral measurements of membrane surfaces, a Thermal Nicolet Nexus 670 FTIR system with an ATR accessory was employed. The ATR accessory contained a ZnSe crystal (25 mm x 5 mm x 2 mm) at a nominal incident angle of 45°, yielding about 12 internal reflections at the sample surface. All spectra were recorded with 256 scans at 4.0 cm^{-1} resolution at room temperature.
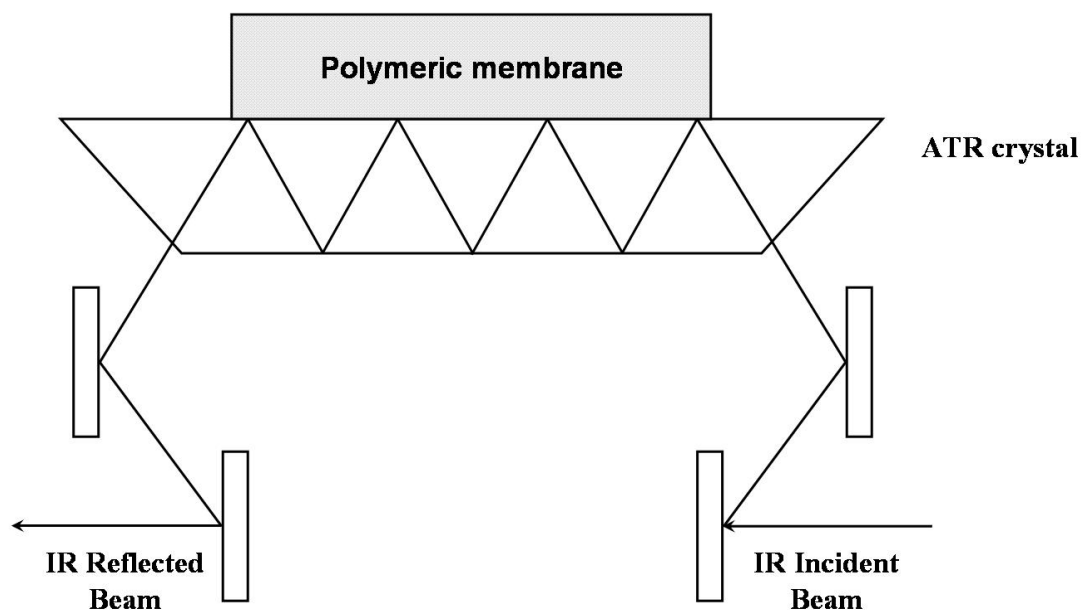
Figure 3.3. Schematic diagram of ATR-FTIR measurement.

3.3.2.5. Atomic Force Microscopy (AFM)

In order to obtain the image of the protein adsorption on the PES surface, a multimode AFM with Nanoscope IIIa Controller (Digital Instruments, Veeco, Santa Barbara, CA) was used. AFM provides capabilities and advantages over other microscopic methods such as scanning electron microscopy (SEM) and transmission electron microscopy (TEM) in studying of solid surfaces and micro structures by providing reliable measurements at nanometer scale (Göken and Kempf, 1999). A typical AFM system consists of a cantilever probe with a sharp tip mounted to a Piezoelectric actuator and a photo detector for receiving a laser beam reflected off the end point of the beam to provide cantilever deflection feedback (Figure 3.4). The principle of AFM is as follows: during the AFM tip scans the sample surface by moving up and down with the contour of the sample surface, the cantilever provides measurements of the difference in light intensities between the upper and lower photo detectors while Piezoelectric scanners maintain the tip at a constant force or constant height above the sample surface (Jalili and Laxminarayana, 2004).

AFM system can be operated in three different modes: i) non-contact mode, ii) contact mode, and iii) tapping mode. The non-contact mode is acquired by moving the cantilever tip slightly away from the sample surface and oscillating the cantilever at its resonance frequency. In non-contact mode, the cantilever tip can detect the attractive van der Waals forces between the tip and the sample surface. The topography of the sample is constructed by scanning the tip above the sample surface. The contact mode is utilized by monitoring interaction forces while the cantilever tip remains in contact with the target sample. In this mode, the interaction forces between the cantilever tip and the sample

surface are mainly repulsive forces. The tapping mode AFM combines both the contact and non-contact modes by gleaning sample data and oscillating the cantilever tip at its resonance frequency while allowing the high resolution imaging of soft samples that are difficult to examine using the contact mode AFM.

In this study tapping mode AFM was used to characterize the surface topography and roughness of PES modified quartz crystal surface and protein adsorbed surface. In order to obtain these surface images, the PES modified quartz crystal and protein adsorbed crystal surfaces were glued onto metal disks and attached to a magnetic sample holder, located on top of the scanner tube.
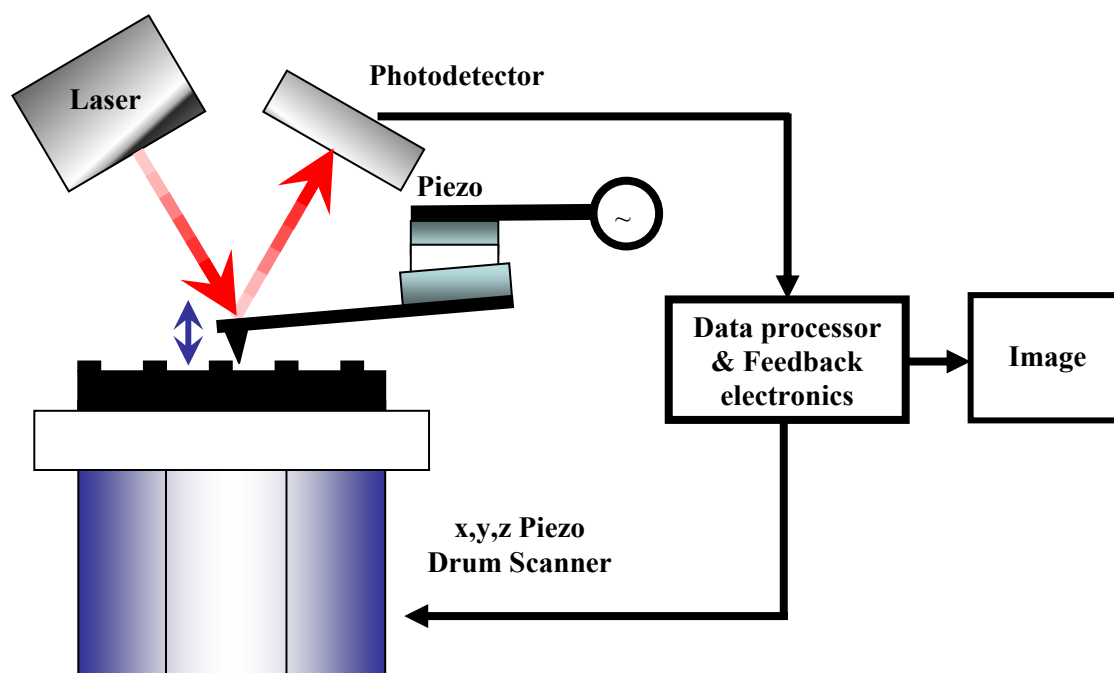
Figure 3.4. Schematic diagram of AFM measurement.

3.4. Results and Discussion

3.4.1. Static Adsorption Studies

The adsorption isotherms of β-lactoglobulin on PES membrane were obtained at various pHs of 3.0, 5.2 (isoelectric point), 7.0, and 9.0 (Figure 3.5). During the protein adsorption process on the polymeric membrane surface, many interactions between the membrane and the protein as well as among proteins themselves might affect on the amount of protein adsorption. Hydrophobic PES membrane is negatively charged in aqueous solution due to the ionization of polar groups at the membrane surface and/or the selective adsorption of anions from the surrounding solution onto the membrane surface (Pujar and Zydney, 1997). Therefore, the protein adsorption can be affected by the charge and density of the polymeric membrane surface as well as the protein charge which is dependent on the pH of the protein solution. The native structure of β-lactoglobulin is predominantly a dimer structure at room temperature and at neutral pH but it can be dissociated into the monomer structure depending on the pH of the solution. Below pH 3.5 and above pH 7.5 the dimer structure of β-lactoglobulin can be usually dissociated into the monomer structure (Verheul et al., 1999; McKenzie and Sawyer, 1967).

3.4.1.1. Effects of pHs

As shown in Figure 3.5 the amount of β-lactoglobulin adsorbed on the PES membrane surface was the lowest at the neutral pH (pH 7.0). The maximum adsorption of β-lactoglobulin on the PES membrane surface was obtained at the acidic condition (pH 3.0), which was below the isoelectric point (pH 5.2) of β-lactoglobulin. In this acidic condition, the protein adsorption might be affected by the electrostatic attraction between

the protein and the PES membrane surface because β-lactoglobulin had positive charges below its isoelectric point (pI) and hydrophobic PES membrane had negative charges in an aqueous solution due to the selective adsorption of anions from the surrounding water or due to the ionization of polar groups at the membrane surface (Pujar and Zydney, 1997). In addition, the hydrophobic interaction between protein and membrane can increase the amount of the protein adsorption. At the pH 3.0, the dimer structure of β-lactoglobulin can be dissociated into the monomeric units which expose the hydrophobic sites as shown in Figure 3.6. These monomeric units are inclinable to interact with the hydrophobic PES surface. Although some other interactions might affect on the protein adsorption, both hydrophobic interaction by the dissociation of dimer structure of β-lactoglobulin and electrostatic attraction between protein and PES membrane are the principal factor to show the higher adsorption than at higher pHs.

At the pI (pH 5.2) where β-lactoglobulin structure was more hydrophobic and compact because β-lactoglobulin aggregates strongly to a tetramer which is cyclic structure and involving four bonds between pH 3.7 to pH 5.2, the protein adsorption was occurred due to the mainly hydrophobic interaction between protein and PES membrane surface (Timasheff and Townend, 1964). The amount of β-lactoglobulin adsorbed at the pI was higher than that at the neutral pH where the electrostatic repulsion existed because both β-lactoglobulin and the PES membrane surface had negative charges above the pI of the protein solution. Also, hydrophobic interaction at pH 7.0 might be weaker than at the pI because β-lactoglobulin is less hydrophobic at neutral pH.

The higher adsorption of β-lactoglobulin, however, was observed at the pH 9.0 comparing with pH 5.2 and pH 7.0 even if the electrostatic repulsion was much stronger in this alkaline condition than in the neutral pH. Because β-lactoglobulin also could be dissociated into monomeric units above pH 7.5, the hydrophobic interaction between the PES surface and the monomeric units of β-lactoglobulin might increase the amount of adsorption at the pH 9.0. This hydrophobic interaction might be much stronger than the electrostatic repulsion so the protein adsorption is much higher at pH 9.0 than at pH 7.0 and at pH 5.2. These results support the earlier explanation that the protein adsorption is not only due to the electrostatic interactions but also due to the change of protein structure and hydrophobic interaction between the protein and the PES membrane as well as among the proteins themselves. Also, hydrophobic interaction by dissociation of dimer structure to monomer structure shows the more adsorption than the electrostatic interactions.
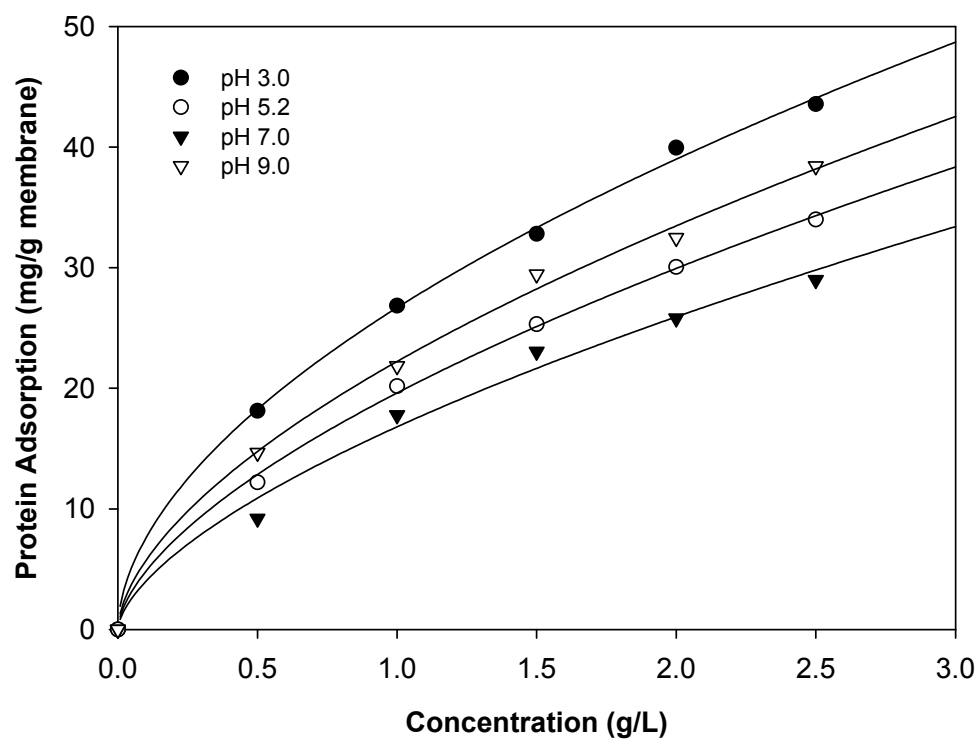
Figure 3.5. Adsorption isotherm for β-lactoglobulin on PES membranes at different pHs: pH 3.0, 5.2, 7.0 and 9.0.
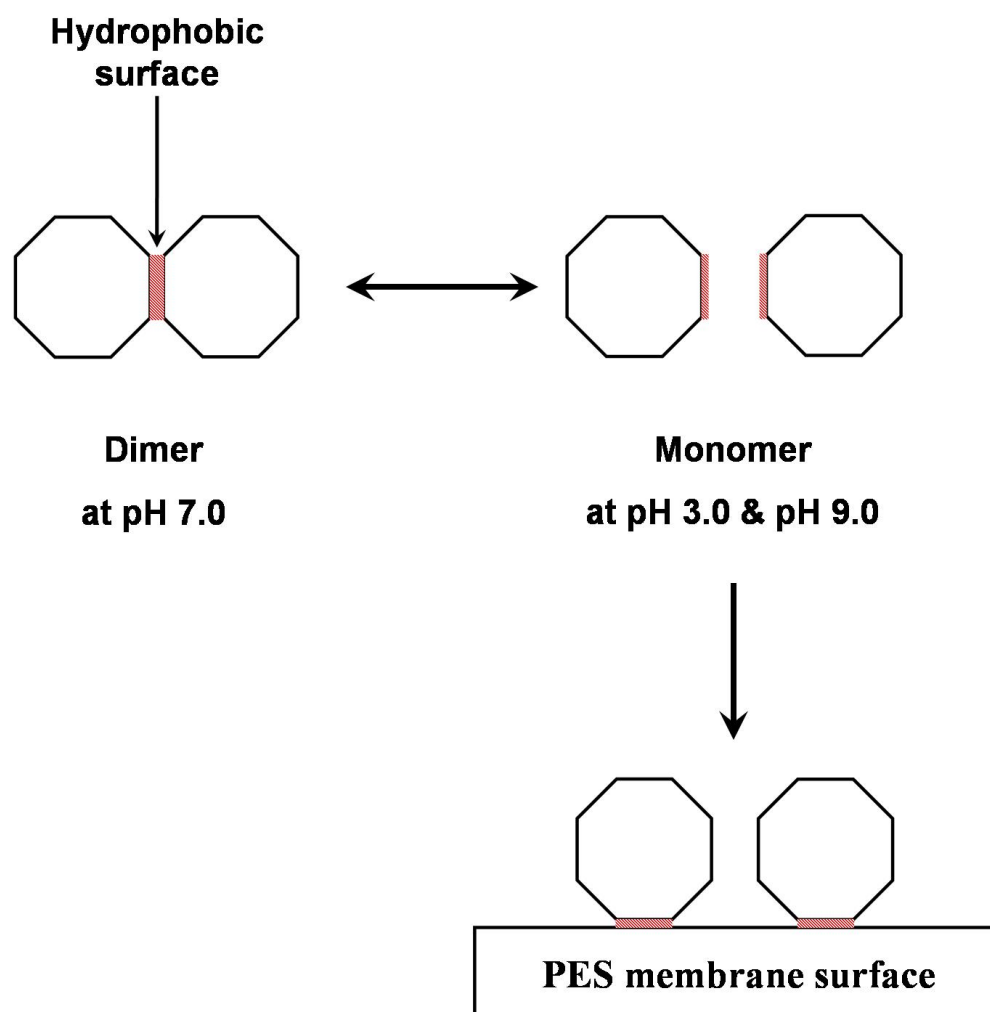
Figure 3.6. Dissociation of dimer structure of B-lactoglobulin to monomer structure depending on pH of protein solution.

The adsorption equilibrium curves of β-lactoglobulin on the PES membrane surface were obtained by plotting *ln q_e* versus *ln C_e*. The parameters of the Freundlich isotherm were determined from the intercept and slop of a linear regression, and then the results were given in Table 3.1. It can be seen clearly that the Freundlich constants such as adsorption capacity, K_F, and adsorption intensity, *1/n*, for β-lactoglobulin were depended on the pH of the protein solution. The adsorption capacity, K_F, which is the measure of bonding energy and indicates the quantity of the adsorbate on the adsorbant, increased with away from the neutral pH (pH 7.0). The K_F values increased about 65% at pH 3.0, 20% at pH 5.2, and 38% at pH 9.0 compared with that at pH 7.0. This result supports that the pH of protein solution is one of the important factors for the protein adsorption process and the amount of protein adsorption would be higher at the acidic (pH 3.0) and the alkaline (pH 9.0) conditions where the hydrophobic interaction by dissociation of dimer to monomer structure is occurred. The intensity constants, *1/n*, were just opposite to the trend of K_F. The intensity constants (*1/n*) decrease with the increasing the adsorption capacity value (K_F). The lower intensity constant means that the protein adsorbed surface is more heterogeneous. As shown in Table 3.1, the more protein adsorbed on the membrane surface (increase the adsorption capacity, K_F), the more heterogeneous surface can be formed on the membrane surface.

Table 3.1. Freundlich constants of β-lactoglobulin adsorbed on PES membrane at different pHs.

pH	K_F	$1/n$	R^2
3.0	26.64	0.551	0.998
5.2	19.41	0.634	0.996
7.0	16.16	0.709	0.972
9.0	22.16	0.596	0.995

3.4.1.2. Effects of NaCl Concentration

Figure 3.7 shows the salt effects on the β-lactoglobulin adsorption on the PES membrane at pH 3.0 where the maximum adsorption was obtained. The increase in ionic strength provided by NaCl reduced the amount of adsorption for β-lactoglobulin on PES membrane at pH 3.0. Although the hydrophobic interaction by the change of β-lactoglobulin structure from dimer to monomer increases the amount of adsorption, the electrostatic attraction between positive charged protein and negative charged PES membrane in acidic condition is also the major factor in the increasing of β-lactoglobulin adsorption on the PES membrane surface. The salt ions, however, can interact to the charged protein molecules and PES membrane surface so the electrostatic attractions between protein molecules and membrane surface could be reduced by the salt addition. Therefore the amount of β-lactoglobulin adsorption on the PES membrane surface was reduced with salt concentration. As shown in table 3.2, the adsorption capacity (K_F) decreases with NaCl concentration. Although the amount of β-lactoglobulin adsorption decreases with salt concentration, the intensity constants ($1/n$) also decrease with salt concentration. This result reveals that the protein adsorbed layers are more heterogeneous with salt concentration.
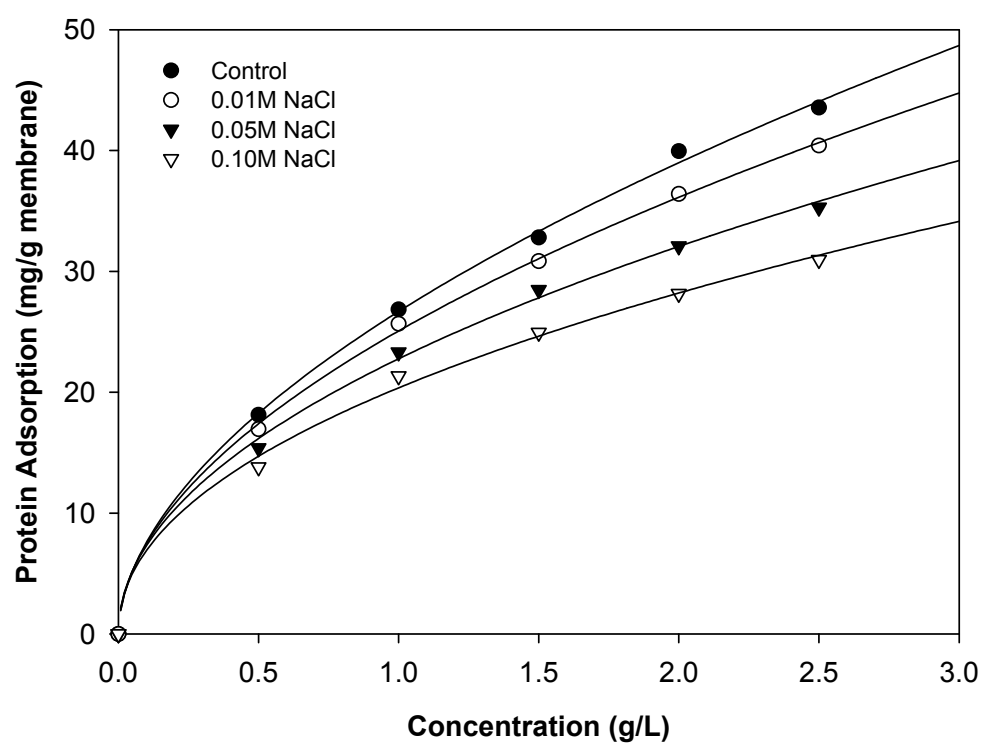
Figure 3.7. NaCl effect on the adsorption isotherm of β-lactoglobulin at pH 3.0.

Table 3.2. Freundlich constants of β-lactoglobulin adsorbed on PES membrane at pH 3.0 depending on the concentration of NaCl.

NaCl	K_F	$1/n$	R^2
Control	26.64	0.551	0.998
0.01 M	24.96	0.538	0.997
0.05 M	22.55	0.516	0.993
0.10 M	20.15	0.496	0.987

3.4.2. Dynamic Adsorption Studies

3.4.2.1. Characterization of PES Modified Surface

In order to study the dynamic adsorption processing of protein onto the PES surface using QCM-D instrument, the PES surface should be created onto the quartz crystal surface. Quartz crystals were spin-coated at 2000 rpm to 4000 rpm with 1% (w/v) PES solution in DMF and evaporated at the room temperature. After crystals were spin-coated some surface properties were characterized to make sure the PES modified crystal surface. Contact angle and FT-IR spectra were measured for the 1% PES solution coated quartz crystal surface and compared with those of the commercial PES membrane. The contact angles measurement using deionized water is the easiest way to characterize the surface hydrophilicity. As shown in Table 3.3, the contact angle of 1% PES modified crystal surface 74.08 ± 1.61 which is similar to that of the commercial PES membrane (71.49 ± 2.57). FT-IR spectra show the exactly same pattern in both PES modified surface and commercial PES membrane (Figure3.8). Aromatic bands of PES are present at 1578 and 1486 cm^{-1}. The peaks at 1322 and 1298 cm^{-1} represent the sulfone groups (S=O) of PES membrane. The possible assignments of spectra of Figure 3.8 are summarized in Table 3.4.

Table 3.3. Contact angles of PES-coated crystal and commercial PES membrane.

Surfaces	Contact angle
PES coated crystal	74.08 ± 1.61
Commercial PES membrane	71.49 ± 2.57
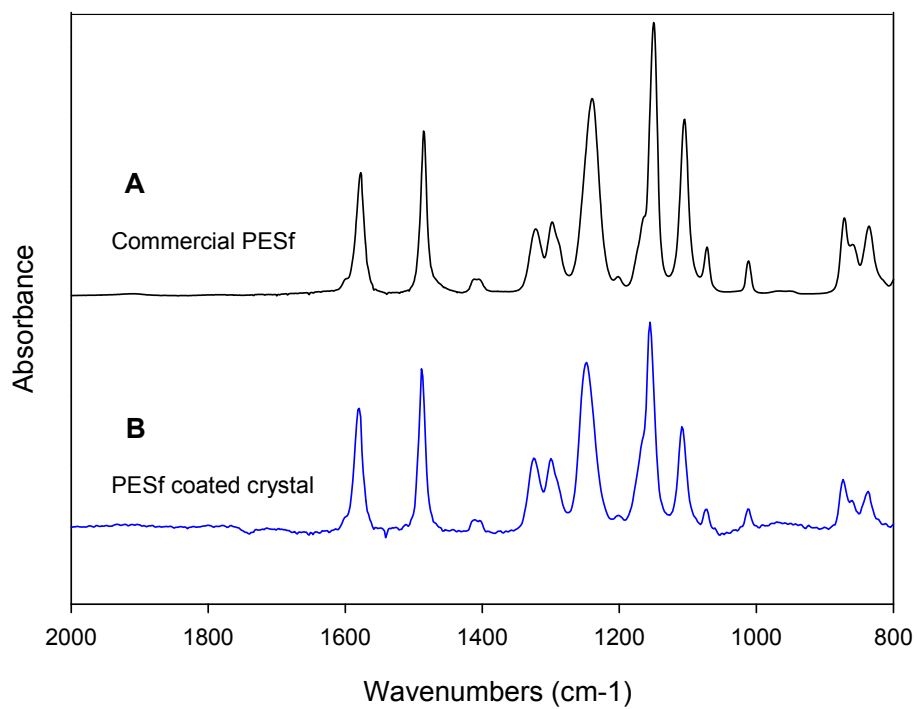
Figure 3.8. ATR-FTIR spectra of (A) the commercial PES membrane and (B) the PES-coated quartz crystal.

Table 3.4. Possible assignments of the FTIR spectra of PES membrane.

Peak (cm^{-1})	Possible assignments
1577	C=C aromatic ring stretching vibrations
1486	C=C aromatic ring stretching vibrations
1412	C=C aromatic ring stretching vibrations
1322	Ar-SO$_2$-Ar asymmetric stretching vibrations
1298	S=O stretching vibrations
1240	Ar-O-Ar stretching vibrations
1150	Ar-SO$_2$-Ar symmetric stretching vibrations
1105	C-C stretching vibrations
1072	C-C stretching vibrations
1012	C-C stretching vibrations
872	C-C stretching vibrations
836	C-H rocking vibrations (aromatic)
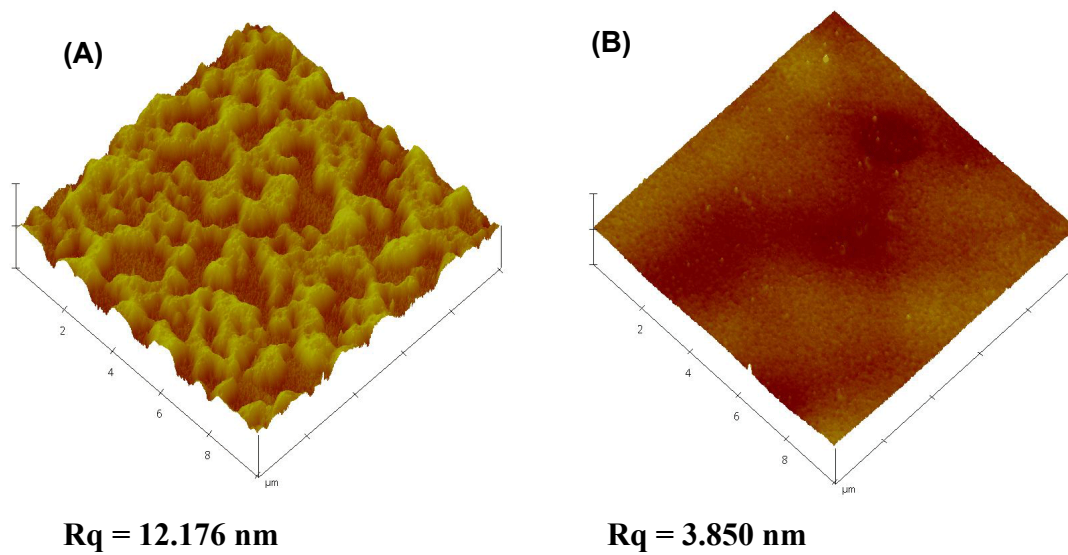
Figure 3.9. AFM images of 1% PES coated crystal surface using spin coater (A) at 2,000 rpm and (B) at 4,000 rpm.

Figure 3.9 shows the surface topography of 1 % PES coated quartz crystal using a spin coater by tapping mode AFM. The rpm of spin coater was changed from 2,000 to 4,000. The root mean square roughness (Rq) of PES coated crystal surface decreased with increasing rpm of spin coater, from 12.176 to 3.850 nm for a scan area of 10 x 10 μm^2 while the root mean square roughness (Rq) of commercial PES membrane was 2.067 nm. The shading intensity shows the vertical profile of the membrane surface with the light regions being the highest points and the dark regions being depressions. As shown in Figure 3.9.A, the surface of PES coated crystal was rough and heterogeneous when the rpm of spin coater was 2,000. On the other hand, the roughness of PES coated surface at 4,000 rpm was close to that (2.067 nm) of the commercial PES membrane.

3.4.2.2. Adsorption of β-Lactoglobulin on PES-Coated Surface

The typical adsorption process of β-lactoglobulin on the PES-modified crystal surface was monitored in real time by simultaneously measuring of frequency shifts (Δf) and dissipation shifts (ΔD). Figures 3.10.A and 3.10.B show the Δf and ΔD of 1% β-lactoglobulin at pH 5.2 as a function of time, respectively. Because viscous layers like protein layers adsorbed on the interfaces exhibit different penetration depths of harmonic acoustic frequencies, Δf and ΔD induced by the adsorbed protein layer were measured simultaneously at three different overtones (n=3, 5, and 7). These multiple frequency and dissipation data can be used to calculate the viscoelastic properties of the adsorbed protein layer. The Δf obtained at three overtones were normalized by their overtones. The arrows indicate the injection time of β-lactoglobulin solution (t_1), and several times of rinsing solutions (t_2, t_3, t_4 and t_5), respectively. The adsorption process of β-lactoglobulin on PES

surface consisted of reversible and irreversible adsorption, as shown in Figure 3.10.A. The Δf remained after rinsing steps indicates the irreversible adsorption and the Δf recovered by rinsing steps indicates the reversible adsorption. Although the reversible adsorption can cause membrane fouling, it can be removed by the high shear stress in the membrane filtration process. The irreversible adsorption, however, was caused by the strong interactions between protein and the membrane surface and between protein molecules, and it could not be removed in the rinsing steps. Therefore, the irreversible adsorption was the principal factor to cause the permanent membrane fouling. The frequency and dissipation data obtained after four times of rinsing were used to explain the permanent adsorption and the viscoelastic properties of the adsorbed protein layer. If the adsorbed protein layers were completely rigid and the energy could not be dissipated, all normalized Δf would be the same ($\Delta f_3/3 = \Delta f_5/5 = \Delta f_7/7$). In our study, all the normalized $\Delta f_n/n$ curves coincided when the concentration of β-lactoglobulin was below 0.1% (w/v) (data are not shown). However, when the concentration of β-lactoglobulin was higher than 1.0% (w/v), the normalized $\Delta f_n/n$ curve at the smaller overtone was usually larger than those at the larger overtones ($\Delta f_3/3 > \Delta f_5/5 > \Delta f_7/7$), as shown in Figure 3.10.A. Similar observations were also reported by Zhou et al. (2004) and Hook et al. (2001). Dissipation shift at smaller overtone was also larger than those at the larger overtones ($\Delta D_3 > \Delta D_5 > \Delta D_7$) until it was rinsed, as shown in Figure 3.10.B. After several times of rinsing steps, there were no significant differences in Δf and ΔD at all overtones because most viscous layers have been removed after rinsing four times.

Figure 3.10. (A) Frequency shift (Δf) and (B) dissipation shift (ΔD) induced by the adsorption of 1% β-lactoglobulin at pH 5.2 on the PES coated-surface as a function of time. Δf and ΔD are measured simultaneously at three overtones (n=3, 5, and 7) and normalized by their overtone numbers. The arrows indicate the time for the injection of protein solution (t_1) and four times of rinsing steps (t_2, t_3, t_4 and t_5).

3.4.2.3. Effects of Concentration and pH

The adsorption process of β-lactoglobulin was investigated at various

concentrations (0.1, 1.0, and 2.0 % (w/v)) and pHs (3.0, 5.2, and 7.0). The adsorption

profiles of β-lactoglobulin at each concentration on 1% PES coated-gold crystal are shown

in Figure 3.11. The magnitudes of Δf and ΔD increase with increase in protein

concentration, as shown in Figure 3.11.A and 3.11.B. The adsorption processes of

β-lactoglobulin on the PES surface in Figure 3.11 were very similar in their patterns

irrespective of the protein concentration. The Δf and ΔD changed rapidly and greatly after

the injection of β-lactoglobulin solution, and followed by minor changes over the

adsorption time until the rinsing steps were reached. During the rinsing steps, some

recoveries of Δf and ΔD were observed in 1% and 2% (w/v) protein concentrations. The Δf

and ΔD at the lowest protein concentration (0.1% (w/v)), however, were rarely recovered

during the rinsing steps. This result revealed that the most adsorbed layer of 0.1% (w/v)

β-lactoglobulin solution was irreversible adsorption even if the amount of Δf and ΔD were

small compared with those of higher concentrations. Figure 3.11.B shows that ΔD

increases with β-lactoglobulin concentration of β-lactoglobulin solution. The more

proteins were adsorbed on the polymer surface, the more energy was dissipated. In

addition, in 0.1% (w/v) β-lactoglobulin solution, the mono-layers of protein layers might

be formed on the polymer surface because the β-lactoglobulin solution concentration was

too low to form multi-layers. This pattern was close to the pattern described by the

Sauerbrey equation because most protein adsorption was occurred by the strong

interactions between the proteins and the polymer surface. The amount of proteins on the

reversible protein layer depends on the protein concentration. In the case of the adsorption

of 2% (w/v) β-lactoglobulin on the polymer surface, about 15% of Δf and 50% of ΔD were reversed by rinsing four times. Thus, in the case of adsorption at higher protein concentrations, β-lactoglobulin multi-layers originating from self-association among β-lactoglobulin molecules may also form. Although these protein multi-layers may cause significant energy dissipation, they were reversible, causing the lost of the mass of protein adlayers during the rinsing steps.
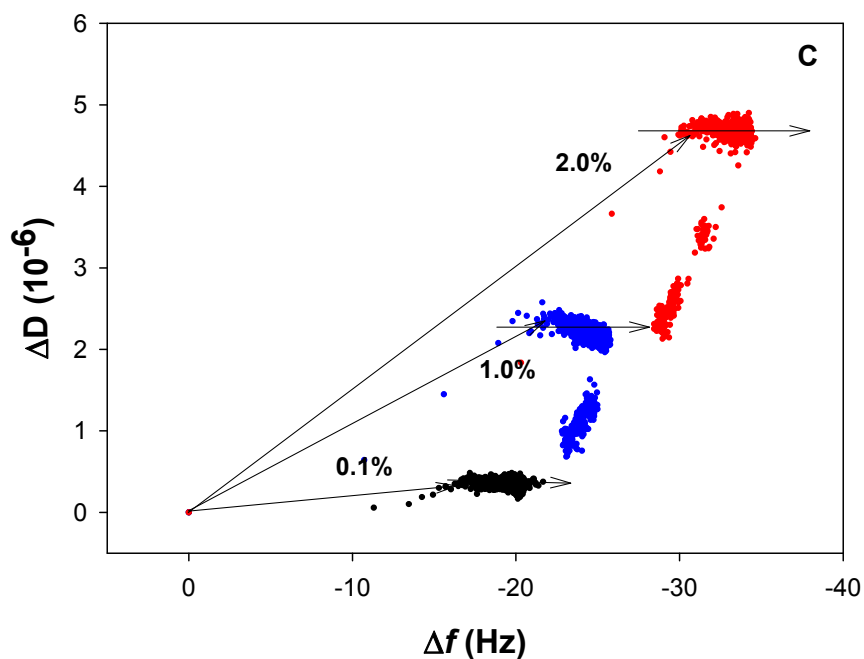
Figure 3.11. (A) Frequency shift (Δf) and **(B)** dissipation shift (ΔD) induced by the adsorption of β-lactoglobulin solutions with three concentrations (0.1, 1.0, and 2.0 %) at pH 7.0 as a function of time. The Δf was obtained at third overtone (f_3=15 MHz) and normalized ($f_3/3$). **(C)** ΔD - Δf plots using the data from **(A)** and **(B)**.

To illustrate the correlation between ΔD and Δf, the ΔD - Δf plots of β-lactoglobulin adsorption on PES surface at different protein concentrations were drawn in Figure 3.11.C using the data from Figures 3.11.A and 3.11.B. From the ΔD - Δf plots, we know the protein adsorption kinetic processes from the different dissipation shift per unit frequency shift ($\Delta D/\Delta f$). The different slopes in ΔD - Δf plots suggest that there exist at least two different processes during protein adsorption on the PES coated-surface. At the initial stage, protein molecules in solution diffuse rapidly to the interface and the conformation of protein molecules on the polymer surface might be occurred at the second stage. The initial slopes in ΔD - Δf plots are 0.020 for 0.1%, 0.111 for 1.0%, and 0.155 for 2.0% of β-lactoglobulin solution, whereas second slopes close to zero for all protein concentrations. These different slopes in ΔD - Δf plots may arise from protein adlayers of different viscoelastic properties, which were affected by the interactions between protein and polymer surface as well as the interactions between protein and protein. The amount of β-lactoglobulin adsorbed and the adsorption rate were higher at the higher concentration.
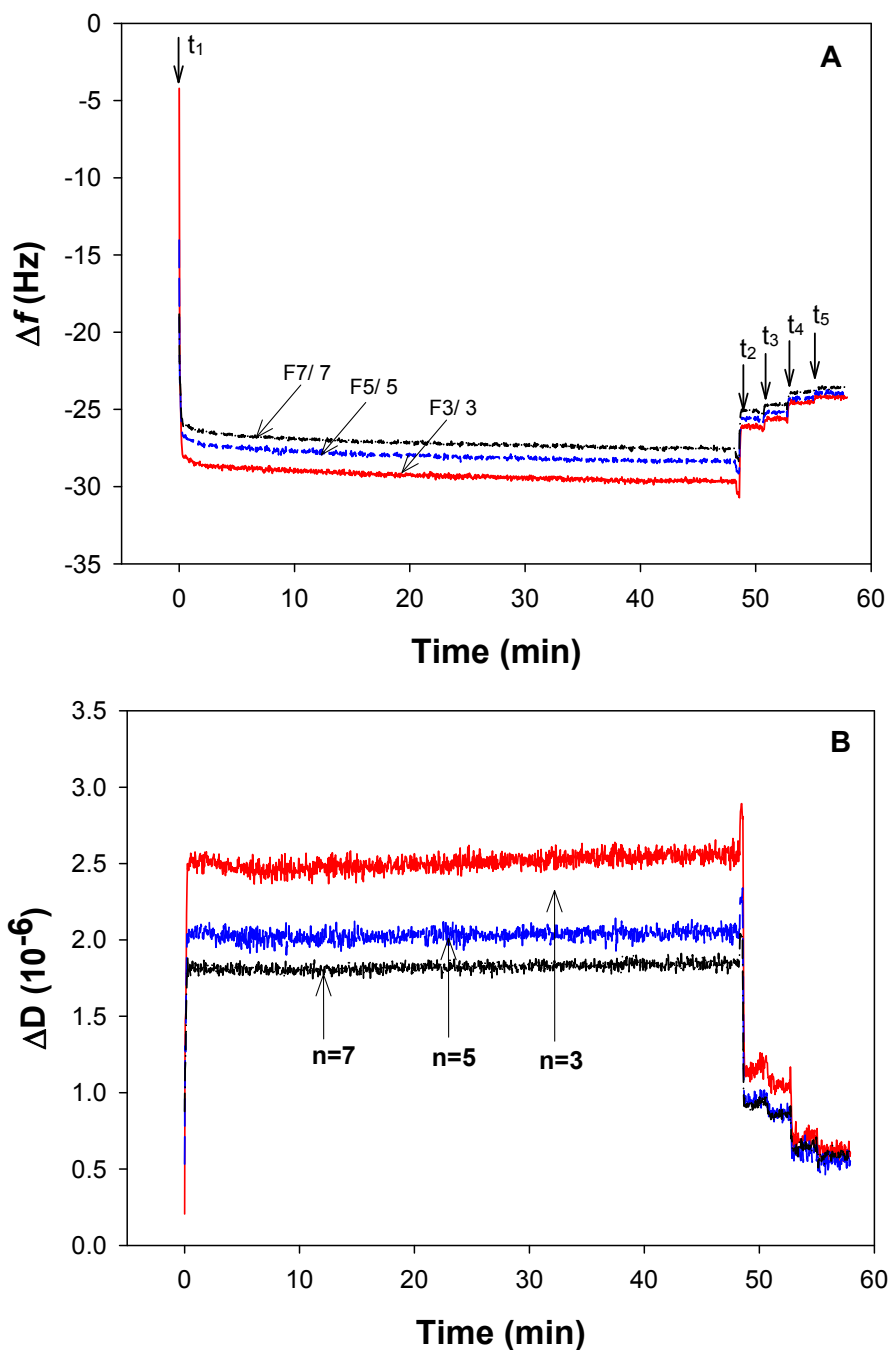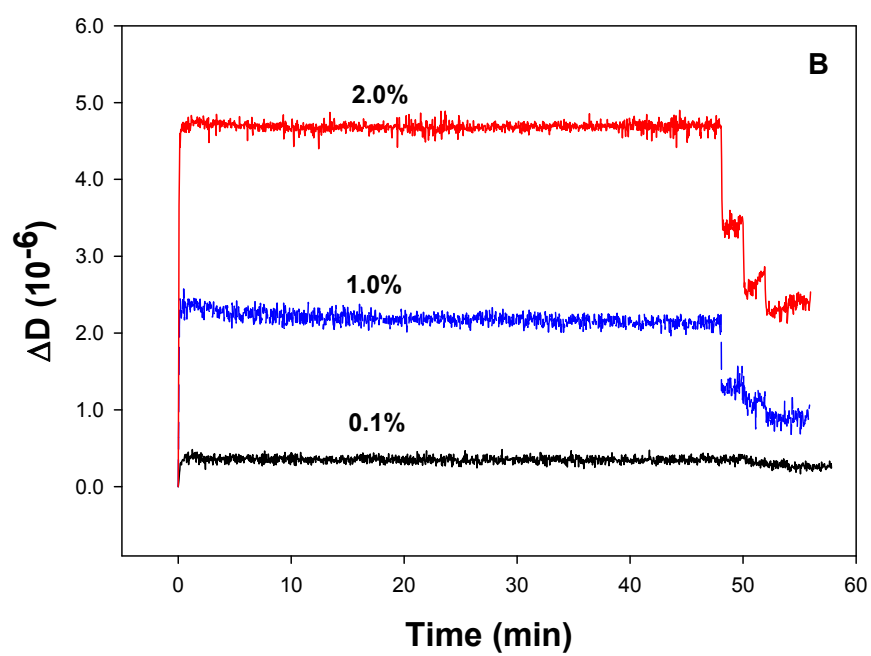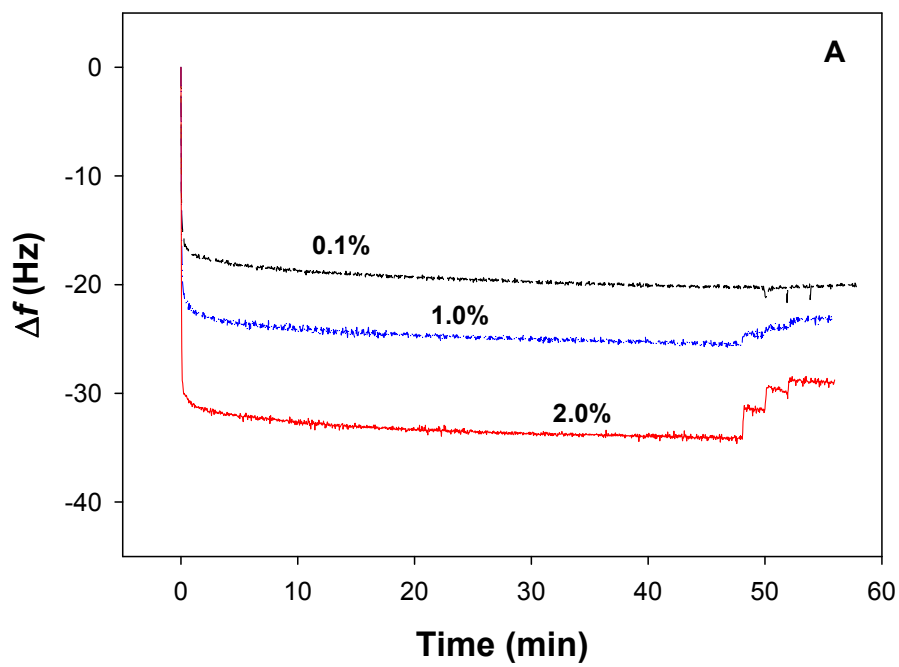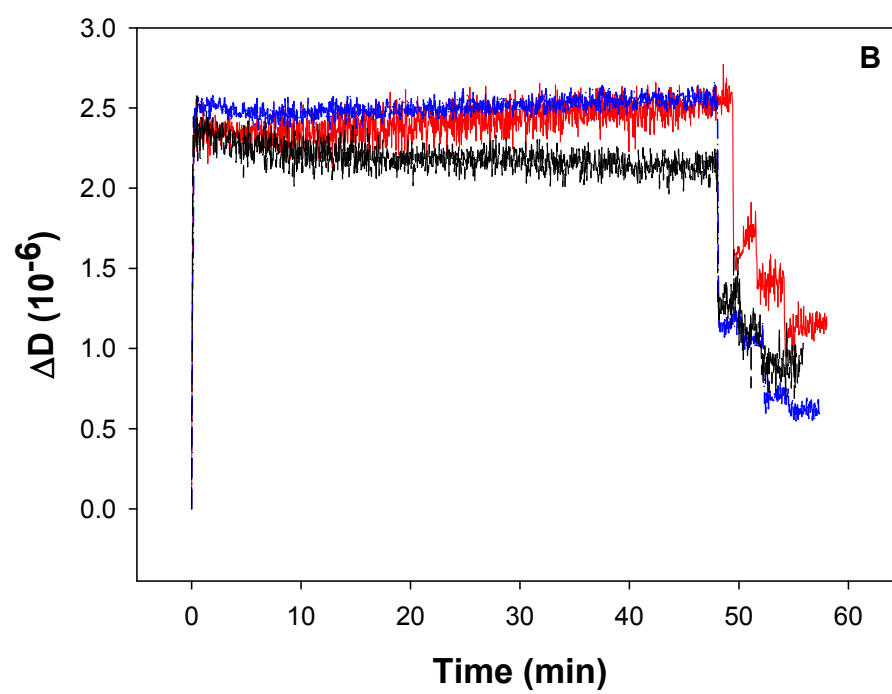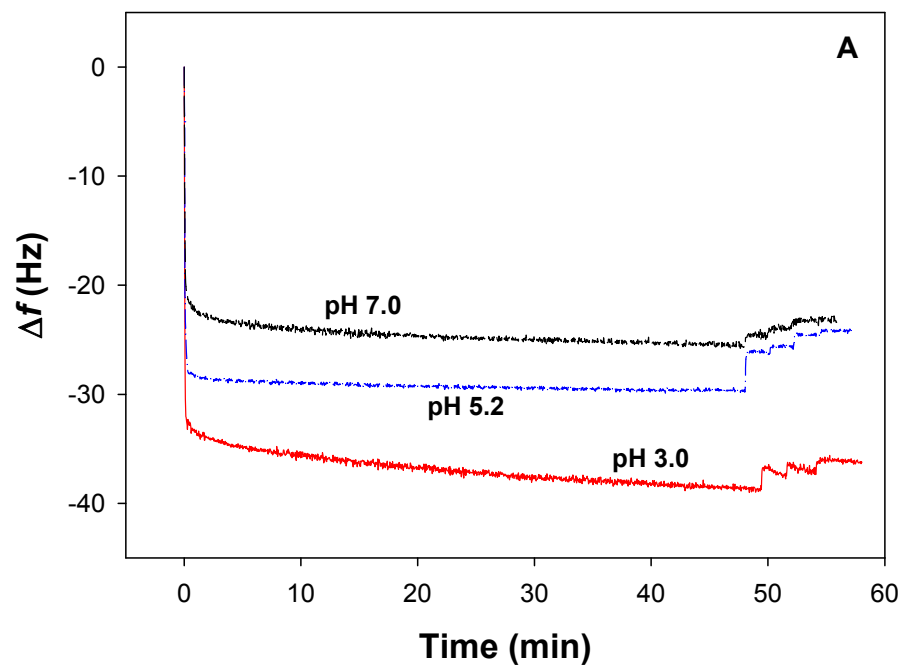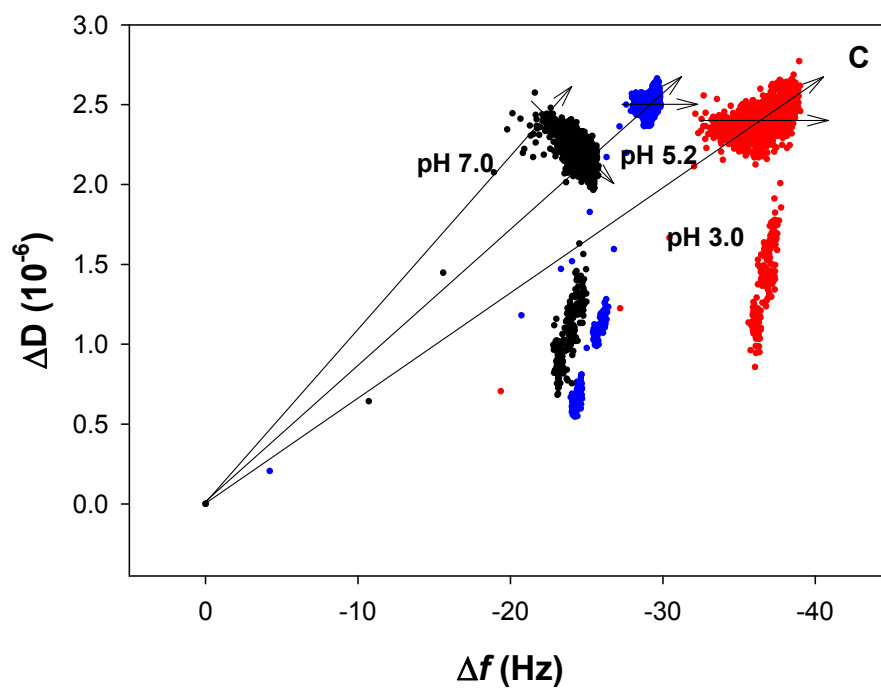
Figure 3.12. (A) Frequency shift (Δ*f*) and (B) dissipation shift (Δ*D*) induced by the adsorption of 1% β-lactoglobulin solutions at three pHs (3.0, 5.2, and 7.0) as a function of time, and (C) Δ*D* - Δ*f* plots using data (A) and (B).

Figure 3.12.A and B show the plots of Δf and ΔD as a function of time for the pH dependent adsorption of 1% β-lactoglobulin solution. The magnitude of Δf in the adsorption of 1% of β-lactoglobulin increased with the decrease of pH of the protein solutions. However, the effects of pH on the dissipation shifts at saturation point were not different significantly, as shown in Figure 3.12.B. From Figure 3.12.A, one notes that the Δf of β-lactoglobulin at pH 3.0 didn't reach the plateau after 50 mins from the onset of the adsorption. Instead, it kept decreasing with the adsorption time without changing the energy dissipation. This result suggested that the protein layers might be formed continuously and completely at the polymeric surface. The magnitude of Δf increases with decrease the pH of solution. As shown in Figure 3.12.C, the initial slopes in ΔD - Δf plots are 0.110 for pH 7.0, 0.086 for pH 5.2, and 0.062 for pH 3.0 of β-lactoglobulin solution.

A)
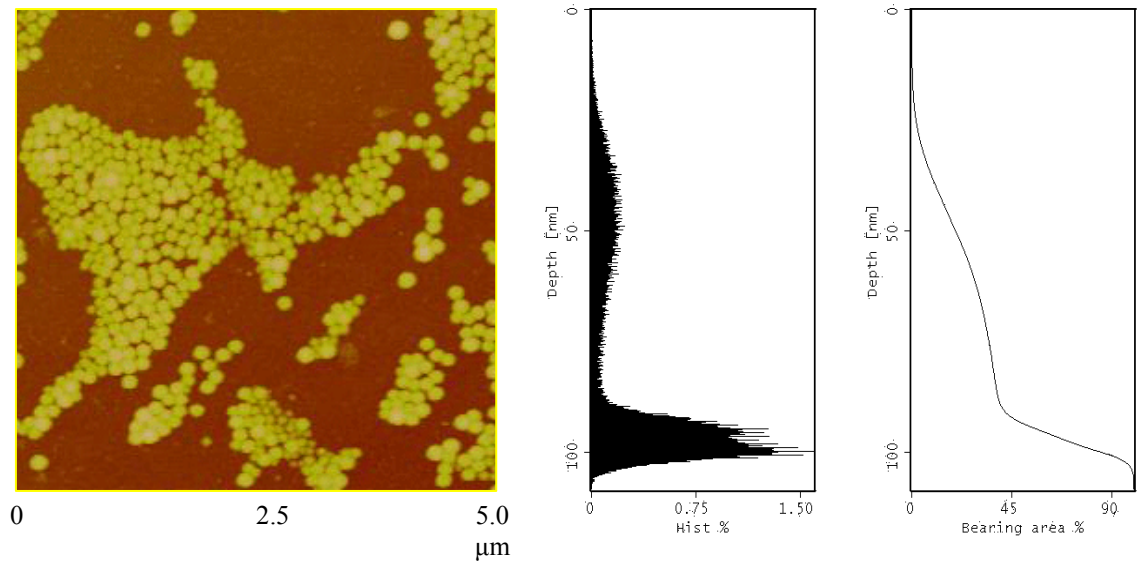
B)
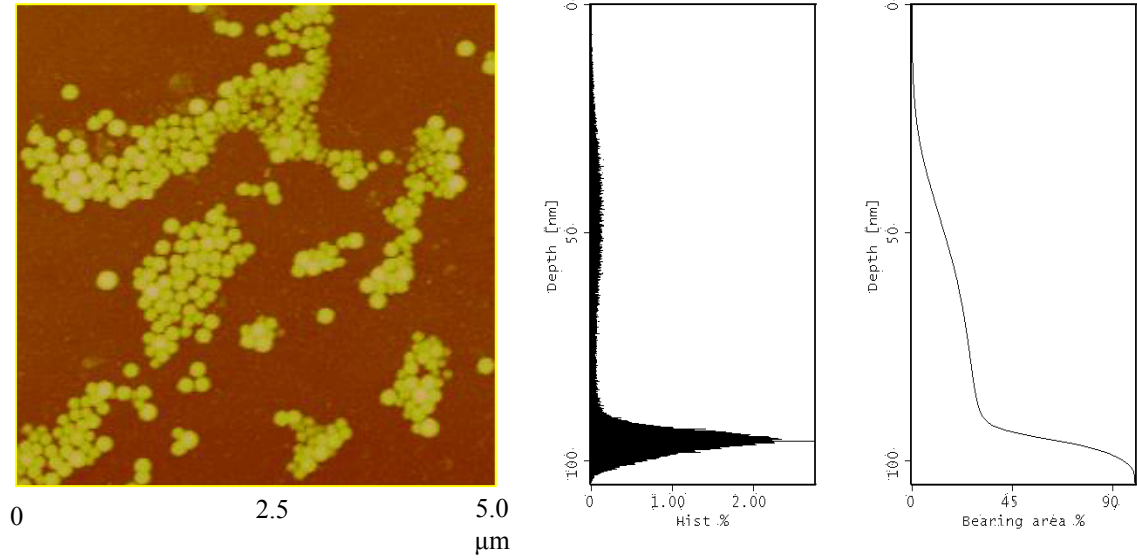
C)
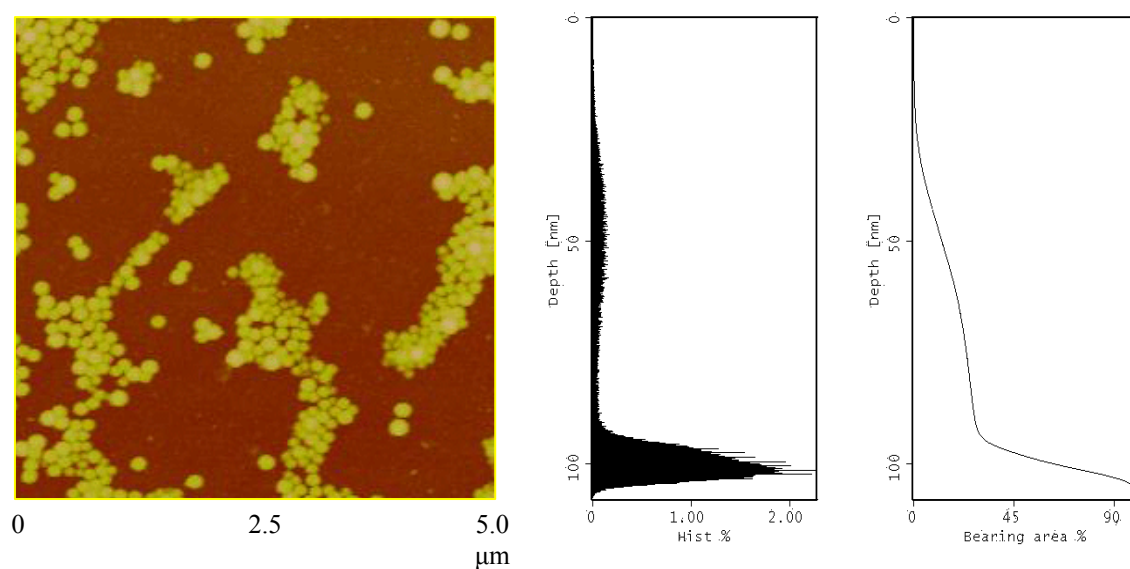
Figure 3.13. Tapping mode AFM images and height distribution of the PES coated crystal surface after 1% (w/v) β-lactoglobulin adsorption (A) at pH 3.0, (B) at pH 5.2, and (C) at pH 7.0.

Figure 3.13 shows the tapping mode AFM images and height distribution of 1%

β-lactoglobulin adsorbed polymer surface varying with the pHs of protein solutions: A) pH

3.0, B) pH 5.2, and C) pH 7.0. β-Lactoglobulin adsorption on the PES surface appeared to

be randomly distributed on the PES modified surface. At pH 7.0, the proteins covered less

surface area comparing to the case of lower pH where a larger surface area was covered by

protein molecules. In order to investigate how much surface area was covered by protein

molecules, the surface coverage was obtained by bearing analysis. Bearing analysis could

reveal that what percentage of surface area was above and below any arbitrarily chosen

height. When bearing depth is 70 nm, the surface coverage of the protein adsorbed surfaces

at pH 3.0, 5.2 and 7.0 were 32.9%, 23.9%, and 22.4%, respectively. The surface coverage

at pH 7.0 and pH 5.2 are not significantly different but the higher surface coverage at pH

3.0 supports that more protein molecules were adsorbed on the PES modified surface.

These AFM images generally supported the QCM-D data that the Δf of β-lactoglobulin at

pH 3.0 didn't reach the plateau within 50 min after injection of the protein solution but kept

decreasing without any more dissipation changes. These results could be explained by the

structure change of β-lactoglobulin depending on the pH of protein solution. At the acidic

condition (pH 3.0), the dominant structure of β-lactoglobulin might be monomer structure

by dissociation of dimer units. The hydrophobic interaction between PES surface and

monomeric units of β-lactoglobulin might increase the amount of the protein adsorption. In

this case, the interaction between protein and PES surface is higher than the interaction in

proteins themselves.

3.4.2.4. Viscoelastic Properties of The Protein Adlayer

We used the Voigt based viscoelastic model, which imposed specific frequency and dissipation on the storage modulus and loss modulus to examine the viscoelastic properties of β-lactoglobulin thin layer adsorbed on the PES-coated surface. The information on the viscoelastic properties of the adsorbed protein layer can be used in assisting the development of cleaning methods and optimizing the processing conditions to prevent or reduce protein adsorption and membrane fouling. Table 3.5 shows the viscosities and the elasticities of the adsorbed protein layer at three different concentrations. The obtained values at various concentrations of β-lactoglobulin ranged from 0.0023 to 0.01 kg/ms for viscosity, from 0.100 to 0.918 MPa for elasticity, and from 3.171 to 6.213 nm for thickness of the adlayer. The thickness of the adlayer increased with increase in concentration of the protein solution but both viscosity and elasticity of the adlayer decreased with increase in concentration. At 0.1% (w/v) of protein solution, the viscosity and elasticity of the β-lactoglobulin adlayer were 0.010 ± 0.001 kg/ms and 0.918 ± 0.334 MPa, respectively. These values were almost twice of those (0.0045 ± 0.0004 kg/ms and 0.555 ± 0.284 MPa) at 1.0% (w/v) and five to nine times of those (0.0023 ± 0.0001 kg/ms and 0.100 ± 0.001 MPa) at 2.0 % (w/v) of protein solution. Even if the adsorbed mass and thickness at lower concentrations were small compared with those at higher concentrations, the viscosity and elasticity of the protein adlayer were much higher at lower concentrations. This indicated that the β-lactoglobulin adlayer at lower concentrations were more completely adsorbed and relatively rigid due to the strong interactions between proteins and the polymer surface. Therefore, it was hard to remove by the rinsing step.

Table 3.5. The viscosities and elasticities of β-lactoglobulin adlayers at various concentrations (0.1, 1.0, and 2.0% (w/v)) after four times of rinsing.

Concentration	Viscosity (kg/ms)	Elasticity (MPa)
0.1%	0.0100 ± 0.0010	0.918 ± 0.334
1.0%	0.0045 ± 0.0004	0.555 ± 0.284
2.0%	0.0023 ± 0.0001	0.100 ± 0.001
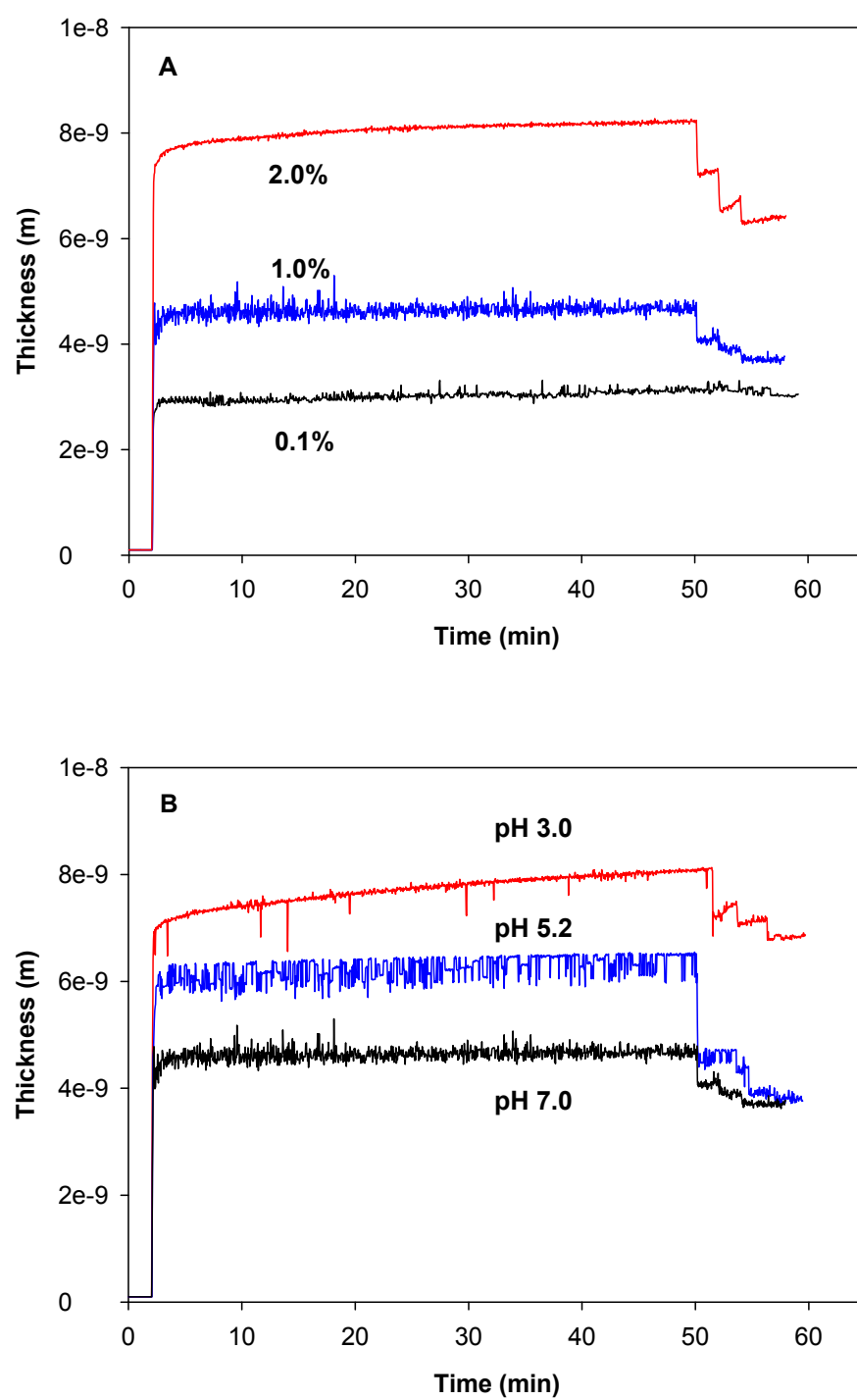
Figure 3.14. The thickness of the β-lactoglobulin adlayers at concentrations (A) and pHs (B).

Figure 3.14 show the thickness changes of the β-lactoglobulin adsorbed layers as a function of adsorption time at various concentrations (A) and pHs (B). In case of (A), the solution pH was 7.0 and in case of (B), the concentration of β-lactoglobulin was 1.0%. The thickness of protein layer adsorbed on PES modified surface increased from 2 nm to 6 nm with the protein concentration from 0.1% to 2.0% after rinsing steps. The thickness also increases from 3.6 nm to 6.5 nm with decrease the pHs from 7.0 to 3.0. Although the thickness of 2.0% protein at pH 7.0 is a little higher than the thickness of 1.0% protein at pH 3.0 before rinsing steps, it is reversed after rinsing four times. As shown in Figure 3.14, the amount of reversible protein is depending on the protein concentration but not depending on the solution pH. This result support that the major interaction in higher concentration is the interaction in proteins themselves which could be recovered easily by rinsing steps but the major interaction in acidic condition is the interaction between protein and PES surface which could not be recovered easily by rinsing steps.

Figures 3.15 shows the adsorbed masses calculated by the Sauerbrey equation and by the Voigt based viscoelastic model at different concentration (Figure 3.15.A) and different pH values (Figure 3.15.B). Since the amount of the adsorbed mass was intimately related to the decrease the permeation flux in the membrane filtration and to the formation of the fouling, the accurate mass of the adsorbed protein layer should be examined. We denoted the adsorbed masses calculated by the Sauerbrey equation as Sauerbrey mass (S-Mass) which is only based on the frequency change and by the Voigt based viscoelastic model as Voigt mass (V-Mass) which is based on both the frequency change and dissipation change. The V-Masses are usually higher than the S-Masses because of the

dissipation effect. The ratios of V-Mass to S-Mass increased with protein concentration because the dissipation changes also increased with protein concentration. As shown in Figure 3.15.A, there is a little difference (less than 10%) between S-Mass and V-Mass at lower concentrations below 1.0% but the difference between S-Mass and V-Mass at 2.0% protein solution is significantly increased by about 50% due to the higher dissipation shift in 2.0% concentration. With the higher concentration, the adsorbed protein layers might be more hydrated and softer and formed as a multilayer. Although the difference between S-Mass and V-Mass increased with decreasing the solution pHs, the ratios of V-Mass to S-Mass are not significantly changed with the solution pHs because dissipation shifts were not significantly changed with pH changes (Figure 3.15.B).
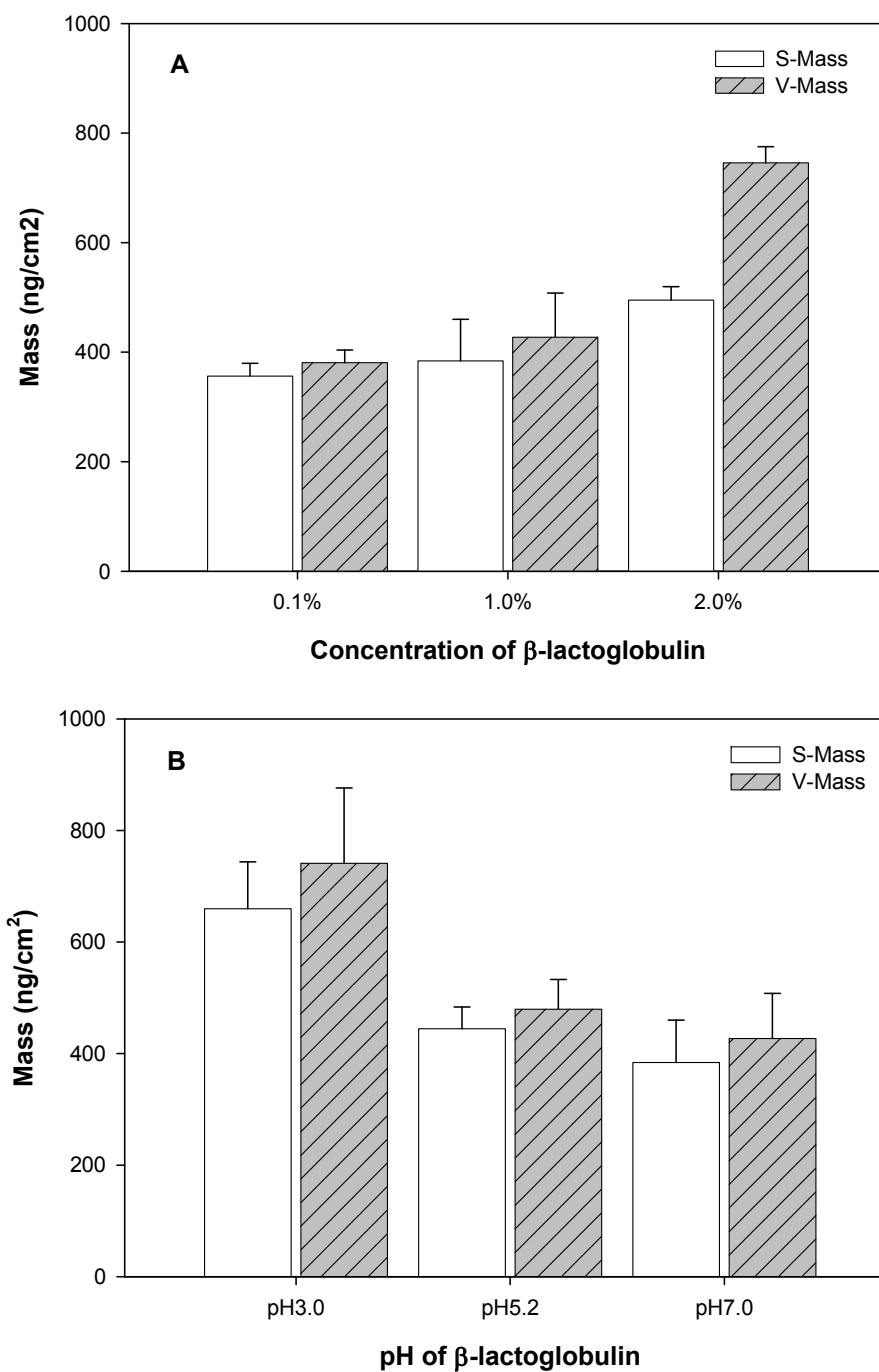
Figure 3.15. The dependence of adsorbed mass on the protein concentration (A) and pH (B). S-Mass is the mass obtained by the Sauerbrey equation and V-Mass is the mass obtained by Voight based viscoelastic model.

3.5. Summary

Static and dynamic adsorption of β-lactoglobulin on PES surface was investigated using UV-spectrophotometer and QCM-D, respectively. In static adsorption experiments, Freundlich isotherm model was used to fit the data and to obtain the isotherm parameters such as K_F and $1/n$. Based on the data of the static adsorption process, the amount of adsorption was highest at the acidic pH (pH 3.0) where is below the isoelectric point of β-lactoglobulin due to the electrostatic attraction and the interactions by the dissociation of β-lactoglobulin from dimer to monomeric unit. On the other hand, the amount of adsorption was lowest at the neutral pH (pH 7.0) due to the electrostatic repulsion. Although the electrostatic repulsion is still strong, the adsorption at the alkaline condition (pH 9.0) was higher than that at the isoelectric point. This result supports that the interactions by the dissociation of β-lactoglobulin are higher than the electrostatic repulsion so the adsorption of β-lactoglobulin increased in the alkaline condition. The addition of salt reduced the adsorption of β-lactoglobulin on PES because the salt ions interact with the charged protein molecules.

In dynamic adsorption experiments, we have investigated the adsorption process of β-lactoglobulin on PES-coated quartz crystal surface and the viscoelastic properties of the adsorbed β-lactoglobulin layer using quartz crystal microbalance with dissipation monitoring (QCM-D). The QCM-D data in various protein concentrations and pHs showed similar trends in the adsorption processes; the frequency shift (Δf) and dissipation shift (ΔD) changed rapidly and greatly after the injection of the β-lactoglobulin solutions, followed by minor changes with the adsorption time until the rinsing steps. The adsorption of protein on the membrane polymer surface consisted of reversible and irreversible

adsorptions. Because irreversible adsorption was the main factor that causes permanent membrane fouling, the information on the mass and viscoelastic properties of the irreversibly adsorbed protein layers were important to optimize the process condition to reduce the membrane fouling. AFM images revealed that β-lactoglobulin adsorption was not homogeneously but randomly distributed on the PES surface. The protein molecules could cover more polymer surface area at acidic condition where the dominant structure of β-lactoglobulin is monomer.

From the QCM-D results the Δf of β-lactoglobulin depended on both protein concentration and pH of the solution, but the ΔD depended only on protein concentration. These results suggested that the amount of adsorbed mass could be affected by concentration and pH of the β-lactoglobulin solution, but the viscoelastic properties of the protein thin layer were mainly altered by the concentration of protein solution.

CHAPTER IV. DEVELOPMENT OF NOVEL MEMBRANES TO REDUCE THE PROTEIN ADSORPTION BY SURFACE MODIFICATION

4.1. Introduction

Many researchers have revealed that increasing the hydrophilicity of membranes significantly reduced the membrane fouling (Musale and Kulkarni, 1996; Hester et al., 1999) because of the decrease of the hydrophobic interaction between protein and membrane surface. With aqueous feed streams, the ideal membrane to minimize fouling is hydrophilic membrane. Unfortunately, the most commercial membranes are relatively hydrophobic because hydrophilic membranes have some drawbacks in their mechanical, thermal, and chemical stability. Hydrophobic polymeric membranes have been commonly used in ultrafiltration system to concentrate and fractionate the protein.

Surface modification of polymeric membrane plays an important role in the membrane performance such as permeation flux, efficiency, and selectivity. By surface modification, two distinct layers were made of two different polymeric materials. The thin surface layer governs the selectivity, flux, and adsorption of solute while the thick substrate layer provides the mechanical strength and chemical stability. The incorporation of hydrophilic polymer through blending (Rajagopalan et al., 2004; Wang et al., 2006), coating (Wei et al., 2005), and surface grafting (Ulbricht and Riedel, 1998; Song et al., 2000; Kim et al., 2002) has been developed to improve the protein adsorption resistance and permeation property of polymeric membranes. Surface modification of hydrophobic membrane to hydrophilic can reduce the hydrophobic interaction between protein and the

polymeric membrane surface, so it can reduce the amount of protein adsorption and membrane fouling.

In this study, poly(vinyl alcohol) (PVA), poly(ethylene glycol) (PEG), and chitosan were used as hydrophilic polymers for grafting due to their excellent hydrophilicity. Poly(vinyl alcohol) has been well known for its excellent film forming property, emulsifying property, and minimal cell and protein adhesion property (Shukla et al., 2005, Peppas and wright, 1998). PVA is also resistant to oil and solvent. Poly(ethylene glycol) showed extraordinary antifouling property to protein adsorption due to its hydrophilicity, flexible long chains, large exclusion volume, and unique coordination with surrounding water molecules in an aqueous solution (Wang et al., 2006). Chitosan is a linear polyelectrolyte carrying positive charges and has been identified as a non-toxic, biodegradable, biocompatible, and hydrophilic polysaccharide. Chitosan based membranes have been used for protein separations (Zeng and Ruckenstein).

4.2. Experimental Rationale and Design

The extent of protein adsorption depends on the various types of interactions between protein molecules and membrane surface such as van der Waals interaction, electrostatic interactions, hydrophobic interaction, dipole-dipole interaction, and hydrogen bonding (Hamza et al., 1997). One of the main factors enhancing the protein adsorption on the polymeric membrane is hydrophobic interaction between the membrane surface and protein molecules. Therefore, protein adsorption on the polymeric membrane can be reduced by modification of hydrophobic membrane surface to hydrophilic surface. It is

also easy to clean the hydrophilic membrane because the adsorbed protein molecules can be easily removed from the hydrophilic surface (Kim et al., 2002).

The hydrophilic polymer grafting using UV/Ozone and the thin film composite (TFC) by interfacial polymerization were studied to improve the hydrophilicity of the PES membrane surface. The polymer grafting methods have been shown to be successful in increasing the surface hydrophilicity and the permeability and decreasing the membrane fouling during the protein filtration (Thom et al., 1998; Kilduff et al., 2000; Pieracci et al., 2002). Among various physical methods for the initiation, UV/Ozone treatment is very easy, fast, and low cost way to activate the polymeric membrane surface. Interfacial polymerization is a powerful technique for fabrication of composite membranes having a very thin active layer. Although it had been used for the membranes of reverse osmosis, interfacial polymerization technique can also be useful for nanofiltration and ultrafiltration (Korikov et al., 2006; Zhao et al., 2006). Interfacial polymerization technique is based on a polycondensation reaction which takes place at the interface between two immiscible phases (one is organic solvent and the other one is water phase). A very fast polymerization reaction often occurs between two very reactive monomers at the interface of two immiscible solvents each containing one of the monomers (polyamine in water phase and polyacyl chloride in organic solvent), and the polymer precipitates quickly, forming a thin dense polyamide film (Kemperman et al., 1998; Chu et al., 2005; Song et al., 2005). Because the thin active layers formed by interfacial polymerization contain hydrophilic polymers, it can reduce the protein adsorption and membrane fouling.

4.3. Materials and Methods

4.3.1. Materials

The flat sheet ultrafiltration membrane, polyethersulfone (PES) (YMPWSP3001), was purchased from Sterlitech Corporation (Kent, WA). MWCO of flat sheet PES membrane is 20,000. Terephthaloyl chloride (TC), *m*-phenylenediamine, polyethylene glycol (PEG) 2000, and poly(vinyl) alcohol (PVA) were purchased from Sigma-Aldrich (St. Louis, MO). Chitosan (MW 300,000, DOD 90%) was purchased from Kunpoong Bio Co., Ltd. (Jeju, South Korea). UV/Ozone cleaner (Jelight Company, Irvine, CA) was used to activate the PES membrane surface for grafting of the hydrophilic polymers on the membrane surface.

4.3.2. Grafting Polymerization Using UV/Ozone

Hydrophilic polymers grafting using UV/Ozone treatment is the combination of physical and chemical modification. Although it is powerful way to improve the hydrophilicity of polymeric membrane, physical modification such as plasma and ion beams could be recovered the surface property over time. Chemical reaction should be followed after physical modification to maintain and improve the hydrophilicity of polymeric membrane. UV/Ozone treatment was carried out to initiate and activate the PES membrane surface for hydrophilic polymers grafting. The dried small piece of PES flat membrane was exposed to UV/Ozone treatment for 1 min to 30 min. Peroxide groups could be formed on the activated membrane surface by ozone treatment. The peroxide groups generated on the membrane surface can react with hydrophilic polymers such as

PVA, PEG, and chitosan. 20% (w/v) PVA, 20% (w/v) PEG $_{2000}$, and 1% (w/v) chitosan

(molecular weight is 300,000) solution were used to react with the activated PES

membranes. The hydrophilic polymer grafting reaction was performed in a glass ampoule

at 70℃ for 2 hr and the chemical schemes are shown in Figure 4.1. After grafting reaction

with hydrophilic polymers, the PES membranes were rinsed with distilled water for 24 hr

to remove excess hydrophilic polymers from the PES membrane surface. Then, the

hydrophilic polymer grafted PES membranes were dried at room temperature under the

vacuum condition.
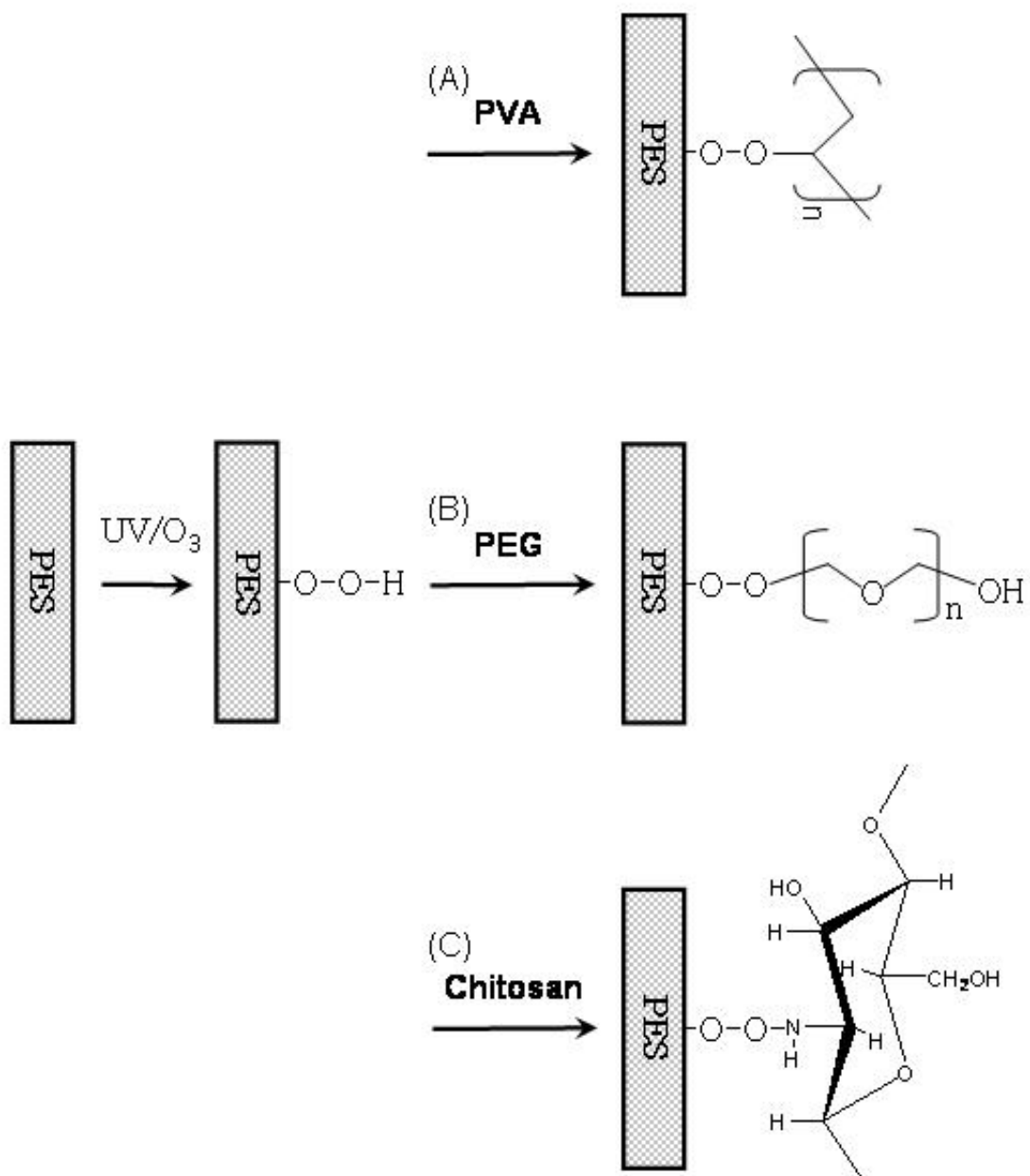
Figure 4.1. Reaction schemes of the hydrophilic polymers grafting onto the PES membrane activated by UV/Ozone treatment: (A) PVA, (B) PEG, and (C) Chitosan.

4.3.3. Thin Film Composite by Interfacial Polymerization

The second surface modification of PES membrane was carried out by fabricating hydrophilic polymers/polyamide thin layer on the PES membrane surface by the interfacial polymerization method. Interfacial polymerization is a powerful method for fabrication of composite membranes with very thin active layer (usually 10 to 20 nm). The schematic of the interfacial polymerization is shown in Figure 4.2. The polymeric membranes were immersed in 1% (w/v) terephthaloyl chloride (TC) in benzene for 20 min. After 20 min, the membranes were exposed in the aerator for one minute to remove the excess TC solution from the membrane surface. Then, membranes were then immersed into the aqueous solution containing *m*-phenylenediamine and hydrophilic polymers such as PVA, PEG, and chitosan to form a composite membrane surface layer by interfacial polymerization. The fabricated PES membranes were rinsed with deionized water and then dried at room temperature for 24 hr.

94
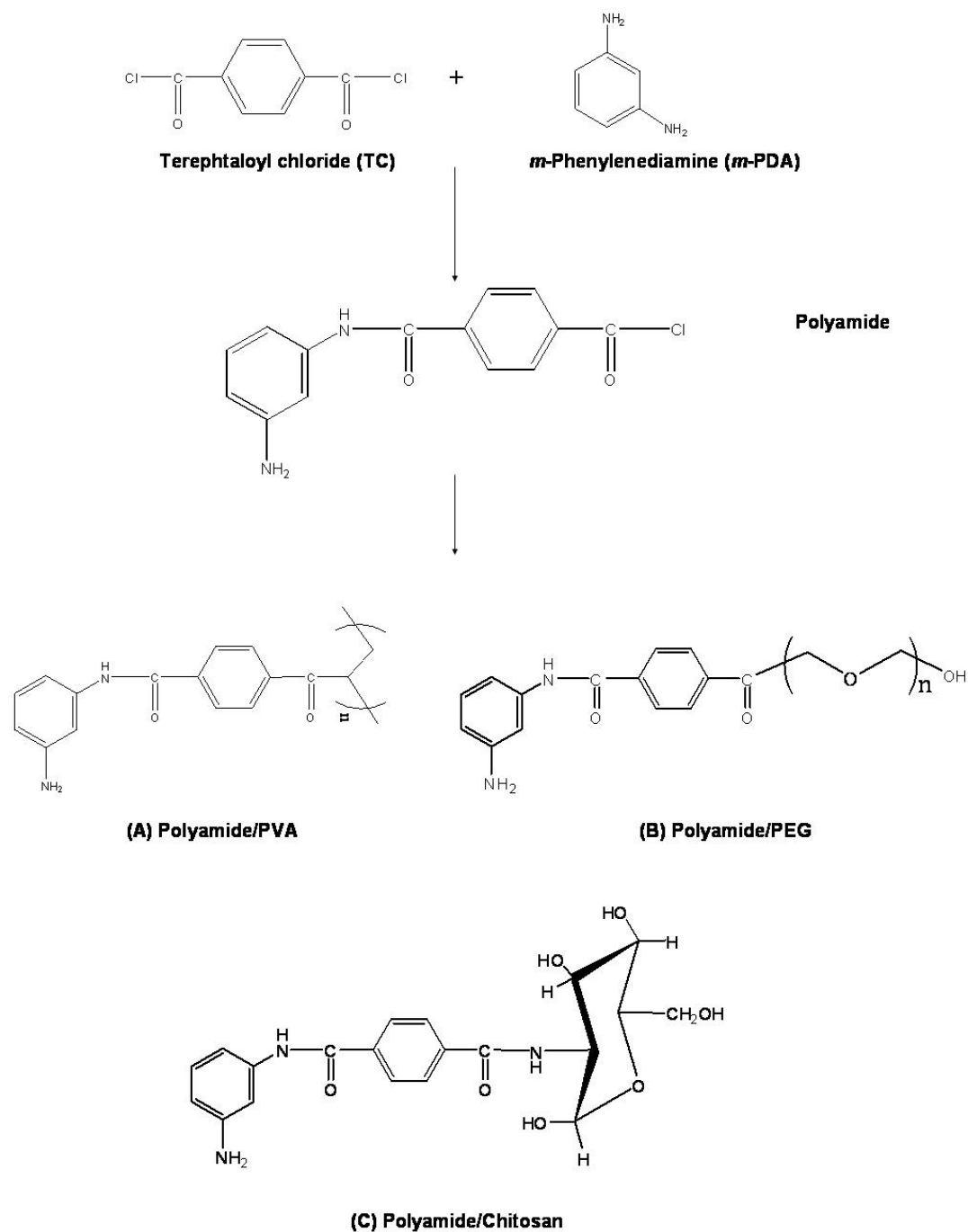
Figure 4.2. Reaction scheme for preparation of the composite membranes with hydrophilic polymers by interfacial polymerization: (A) PVA/polyamide, (B) PEG/polyamide, and (C) Chitosan/polyamide.

Table 4.1 Experimental design for surface modification of PES membrane

Sample NO	Description of modification ways
NO 1	Virgin PES membrane
NO 2	UV/Ozone for 20 min and 20% PVA grafting
NO 3	UV/Ozone for 20 min and 20% PEG $_{2000}$ grafting
NO 4	UV/Ozone for 20 min and 1% Chitosan grafting
NO 5	Interfacial polymerization and 1% PVA
NO 6	Interfacial polymerization and 1% PEG $_{2000}$
NO 7	Interfacial polymerization and 1% Chitosan

4.3.4. Characterization of Modified PES Membranes

In order to understand the interactions between the modified membrane surface and protein molecules, it is important to have good knowledge of the various surface properties of the modified PES membranes. The surface topography, roughness, wettability, and chemical composition of modified PES membranes were characterized using AFM, contact angle, and XPS. ATR-FTIR was used to characterize the modified functional groups on the PES membrane surface.

4.3.4.1. Contact Angle Measurement

The contact angles of the unmodified and modified PES membranes were measured using the sessile drop method on a VCA Optima surface analysis system. A 28 gauge blunt-tip needle was attached to a VCA Optima mechanically controlled micrometer for dispensing a 2 µL deionized water droplet onto the surface of membrane samples. Five measurements were made for each sample and used to determine the average and standard deviation for the data.

4.3.4.2. ATR-FTIR Spectra

ATR-FTIR spectra of unmodified and modified PES membranes were measured using a Thermal Nicolet Nexus 670 FTIR system with an ATR accessory. The ATR accessory contained a ZnSe crystal (25 mm x 5 mm x 2 mm) at a nominal incident angle of 45°, yielding about 12 internal reflections at the sample surface. All spectra were recorded with 256 scans at 4.0 cm^{-1} resolution at room temperature.

4.3.4.3. Electron Spectroscopy for Chemical Analysis (ESCA)

ESCA (electron spectroscopy for chemical analysis), also known as XPS (x-ray photoelectron spectroscopy), is a powerful technique for characterizing the chemical composition of the top few atomic layers at the surface of a solid. A beam of X-rays impinging on a surface causes the ejection of electrons from core levels in the atoms due to the photoelectric effect as shown in Figure 4.3. When a monochromatic source of X-rays of known energy (1253.6 eV for Mg $K\alpha$ and 1486.6 eV for Al $K\alpha$) is used, the binding energy can be determined if the kinetic energy of the electrons is measured. The kinetic energy of the ejected electrons is equal to the difference between the energy of the X-rays and the binding energy, E_b:

$$E_k = h\upsilon - E_b \qquad\qquad\qquad (4\text{-}1)$$

in where v is the wavelength of the incident photons, E_b is the energy of the core level from which the electron is ejected. ESCA can not only give the elemental composition of a surface (C, O, N, S etc) but also provide insights into the chemical bonding at the surface. XPS is a highly surface specific analytical technique used to obtain the chemical structure and atomic composition of a material.

XPS spectra of virgin and modified PES membranes were recorded with a Kratos XSAM 800 X-Ray Photoelectron Spectrometer using a monochromatic Al $K\alpha$ X-ray source (1486.6 eV photons) at 350 W and 15 kV. The take off angle was 90°. Analysis of the high-resolution XPS spectra for unmodified and modified PES membranes was based on the reference (Beamson and Briggs, 1992). In all cases, a Gaussian peak shape was used

and the analyses were performed with the binding energies and full-width-at-half-mazima (fwhm) of the peaks kept constant at the literature values but with the intensities varied.

4.3.4.4. Atomic Force Microscopy (AFM)

The surface topography and phase imaging of modified PES membrane were characterized using tapping mode atomic force microscope (Multimode SPM, Nanoscope IIIa, Digital Instruments) with a silicon probe. Several specimens were scanned in different areas in order to analyze their morphologies.

4.3.5. Protein Adsorption on Modified PES Membranes

Static adsorption of β-lactoglobulin on the modified PES membrane surface was studied using UV-Vis spectrophotometer via the absorbance at 280 nm to compare the decrease of the amount of protein adsorption by surface modification. For this study, the concentration of β-lactoglobulin was 2.5 mg/mL and solution pH was 3.0 where the maximum adsorption was observed in chapter III.
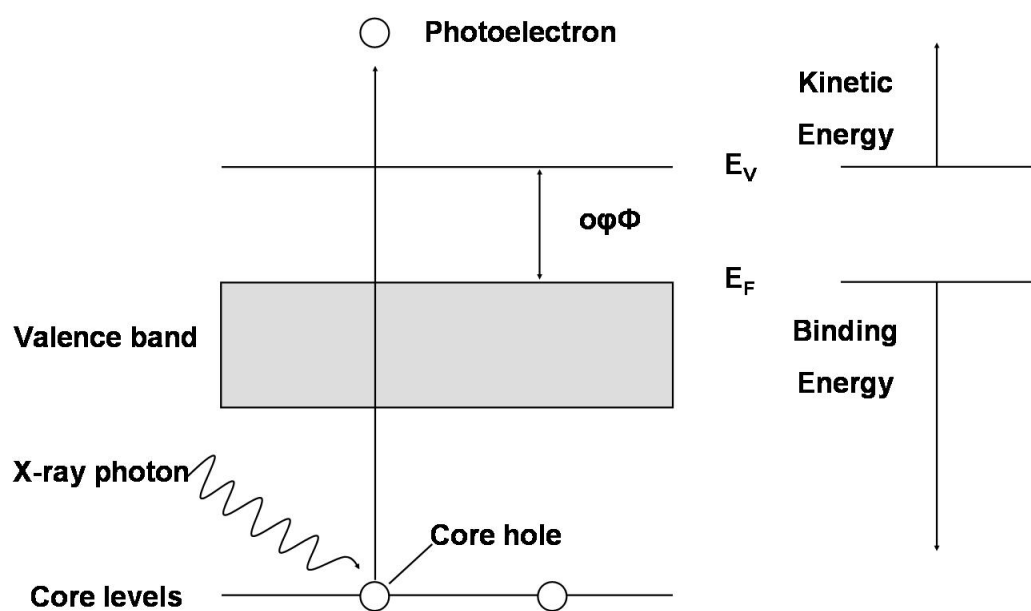
Figure 4.3. Photoelectric effect of XPS

4.4. Results and Discussion

4.4.1. Characterization of Virgin PES Membrane Using ATR-FTIR

In the commercial polymeric membrane manufacture processing, preservatives have commonly been used to stabilize membranes, to prevent the membranes from microbial attack, and to extend their shelf life. As shown in Figure 4.4.(A), preservatives present a very strong band at 3313 cm^{-1} and three bands at 1647, 1037, and 923 cm^{-1} which are the same spectra of the preservatives in previous research (Belfer et al., 2000). Preservatives were washed out with DI water and dried at room temperature for several days for characterization of the native PES membrane. All PES membranes used for surface modification are washed with DI water for 24 hr to remove preservatives and dried at room temperature. The spectra of the washed PES membrane have no strong band at 3400 cm^{-1}, which indicates the aliphatic C-H stretching but two small bands associated with aromatic C-H vibration are present at 3095 and 3069 cm^{-1} as shown in Figure 4.4. (B). There is no band at around 3500 to 3600 cm^{-1} which is associated with the O-H stretching vibration of water molecules, so this IR spectrum supports that PES membrane was dried completely after washing out the preservatives.
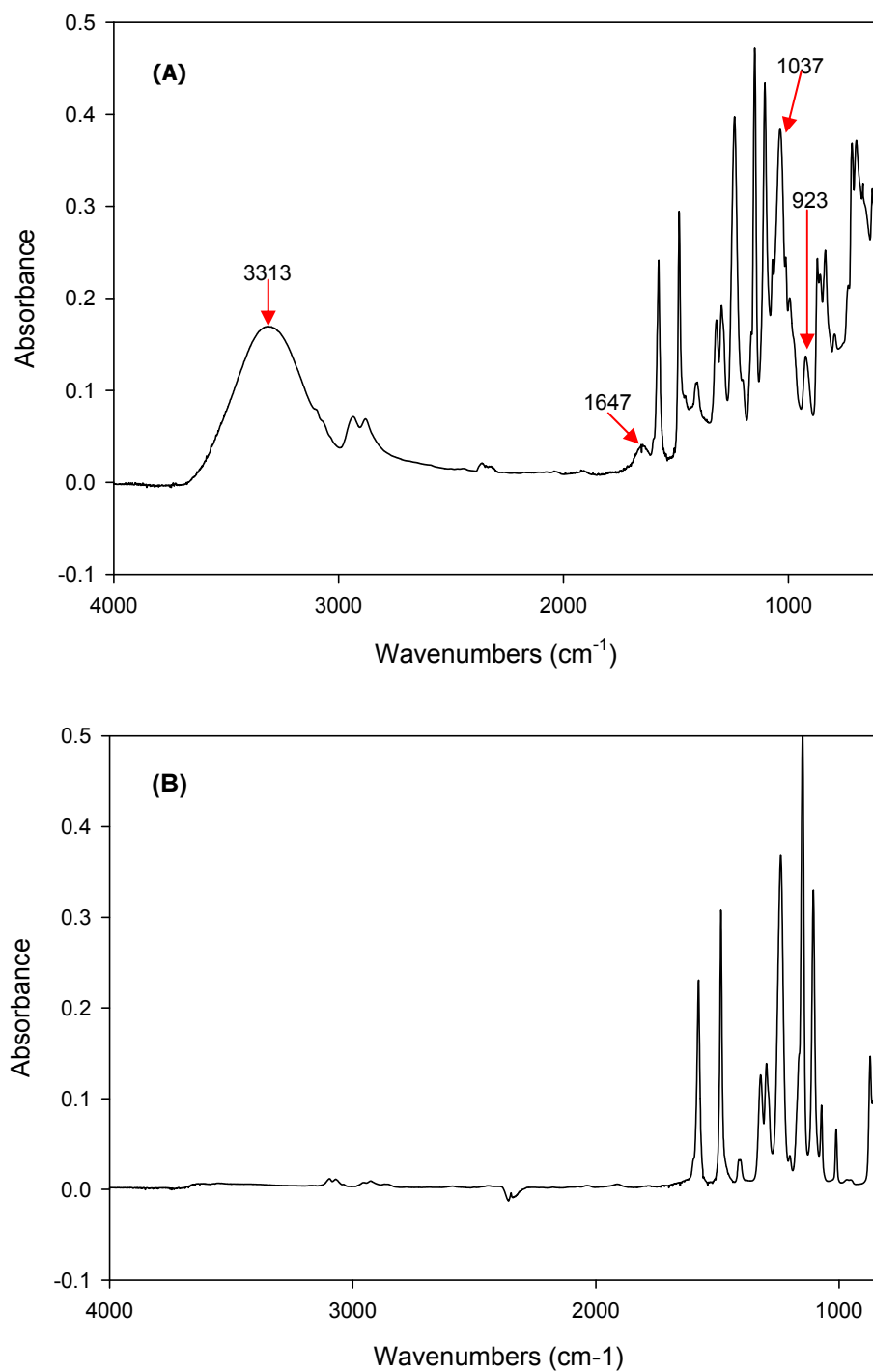
Figure 4.4. ATR-FTIR spectra of the PES membrane (A) before washing and (B) after washing with DI water.

4.4.2. Surface Recovery of UV/Ozone Treatment

Before the grafting reaction with hydrophilic polymers, UV/Ozone treatment was used to activate the membrane surface. However, physical modifications such as plasma, radiation, and ion beams treatments have a major drawback that the surface reactivity can be gradually deteriorated over time. To investigate the surface recovery of UV/Ozone treated PES membrane over time, the contact angle of PES membrane exposed to UV/Zone for 20 min was measured from 0 to 48 hrs. Figure 4.5 shows the recoveries of contact angle of UV/Ozone treated PES membrane over time. The contact angle of the PES membrane exposed to UV/Ozone for 20 min increased back from 11 degrees to 38 degrees in 48 hr. Since the contact angle of original PES membrane was 71 degrees, it could be recovered to the about 50 % of the original PES membrane in 48 hr. The rate of surface recovery decreased over time. Most recovery was occurred in 5 hr after UV/Ozone treatment. After 48 hr, the contact angle was rarely recovered anymore over time. Based on this result, all surface characterization was conducted after 48 hr with UV/Ozone treatment.

When the PES membrane treated by UV/Ozone was stored in air condition, the surface property like contact angle is not changed significantly after 48 hr. However, if the UV/Ozone treated PES membrane was exposed to solution, the contact angle of the PES membrane increased up to 60 degrees. So, the hydrophilic polymer grafting is necessary to prevent the recovery of the surface properties of PES membrane.
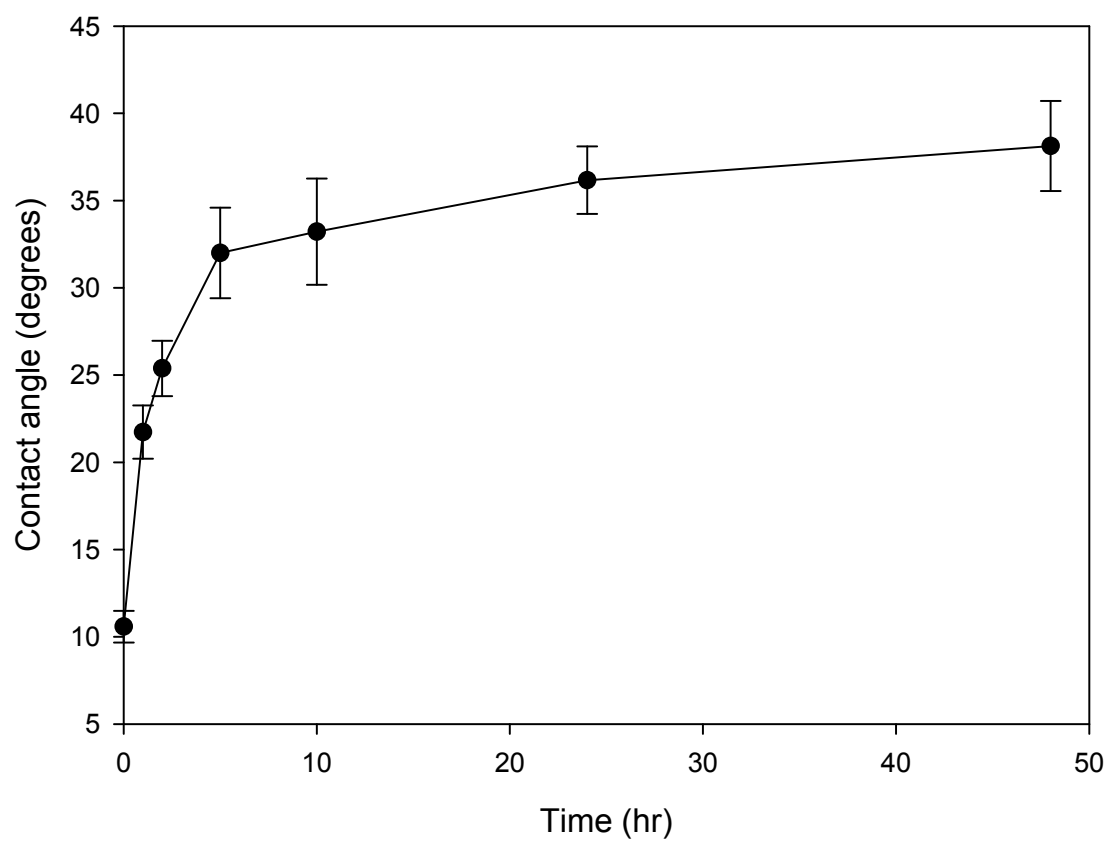
Figure 4.5. Contact angle recoveries of UV/Ozone treated PES membrane over time

4.4.3. Effect of UV/Ozone Treatment Time on Contact Angle

To optimize the UV/Ozone treatment time, contact angle was measured in 48 hr after UV/Ozone treatment from 0 min to 30 min. The contact angle of virgin PES membrane was about 71 degrees but the contact angle of UV/Ozone treated PES membrane decreases greatly with UV/Ozone treatment. As shown in Figure 4.6, the contact angle of PES membrane treated by UV/Ozone decreases continuously with UV/Ozone treatment time but it does not decrease anymore after 20 min. The contact angle of PES membrane decreased greatly within initial 5 min of UV/Ozone treatment and followed by slowly decrease with UV/Ozone treatment time. The contact angle of PES membrane treated by UV/Ozone for 20 min was almost half of the contact angle of the virgin PES membrane. UV/Ozone treatment for 20 min could decrease the contact angle of PES membrane to 36 degrees but it could be recovered after it was exposed to any solution. In order to prevent the recovery of hydrophilicity and maintain the hydrophilic properties of PES membrane activated by UV/Ozone, some hydrophilic polymers such as PVA, PEG, and chitosan were grafted after UV/Ozone treatment for 20 min.
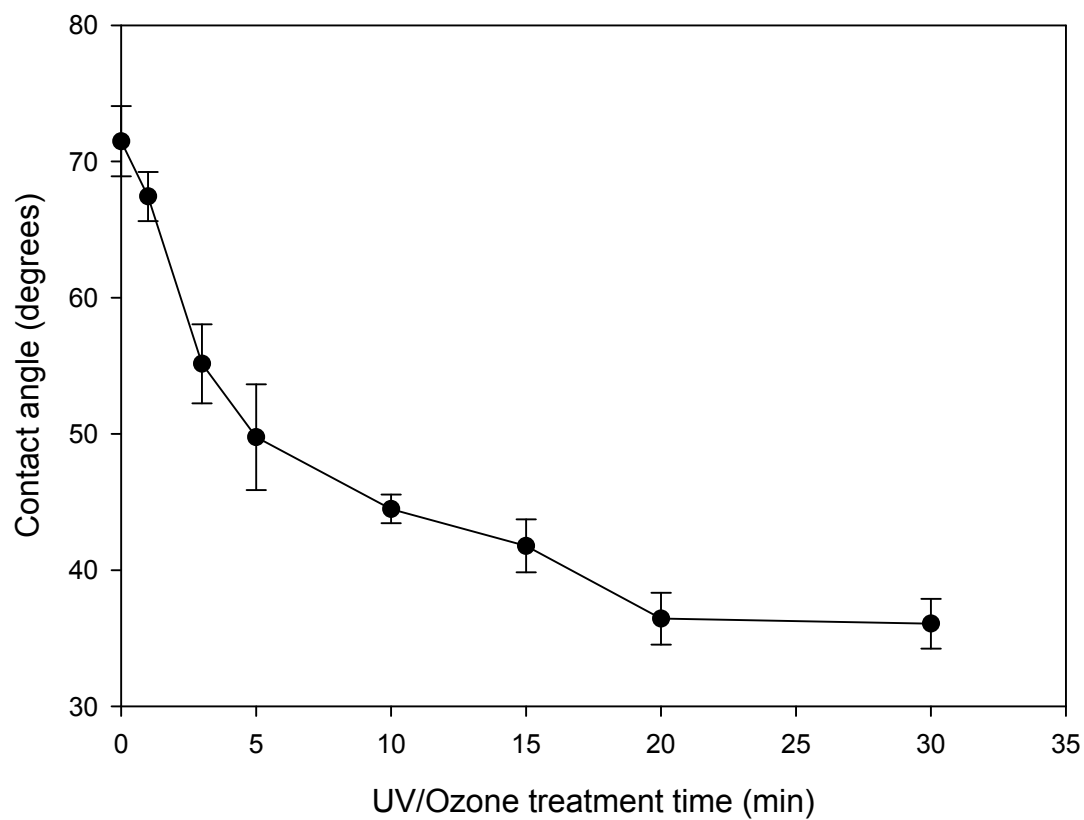
Figure 4.6. Contact angle of PES membrane in 48 hr after UV/Ozone treatment

4.4.4. Effect of Concentration of Hydrophilic Polymers

To initiate and activate PES membrane surface PES membrane was exposed to UV/Ozone and was followed by reaction with hydrophilic polymers. Since PES polymer can be photodegraded and oxidized by UV and ozone treatment (Rivaton and Gardette, 1999), a new peak was observed at 1728 cm^{-1} which is associated with C=O group after UV/Ozone treatment as shown in Figure 4.7. The intensities of this band at 1728 cm^{-1} increased as the UV/Ozone treatment time. This means that more PES membrane structure was degraded and could form more aldehyde C=O groups with increasing the UV/Ozone treatment time.

Figure 4.8 shows the FTIR spectra of Poly(vinyl alcohol) grafted PES membrane using UV/Ozone treatment. Pure poly(vinyl alcohol) have exhibited a broad band from 3600 cm^{-1} to 3650 cm^{-1} which may be attributed to stretching hydroxyl (-OH) group of free alcohol, a broad band from 2850 cm^{-1} to 3000 cm^{-1} which may be attributed to stretching alkyl C-H groups, and from 3200 cm^{-1} to 3570 cm^{-1} for hydrogen bonds (Peppas and Wright, 1996; Mansur et al., 2004). PVA grafted PES membrane have exhibited a broad band at 3312 cm^{-1} and at 2939 cm^{-1} which are assigned to stretching hydroxyl (-OH) group of free alcohol and stretching alkyl C-H group of PVA, respectively. The intensities of these bands at 3312 cm^{-1} and at 2939 cm^{-1} increased with PVA concentration. These observations suggested that hydrophilic PVA polymer should be effectively grafted on the PES membrane surface.

1728 cm⁻¹

20 min

10 min

5 min

3 min

1 min

Wavenumbers (cm⁻¹)
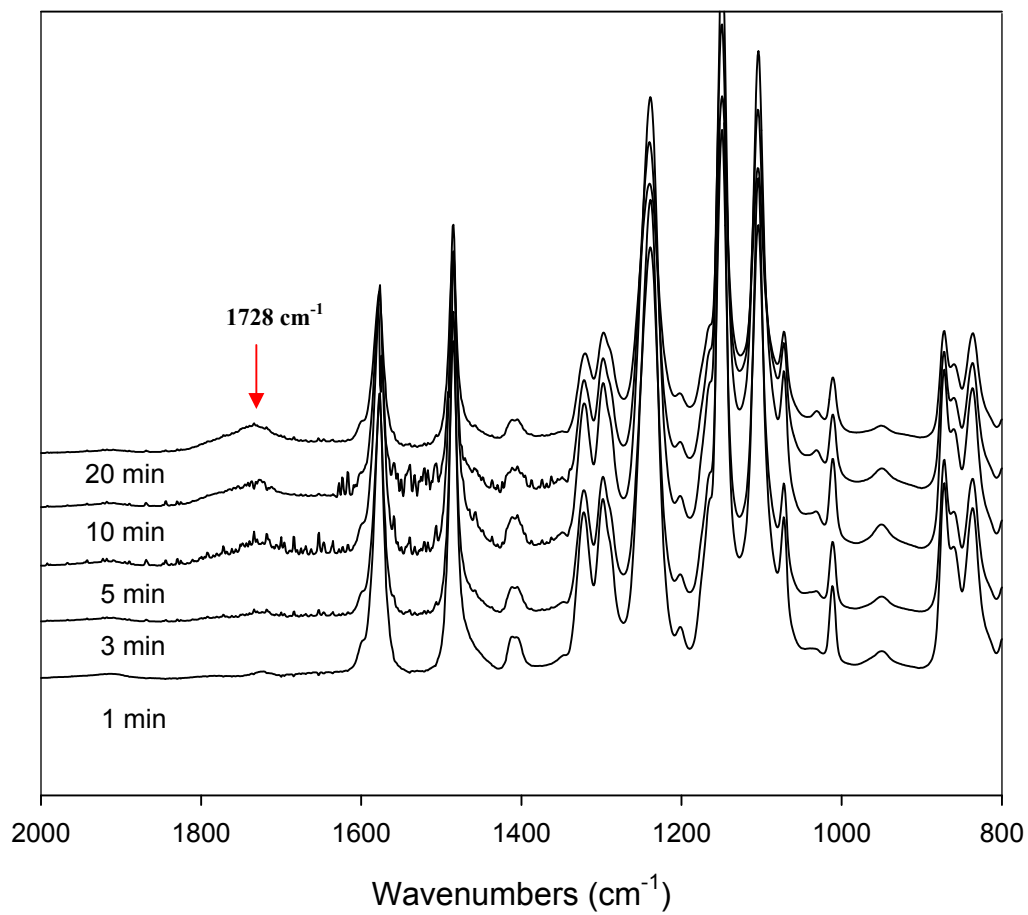
Figure 4.7 ATR-FTIR spectra of the PES membranes exposed to UV/Ozone for 1 min to 20 min.
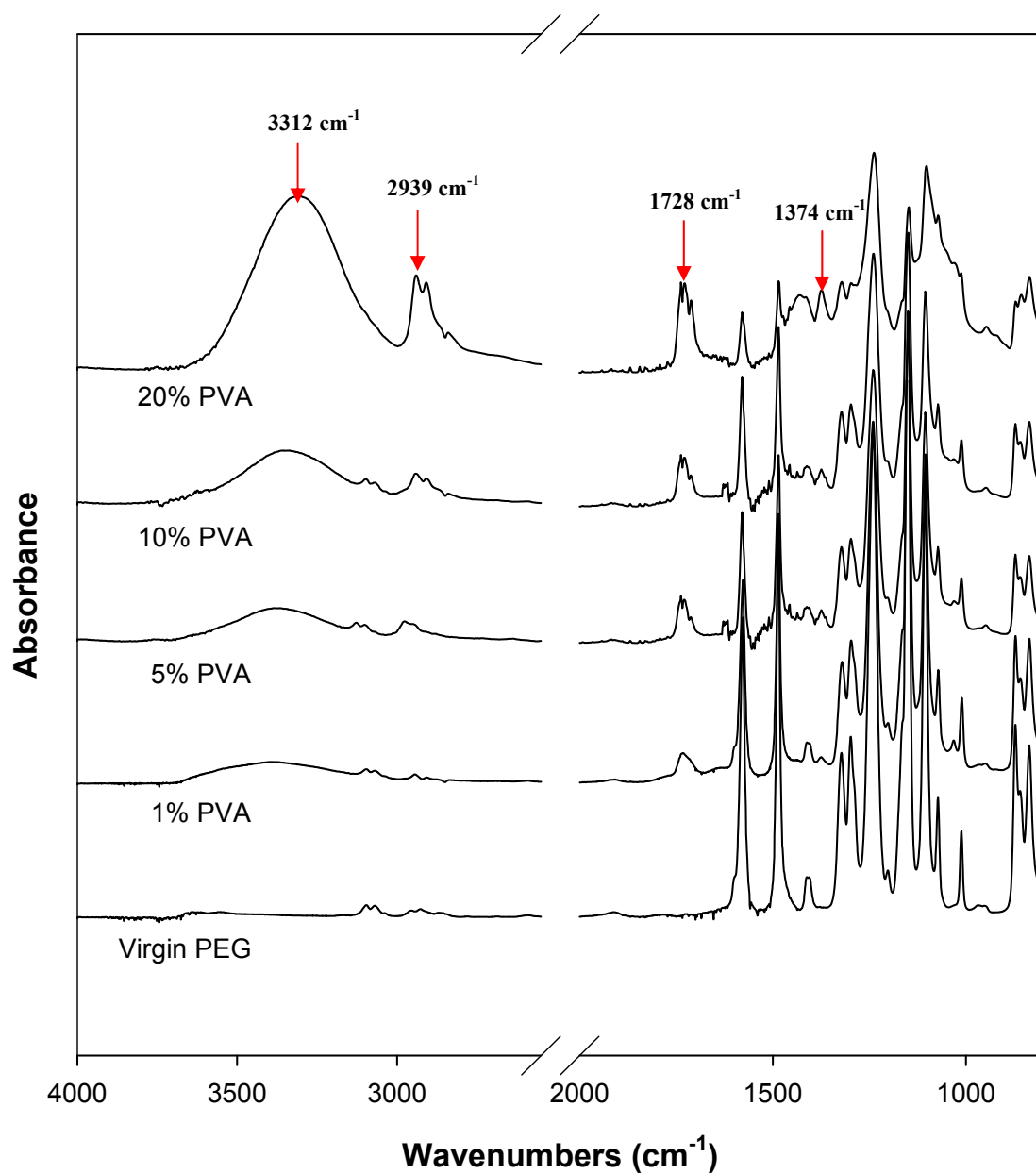
Figure 4.8. ATR-FTIR spectra of PVA grafted PES membrane using UV/Ozone treatment. The concentration of PVA was ranged 1%, 5%, 10%, and 20 %.
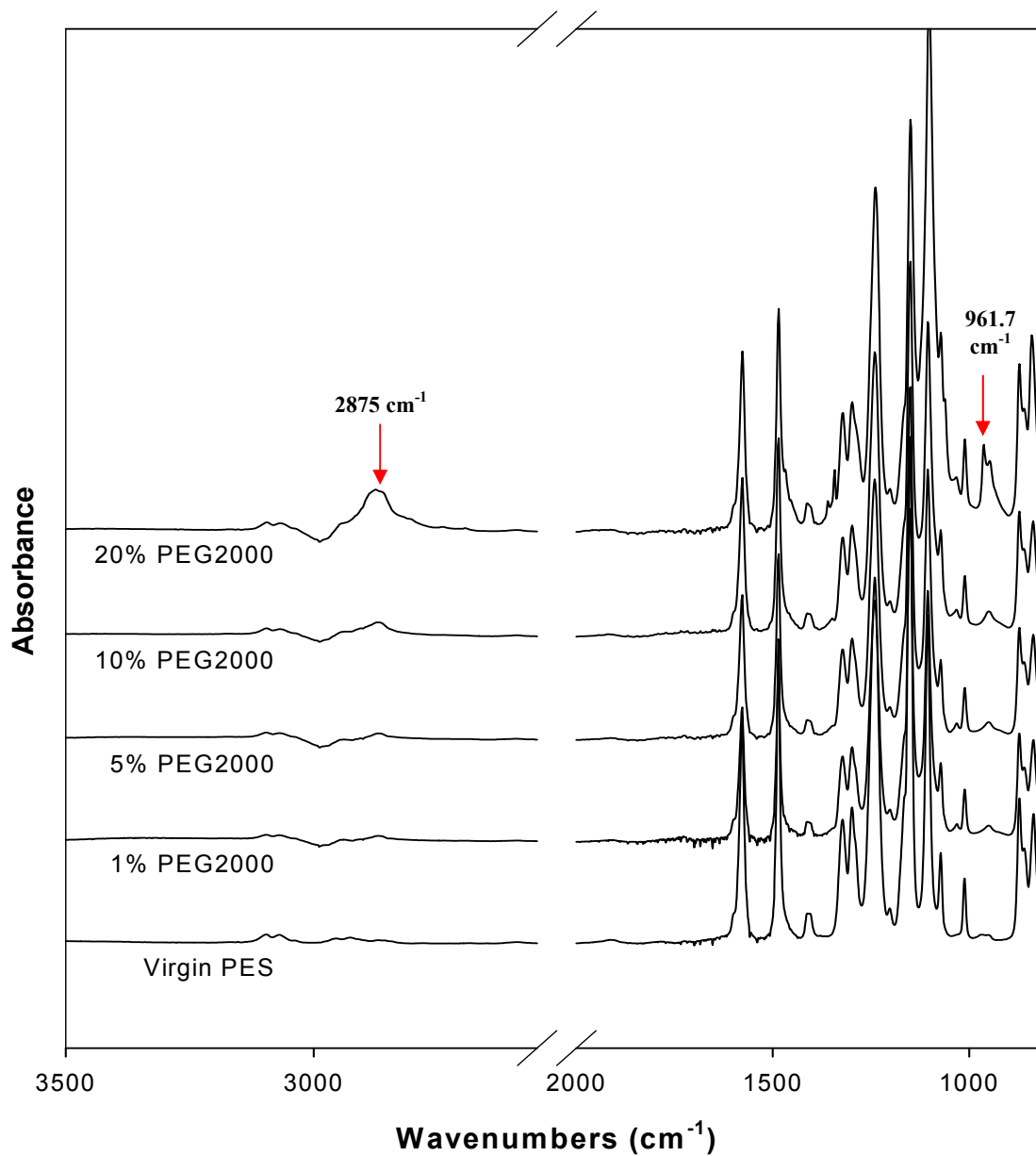
Figure 4.9. ATR-FTIR spectra of PEG $_{2000}$ grafted PES membrane using UV/Ozone treatment. The concentration of PEG $_{2000}$ was ranged 1%, 5%, 10%, and 20 %.

Based on some literatures, poly(ethylene glycol) with molecular chemical structure ($HO-CH_2-(CH_2-O-CH_2)_n-CH_2-OH$) have exhibited important strong absorption bands from 1050 cm^{-1} to 1150 cm^{-1} for the stretching of ether groups, from 2850 cm^{-1} to 3000 cm^{-1} for stretching alkyl (CH_2) groups, and from 3200 cm^{-1} to 3600 cm^{-1} for hydroxyl (-OH) group from FTIR spectroscopy measurements (Mansur et al., 2004). The major characteristic bands of PEG grafted membrane showed some new or intensity increased peaks at 961.7 cm^{-1} and at 2875 cm^{-1}, which were ascribed to C-H rock and C-C stretch, and C-H symmetric stretch of PEG, respectively. These observations suggested that the PEG chains should be effectively grafted on the surface of modified membrane.

4.4.5. Interfacial Polymerization

To optimize the reaction time in the interfacial polymerization processing, contact angle changes were measured depending on the reaction time between organic solvent (terephtahloyl chloride in benzene) and water phase (*m*-phenylenediamine). As shown in Figure 4.10, contact angle decreased with reaction time and minimum contact angle showed at 3 min. After 3 min, the contact angle increased over reaction time. Therefore, all interfacial polymerization processing was reacted for 3 min.

Contact angle of the modified PES membranes was measured and compared to that of virgin PES membrane. As shown in Figure 4.13, contact angle of PES membranes was reduced from 20% to 50 % by surface modification. Generally, the contact angle of the modified PES membranes was more reduced by hydrophilic polymer grafting using UV/Ozone treatment than by the interfacial polymerization. UV/Ozone treatment could reduce the contact angle of PES membrane to about 36 degrees (as shown in Figure 4.6)

but the contact angle could be recovered to about 60 degrees when UV/Ozone treated PES

was immersed in the solution like DI water. When PES membrane, however, was grafted

with hydrophilic polymers such as PVA, PEG, and chitosan after UV/Ozone treatment, the

contact angle of the modified PES membranes was lower than 60 degrees. This proves that

hydrophilic polymers were grafted successfully onto the PES membrane. PEG and

chitosan grafted PES membranes showed the lowest contact angle about 35 degrees to 36

degrees. Based on the contact angle data, these two modified PES membranes were

expected to show the lowest protein adsorption. The PES membranes modified by

interfacial polymerization could form the polyamide layers on the membrane surface.

These modified membranes showed relatively higher contact angles from 40 to 50 degrees

comparing with the hydrophilic polymer grafted PES membranes using UV/Ozone. Lower

contact angle means that the modified membrane was changed to more hydrophilic surface

and it could be expected to lower protein adsorption because the hydrophobic interaction

might be reduced.
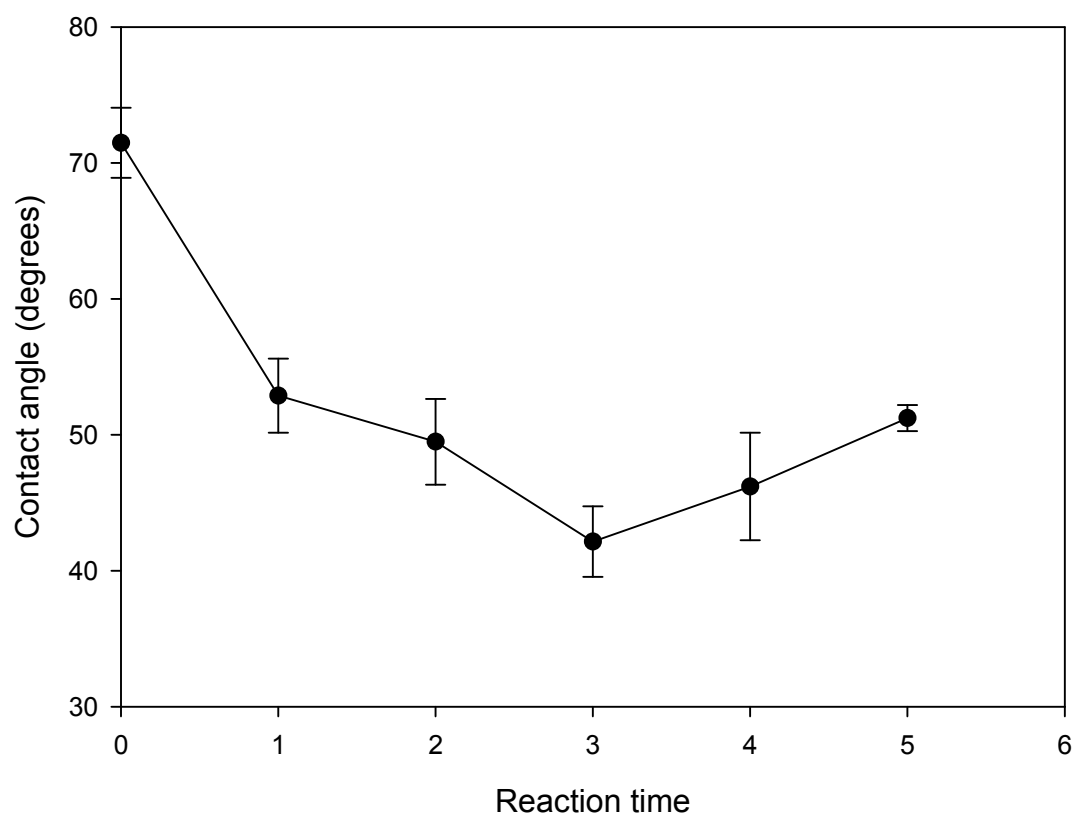
Figure 4.10. Contact angle changes by reaction time in interfacial polymerization
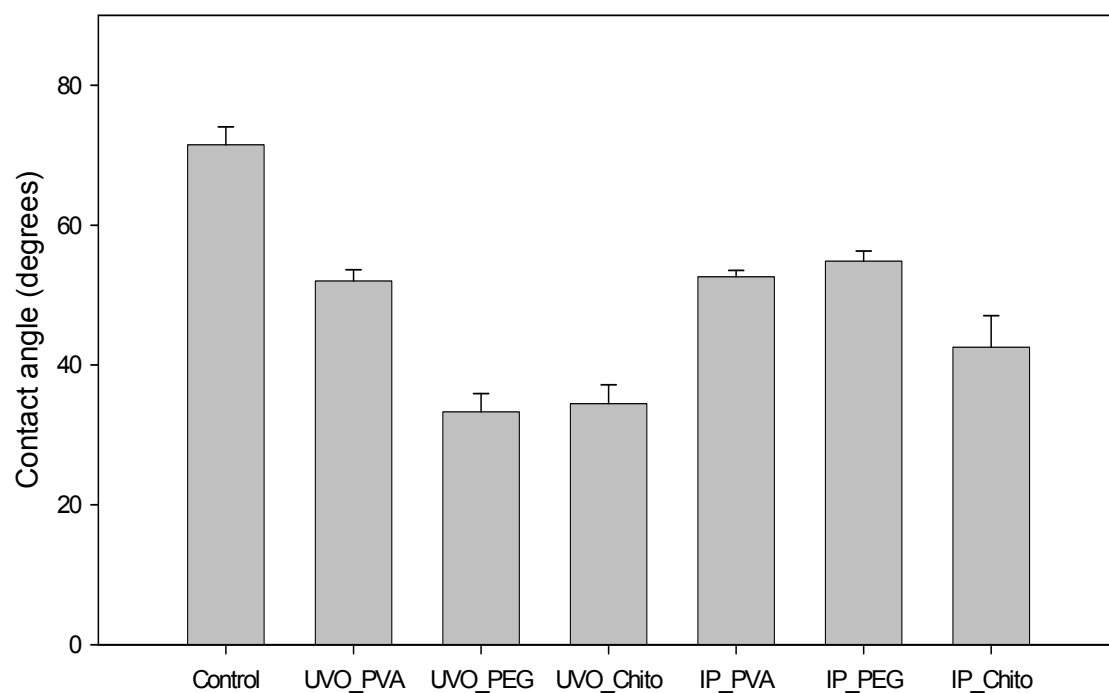
Figure 4.11. Contact angle of modified PES membranes.

Contact angles of modified PES membranes were reduced by 20% to 50% of virgin PES membrane. Generally, contact angles of hydrophilic polymer grafted PES membranes by UV/Ozone treatment were lower than those by interfacial polymerization because UV/Ozone is more powerful to improve the hydrophilicity of polymeric membrane and can form free oxygen groups on the membrane surface. Contact angles of modified PES membranes are different with the type of hydrophilic polymers. Both PVA modified membranes by UV/Ozone and interfacial polymerization showed almost same contact angles which is about 52 degrees. But PEG and chitosan modified membranes showed significant difference in their contact angle by UV/Ozone and interfacial polymerization. Among the modified PES membranes, PEG and chitosan grafted membranes using UV/Ozone showed lowest contact angle which is about 36 to 37 degrees. Based on the contact angle results, these two membranes (UVO-PEG and UVO-chitosan) can be expected to show the lowest protein adsorption.

4.4.6. Electron Spectroscopy for Chemical Analysis (ESCA)

In order to obtain further information about the composition change of the modified PES membrane surface, unmodified and modified PES membranes were subjected to X-ray photoelectron spectroscopy (XPS). First of all, the surface compositions and the atomic percentages of virgin PES membrane are shown in Table 4.2 and shown in Figure 4.12. As shown in Table 4.2 the atomic percentages of unmodified PES membrane were 71.75 % for carbon, 21.99% for oxygen, and 5.32% for sulfur, respectively. The ratio of oxygen to carbon is 0.306 and the ratio of sulfur to carbon is 0.074. Figure 4.12 shows the high-resolution C_{1s}, O_{1s}, N_{1s}, and S_{2p} XPS spectra of virgin PES membrane surface layer. In case of the virgin PES membrane surface layer, the C_{1s} core-level spectrum can be deconvoluted into three peak components. Carbon atoms at the PES surface exhibit core-level binding energies of 285.16 eV for the C-H and C-C species, 286.57 eV for the C-O species, and 292.00 eV for the C-C species on the aromatic benzene rings, respectively (Figure 4.12.A). The atom percentages are 50.01% for the C-C species, 17.47% for the C-S species, and 4.27% for the C-C species in aromatic benzene rings, respectively. The O_{1s} core-level spectrum can be deconvoluted into two peaks components at 531.79 eV for the O=S species and 533.50 eV for the O-C species. The atom percentages are 14.66% for the O=S=O species and 7.33% for the O-C species. The S_{2p} core-level spectrum of virgin PES membrane can be deconvoluted into one peak component with binding energy at 168.60 eV, this can be associated with the sulfone group of PES membrane. The atom percentage of sulfone is 5.18%.

Table 4.2 Relative surface atomic concentration of the virgin PES membrane calculated from XPS spectra.

Peak	Position	Assignment	Atoms percent (%)
C_{1s}	285.16	-C-C-	50.01
	286.57	-C-S-	17.47
	292.00	Aromatic ring	4.27
O_{1s}	531.79	O=S=O	14.66
	533.50	-O-C-	7.33
S_{2p}	168.60		5.18
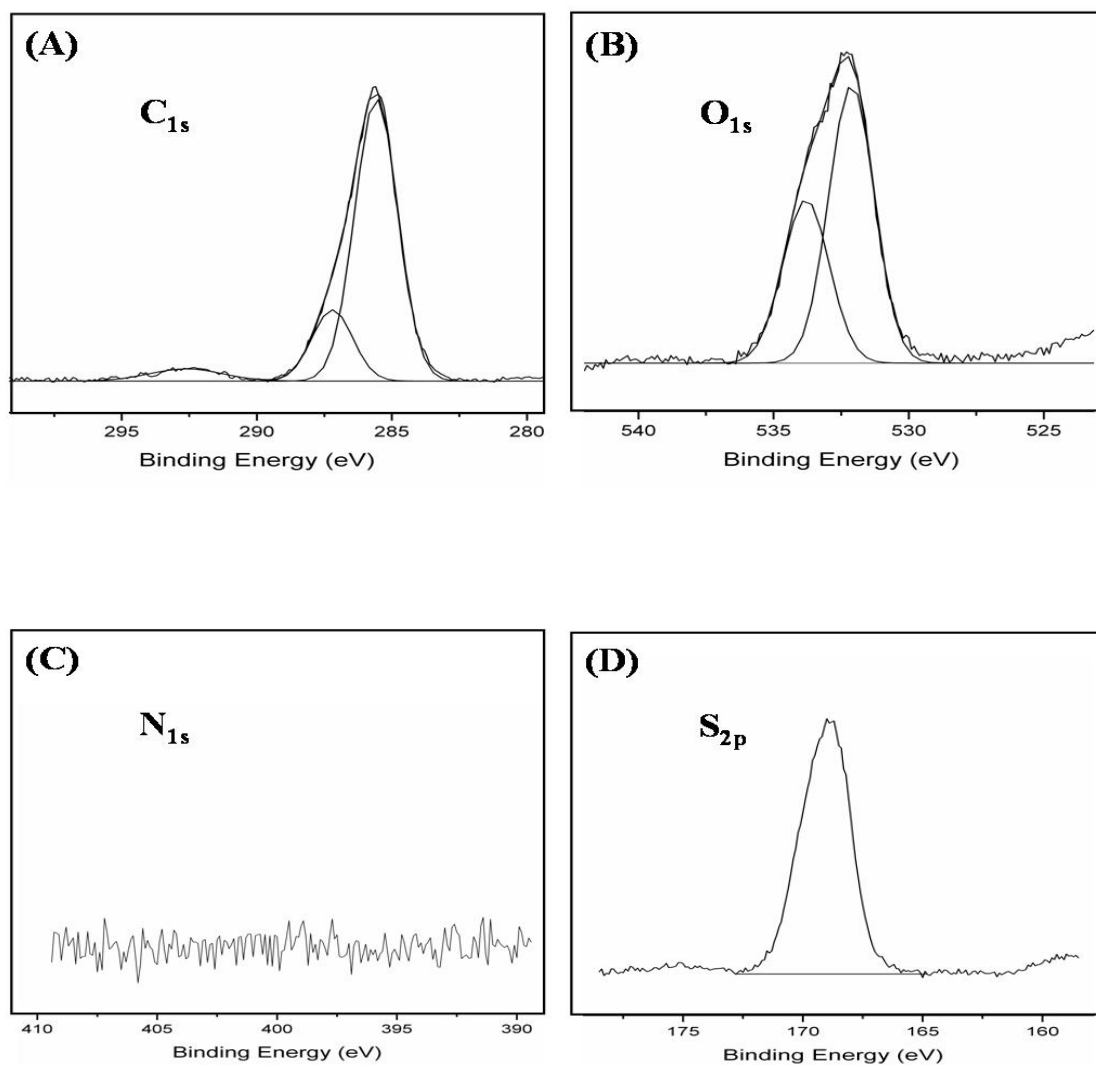
Figure 4.12. High-resolution (A) C_{1s}, (B) O_{1s}, (C) N_{1s}, and (D) S_{2p} XPS spectra of virgin PES membrane (NO. 1).

Figure 4.13 shows the high-resolution C_{1s}, O_{1s}, N_{1s}, and S_{2p} XPS spectra of 20% (w/v) PVA grafted PES membrane surface layer using UV/Ozone treatment (sample NO. 2). The C_{1s} core-level spectrum of PVA grafted PES membrane using UV/Ozone can be deconvoluted into three peak components with binding energies at 284.69 eV for the C-H and C-C species, at 286.16 eV for the C-O species and at 288.91 eV for the C=O species. The new peak component at the binding energy of 288.91 eV is assigned to the C=O species formed by UV/Ozone treatment. The O_{1s} core-level spectrum of PVA grafted PES membrane using UV/Ozone can be deconvoluted into three peak components with binding energies at 531.69 eV for the O-S and O-H species, at 532.05 eV for the O=C species, and at 533.20 eV for the O-C species. The new peak component at the binding energy of 532.05 eV is assigned to the O=C species formed by UV/Ozone treatment. PVA grafted PES membrane has no peak for sulfur component. This means that PVA grafted layer might formed thick layer which could cover the entire membrane surface, so XPS couldn't detected the sulfone groups of PES membrane.

Figure 4.13. High-resolution (A) C_{1s}, (B) O_{1s}, (C) N_{1s}, and (D) S_{2p} XPS spectra of 20% (w/v) PVA grafted PES membrane using UV/Ozone (NO. 2).

Figure 4.14 shows the high-resolution C_{1s}, O_{1s}, N_{1s}, and S_{2p} XPS spectra of 20%

(w/v) PEG $_{2000}$ grafted PES membrane surface layer using UV/Ozone treatment. The C_{1s}

core-level spectrum of PEG $_{2000}$ grafted PES membrane using UV/Ozone can be

deconvoluted into four peak components with binding energies at 284.72 eV for the C-H

and C-C species, at 286.07 eV for the C-O species, at 287.03 eV for the C=O species, and

at 291.49 eV for the C-C species on the aromatic benzene rings, respectively (Figure

4.14.A). The new peak component at the binding energy of 287.03 eV is assigned to the

C=O species formed by UV/Ozone treatment. The O_{1s} core-level spectrum of PEG $_{2000}$

grafted PES membrane using UV/Ozone can be deconvoluted into three peak components

with binding energies at 531.69 eV for the O-S and O-H species, at 532.05 eV for the O=C

species, and at 533.20 eV for the O-C species. The new peak component at the binding

energy of 532.05 eV is assigned to the O=C species formed by UV/Ozone treatment. Sulfur

was still observed in the spectrum after PEG $_{2000}$ grafting onto the PES membrane surface.

The S_{2p} core-level spectrum of PEG $_{2000}$ grafted PES membrane can be deconvoluted into

one peak components with binding energy at 167.80 eV, this can be taken as being

characteristic of the sulfone group of PES membrane. This result indicates that the

membrane surface was not thoroughly covered by the thick layer of the grafted PEG chains

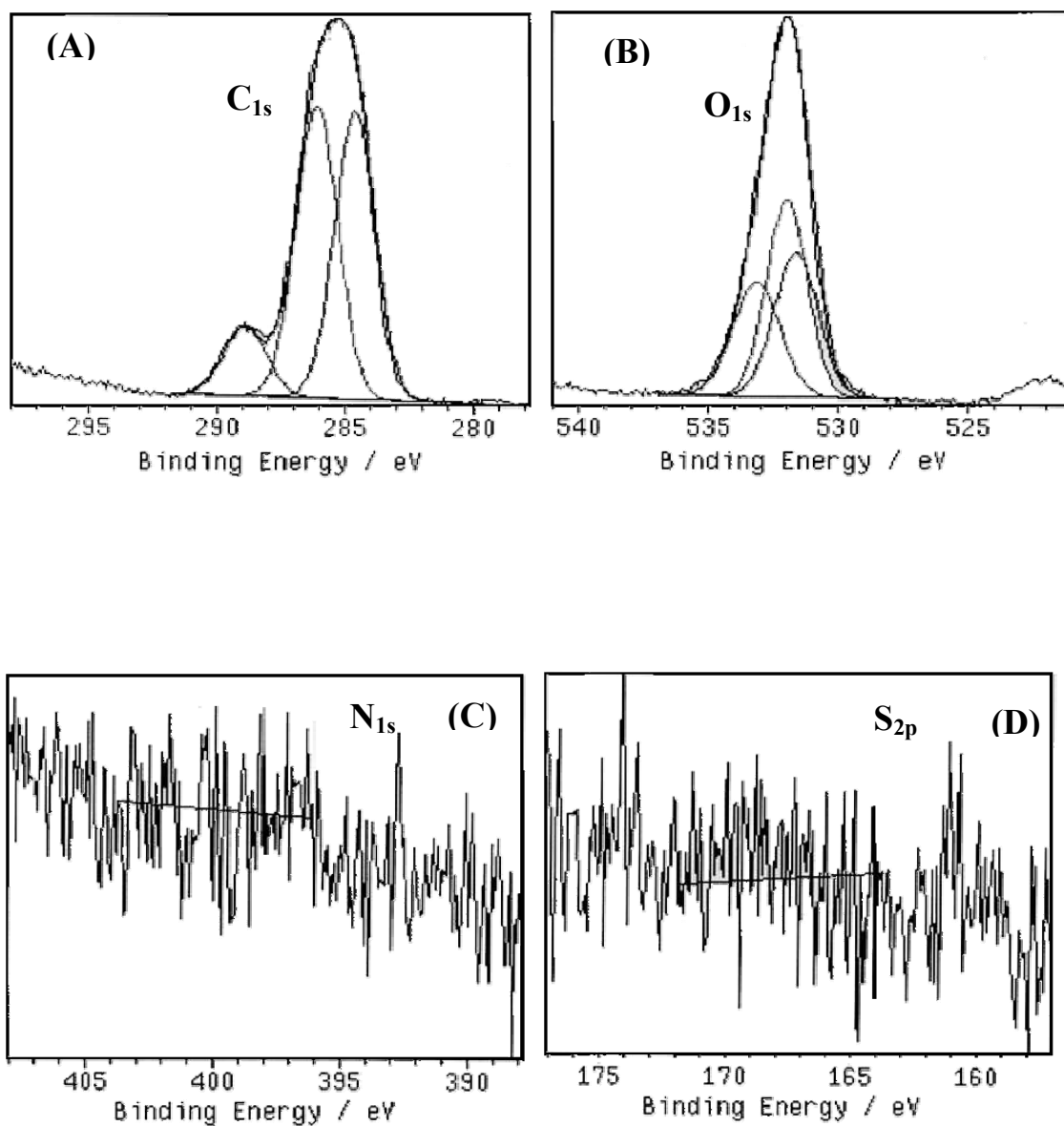but PEG grafting clearly occurred onto PES membrane.

Figure 4.14. High-resolution (A) C_{1s}, (B) O_{1s}, (C) N_{1s}, and (D) S_{2p} XPS spectra of 20% (w/v) PEG $_{2000}$ grafted PES membrane using UV/Ozone (NO. 3).

Figure 4.15 shows the high-resolution C_{1s}, O_{1s}, N_{1s}, and S_{2p} XPS spectra of 1% (w/v) chitosan grafted PES membrane surface layer using UV/Ozone treatment. The C_{1s} core-level spectrum of PVA grafted PES membrane using UV/Ozone can be deconvoluted into three peak components with binding energies at 284.88 eV for the C-H and C-C species, at 286.05 eV for the C-O species and at 288.01 eV for the C=O species. The new peak component at the binding energy of 288.01 eV is assigned to the C=O species formed by UV/Ozone treatment. The O_{1s} core-level spectrum of chitosan grafted PES membrane using UV/Ozone can be deconvoluted into two peak components with binding energies at 531.82 eV for the O-S and O-H species and at 533.20 eV for the O-C species. The new peak in the N_{1s} core-level spectrum of chitosan grafted PES membrane verifies that chitosan has been fabricated on the PES membrane surface because chitsan has free amine groups. Sulfur was still observed in the spectrum after chitosan grafting onto the PES membrane surface. The S_{2p} core-level spectrum of chitosan grafted PES membrane can be deconvoluted into one peak components with binding energy at 168.70 eV, this can be taken as being characteristic of the sulfone group of PES membrane. This result indicates that the membrane surface was not thoroughly covered by the thick layer of the grafted chitosan molecules, but chitosan grafting clearly occurred onto PES membrane. Among hydrophilic polymer grafted PES membranes, only PVA grafted PES membrane formed thick PVA layer which could entirely cover the virgin PES membrane.
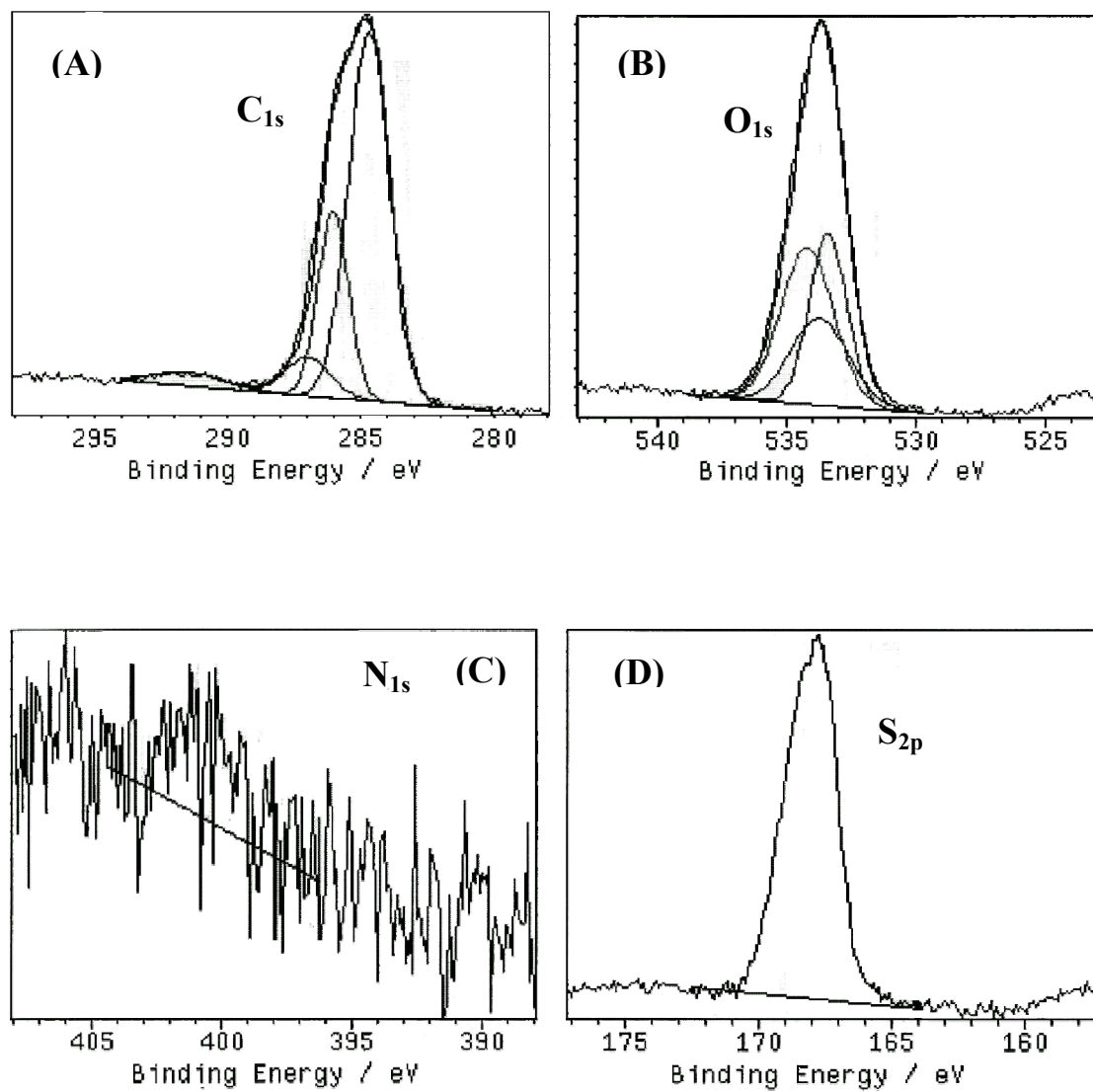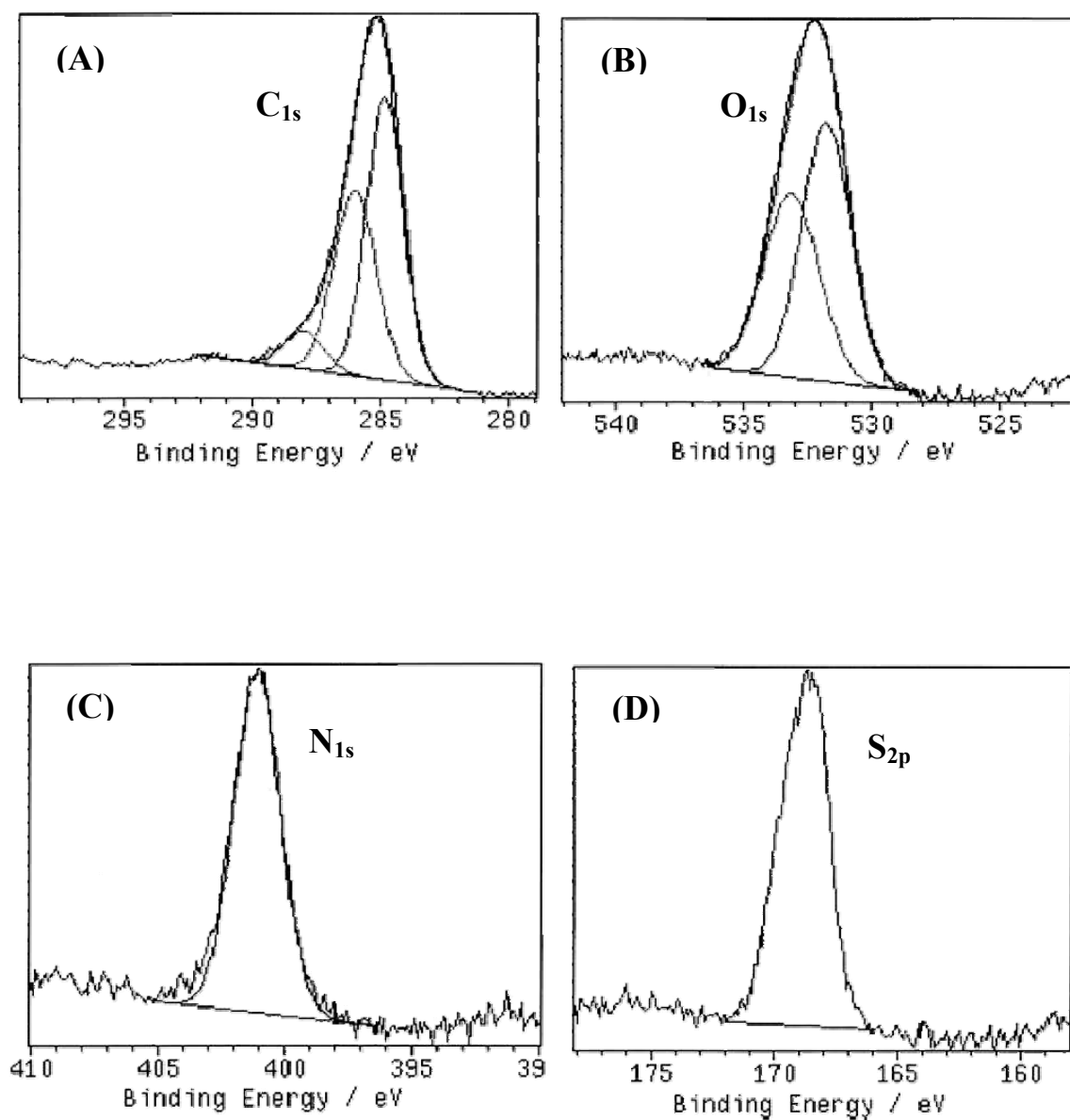
Figure 4.15. High-resolution (A) C_{1s}, (B) O_{1s}, (C) N_{1s}, and (D) S_{2p} XPS spectra of 1% (w/v) chitosan grafted PES membrane using UV/Ozone (NO. 4).

Figure 4.16 shows the high-resolution C_{1s}, O_{1s}, N_{1s}, and S_{2p} XPS spectra of polyamide/PVA modified PES membrane surface by interfacial polymerization. The C_{1s} core-level spectrum of polyamide/PVA modified PES membrane can be deconvoluted into three peak components with binding energies at 284.40 eV for the C-H and C-C species, at 285.89 eV for the C-O species and at 288.69 eV for the C=O species. The new peak component at the binding energy of 288.69 eV is assigned to the C=O species of the synthesized polyamide in polyamide/PVA modified PES membrane. The O_{1s} core-level spectrum of polyamide/PVA modified PES membrane surface by interfacial polymerization can be deconvoluted into three peak components with binding energies at 531.05 eV for the O-S and O-H species, at 532.02 eV for the O=C species, and at 533.40 eV for the O-C species. The new peak component at the binding energy of 532.02 eV is assigned to the O=C species of the synthesized polyamide in polyamide/PVA modified PES membrane. The new peak in the N_{1s} core-level spectrum of polyamide/PVA modified PES membrane can be deconvoluted into two peak components with binding energy at 399.36 eV and at 400.83 eV which are associated with amide groups. The new N_{1s} core-level spectrum verifies that polyamide layers have been fabricated successfully on the PES membrane surface by interfacial polymerization. Sulfur was still observed in the spectrum of polyamide/PVA modified PES membrane surface. The S_{2p} core-level spectrum of polyamide/PVA modified PES membrane can be deconvoluted into one peak components with binding energy at 168.60 eV, this can be taken as being characteristic of the sulfone group of PES membrane. This result indicates that the membrane surface was not thoroughly covered by the thick polyamide layer with PVA, but polyamide/PVA layers clearly occurred onto PES membrane.

Figure 4.16. High-resolution (A) C_{1s}, (B) O_{1s}, (C) N_{1s}, and (D) S_{2p} XPS spectra of PVA/polyamide formed PES membrane by interfacial polymerization (NO. 5).

Figure 4.17 shows the high-resolution C_{1s}, O_{1s}, N_{1s}, and S_{2p} XPS spectra of polyamide/PEG $_{2000}$ modified PES membrane surface by interfacial polymerization. The C_{1s} core-level spectrum of polyamide/PEG $_{2000}$ modified PES membrane can be deconvoluted into four peak components with binding energies at 284.95 eV for the C-H and C-C species, at 286.41 eV for the C-O species and at 287.99 eV and at 289.93 eV for the C=O species. The new peak components at the binding energy of 287.92 eV and 289.93 eV are assigned to the C=O species of the synthesized polyamide in polyamide/PEG $_{2000}$ modified PES membrane. The O_{1s} core-level spectrum of polyamide/PEG $_{2000}$ modified PES membrane surface by interfacial polymerization can be deconvoluted into three peak components with binding energies at 531.10 eV for the O-S and O-H species, at 532.52 eV for the O=C species, and at 533.60 eV for the O-C species. The new peak component at the binding energy of 532.52 eV is assigned to the O=C species of the synthesized polyamide in polyamide/PEG $_{2000}$ modified PES membrane. The new peak in the N_{1s} core-level spectrum of polyamide/PEG modified PES membrane can be deconvoluted into two peak components with binding energy at 399.94 eV and at 401.60 eV which are associated with amide groups. The new N_{1s} core-level spectrum verifies that polyamide layers have been fabricated on the PES membrane surface by interfacial polymerization. Sulfur was still observed in the spectrum of polyamide/PEG modified PES membrane surface. The S_{2p} core-level spectrum of polyamide/PEG modified PES membrane can be deconvoluted into one peak components with binding energy at 168.30 eV, this can be taken as being characteristic of the sulfone group of PES membrane. This result indicates that the membrane surface was not thoroughly covered by the thick polyamide layer with PEG, but polyamide/PEG layers clearly occurred onto PES membrane.
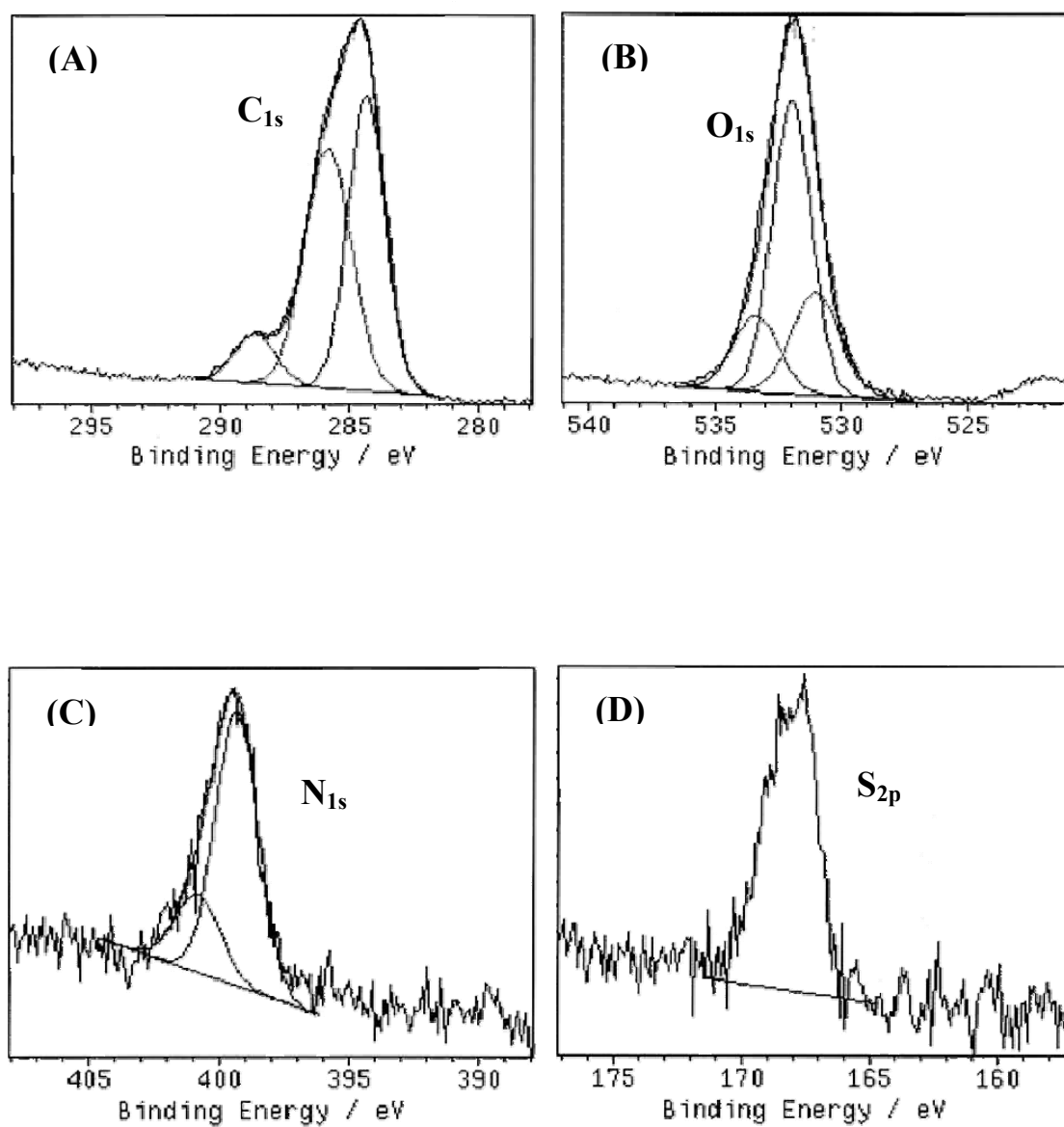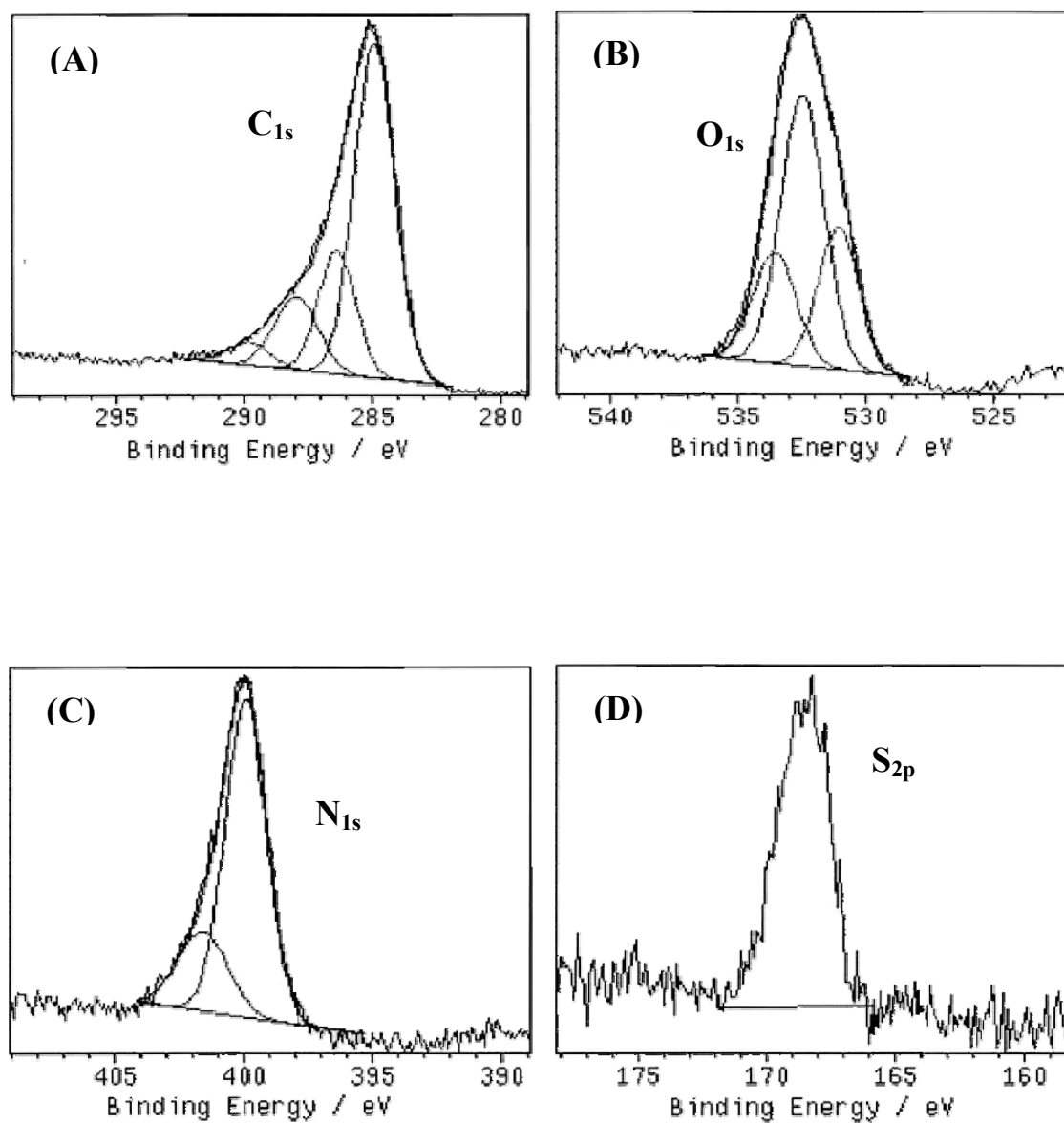
Figure 4.17. High-resolution (A) C_{1s}, (B) O_{1s}, (C) N_{1s}, and (D) S_{2p} XPS spectra of PEG/polyamide formed PES membrane by interfacial polymerization (NO. 6).

Figure 4.18 shows the high-resolution C_{1s}, O_{1s}, N_{1s}, and S_{2p} XPS spectra of polyamide/chitosan modified PES membrane surface by interfacial polymerization. The C_{1s} core-level spectrum of polyamide/chitosan modified PES membrane can be deconvoluted into three peak components with binding energies at 284.71 eV for the C-H and C-C species, at 286.34 eV for the C-O species and at 287.92 eV for the C=O species. The new peak component at the binding energy of 287.92 eV is assigned to the C=O species of the synthesized polyamide in polyamide/chitosan modified PES membrane. The O_{1s} core-level spectrum of polyamide/chitosan modified PES membrane surface by interfacial polymerization can be deconvoluted into three peak components with binding energies at 531.50 eV for the O-S and O-H species, at 532.67 eV for the O=C species, and at 533.34 eV for the O-C species. The new peak component at the binding energy of 532.67 eV is assigned to the O=C species of the synthesized polyamide in polyamide/chitosan modified PES membrane. The new peak in the N_{1s} core-level spectrum of polyamide/chitosan modified PES membrane can be deconvoluted into two peak components with binding energy at 399.23 eV and at 401.47 eV which are associated with amide groups of polyamide layer and amine groups of chitosan. The new N_{1s} core-level spectrum verifies that polyamide layers have been fabricated successfully on the PES membrane surface by interfacial polymerization. Sulfur was still observed in the spectrum of polyamide/chitosan modified PES membrane surface. The S_{2p} core-level spectrum of polyamide/chitosan modified PES membrane can be deconvoluted into one peak components with binding energy at 168.00 eV, this can be taken as being characteristic of the sulfone group of PES membrane. This result indicates that the membrane surface was

not thoroughly covered by the thick polyamide layer with chitosan, but polyamide/chitosan layers clearly occurred onto PES membrane.

Table 4.3 shows the XPS atomic percent and the ratio of O/C, N/C, and S/C for modified PES membranes. Generally the carbon composition decreased and the oxygen composition increased by surface modification. Polymeric membrane surface might be changed more hydrophilic with more oxygen components which could interact with water molecules. Because many free oxygen groups could be generated by UV/Ozone treatment, the oxygen composition of the modified membranes using UV/Ozone increased but chitosan grafted membrane showed a little higher carbon composition and lower oxygen composition. The nitrogen composition of chitosan grafted membrane was about 5% and sulfur composition was reduced from 5.32% to 1.88%. These results support that chitosan molecules were grafted successfully on the PES membrane surface.
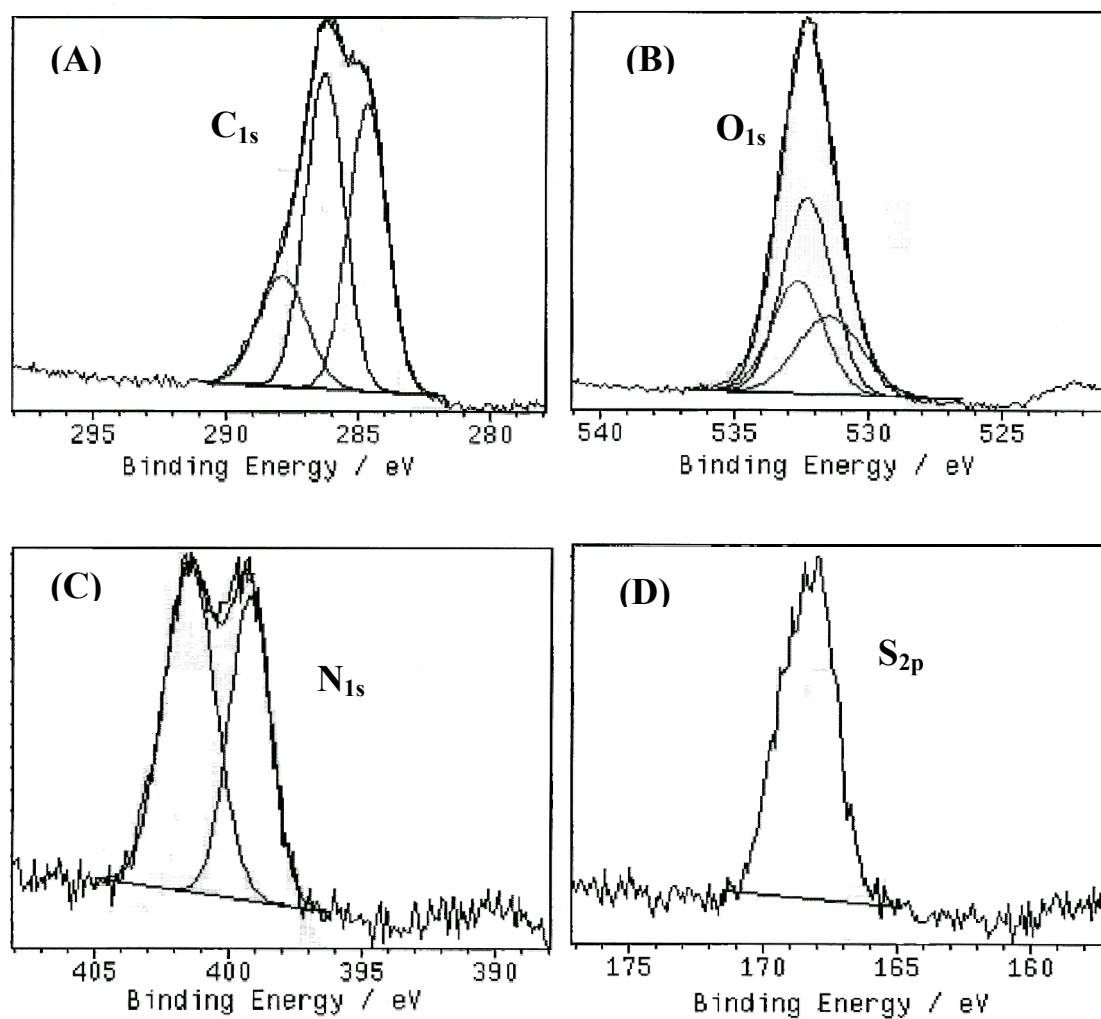
Figure 4.18. High-resolution (A) C_{1s}, (B) O_{1s}, (C) N_{1s}, and (D) S_{2p} XPS spectra of chitosan/polyamide formed PES membrane by interfacial polymerization (NO. 7).

Table 4.3. XPS atomic percent for modified PES membranes

Sample NO	XPS atoms percent				O/C	N/C	S/C
	C	O	N	S			
NO. 1	71.75	21.99	-	5.32	0.306	-	0.074
NO. 2	63.63	36.36	-	-	0.571	-	-
NO. 3	64.91	31.4	-	3.40	0.484	-	0.052
NO. 4	72.27	20.79	5.06	1.88	0.288	0.070	0.026
NO. 5	62.57	34.80	2.11	0.52	0.556	0.034	0.008
NO. 6	68.15	24.17	6.92	0.76	0.355	0.102	0.011
NO. 7	57.88	34.69	5.92	1.34	0.599	0.102	0.023

4.4.7. Atomic Force Microscopy (AFM)

Figure 4.19 to 4.25 represent AFM surface images of virgin PES and all modified PES membranes with a projection area of 2 μm x 2 μm, in which the unique and characteristic ridge-and-valley structure of the PES membranes is clearly shown. The bar at the right side of each image indicates the vertical deviations in the membrane surface; the white region indicates the highest level and the dark region indicates the lowest level. The surface of virgin PES membrane is not homogeneous but heterogeneous surface. Generally, the surface of the modified PES membranes by hydrophilic polymer grafting using UV/Ozone treatment has higher roughness while the surface of the modified PES membranes by interfacial polymerization has lower roughness than that of the virgin PES membrane.
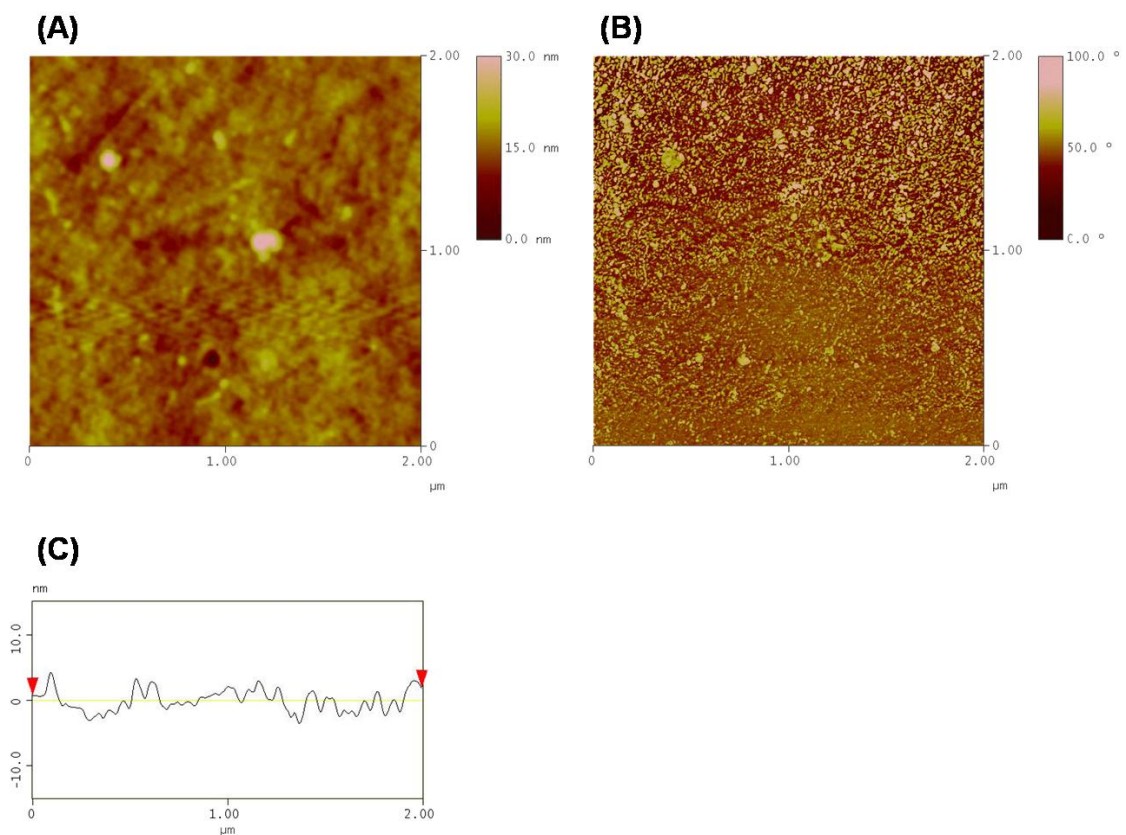
Figure 4.19. Tapping mode AFM images of Virgin PES membrane (NO. 1). (A) topography, (B) phase image, and (C) cross-section. Image size 2µm x 2µm. The root mean square roughness in (A) is 2.067 nm.
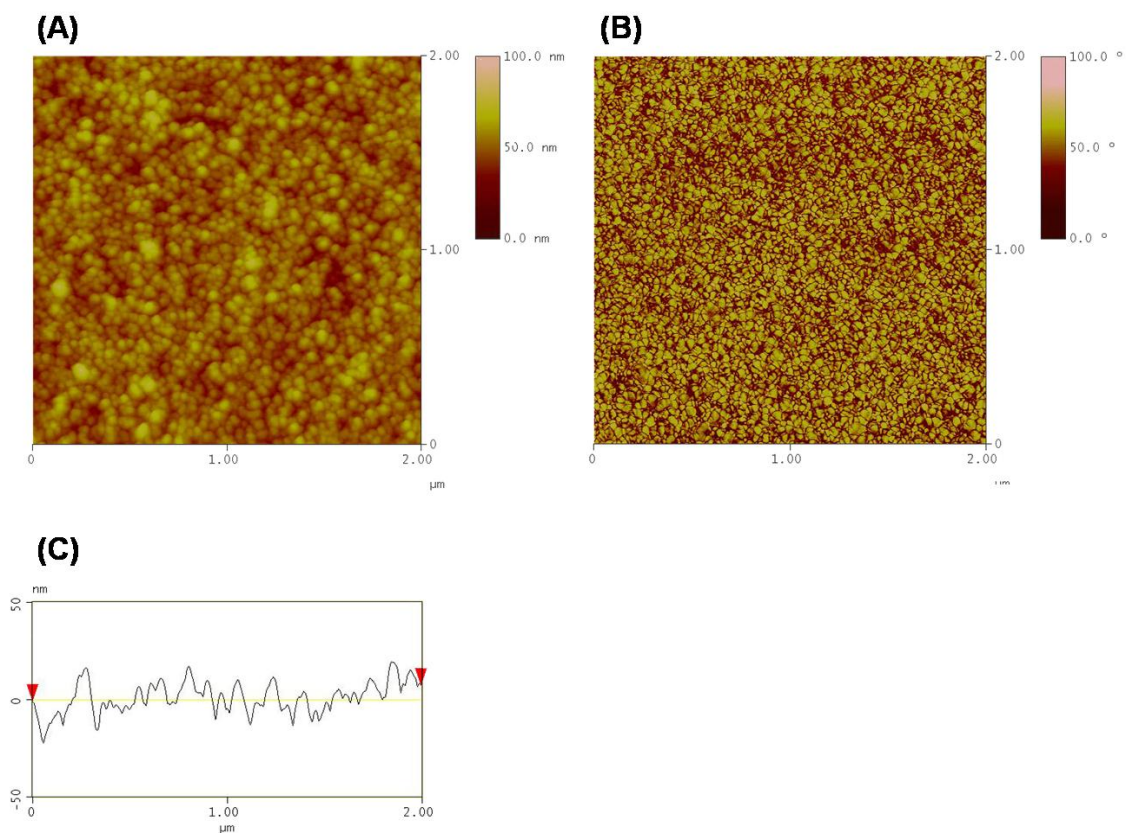
Figure 4.20. Tapping mode AFM images of PVA grafted PES membrane using UV/Ozone (NO. 2). (A) topography, (B) phase image, and (C) cross-section. Image size 2µm x 2µm. The root mean square roughness in (A) is 7.021 nm.

(A)

(B)

(C)
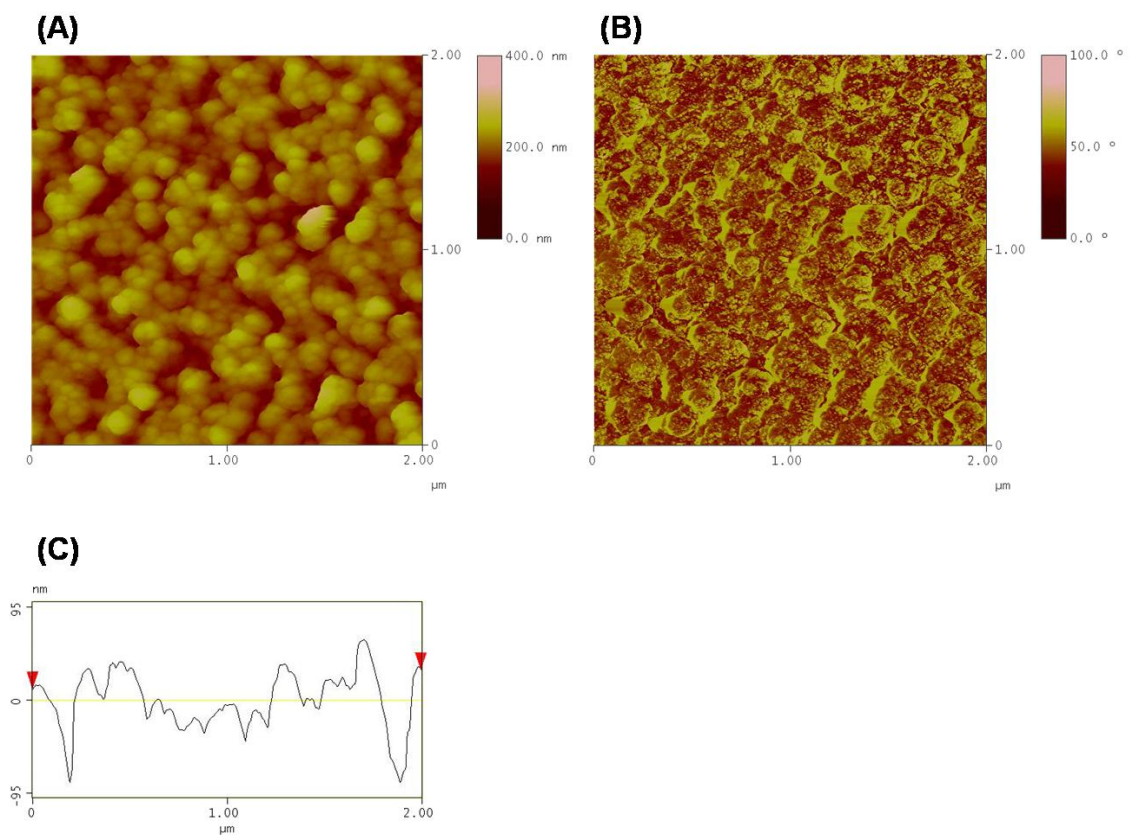
Figure 4.21. Tapping mode AFM images of PEG grafted PES membrane using UV/Ozone (NO. 3). (A) topography, (B) phase image, and (C) cross-section. Image size 2µm x 2µm. The root mean square roughness in (A) is 25.695 nm.
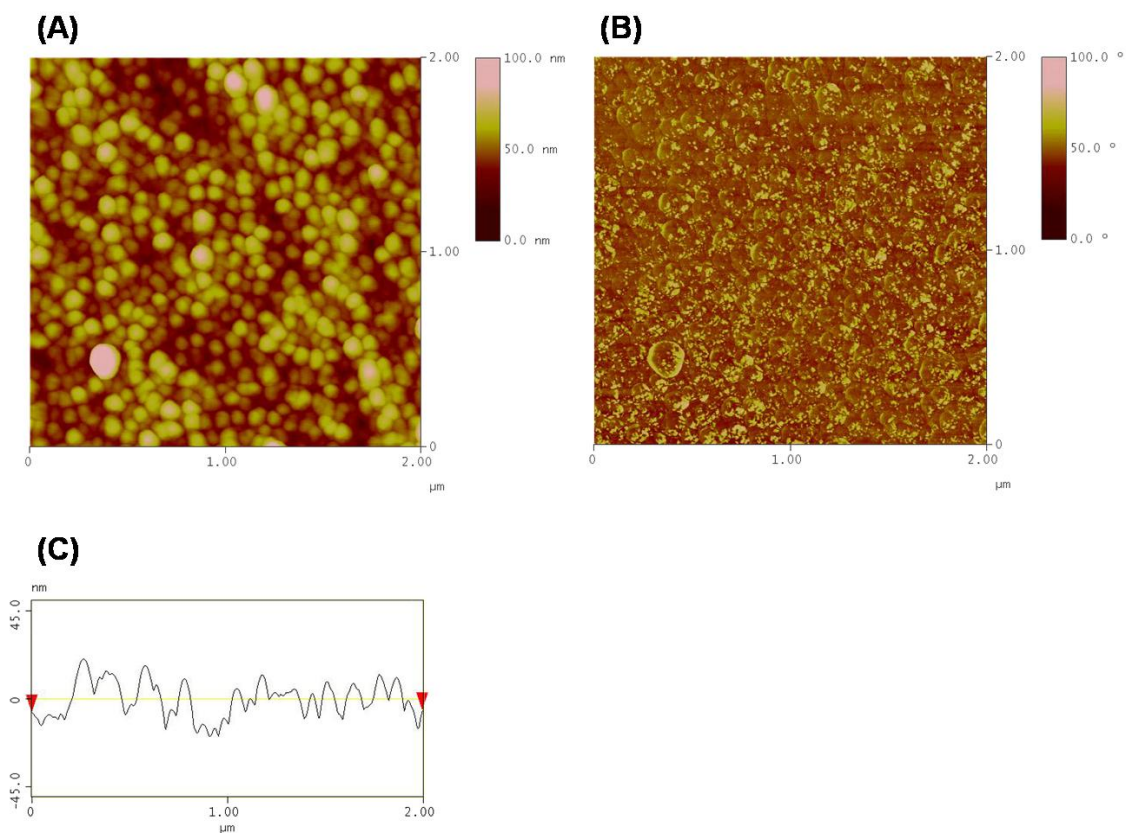
Figure 4.22. Tapping mode AFM images of Chitosan grafted PES membrane using UV/Ozone (NO. 4). (A) topography, (B) phase image, and (C) cross-section. Image size 2µm x 2µm. The root mean square roughness in (A) is 10.107 nm.
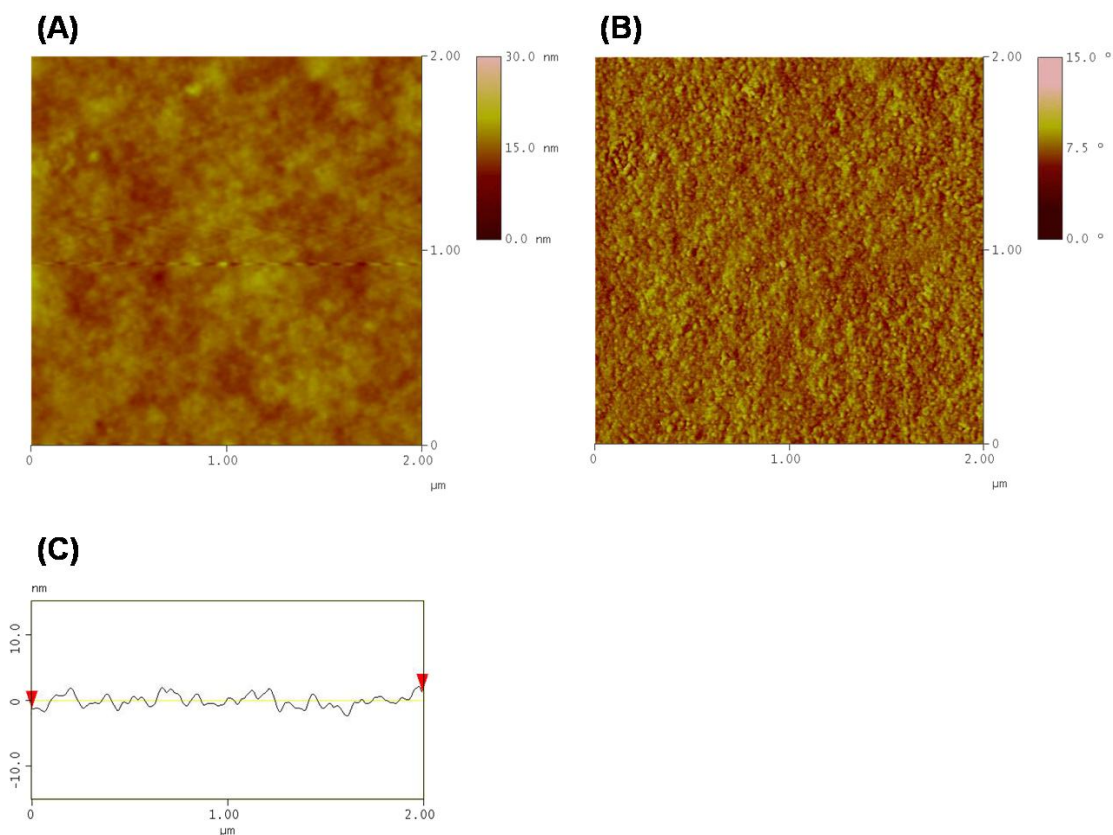
Figure 4.23. Tapping mode AFM images of thin film composite with PVA formed PES membrane by interfacial polymerization (NO. 5). (A) topography, (B) phase image, and (C) cross-section. Image size 2µm x 2µm. The root mean square roughness in (A) is 1.187 nm.
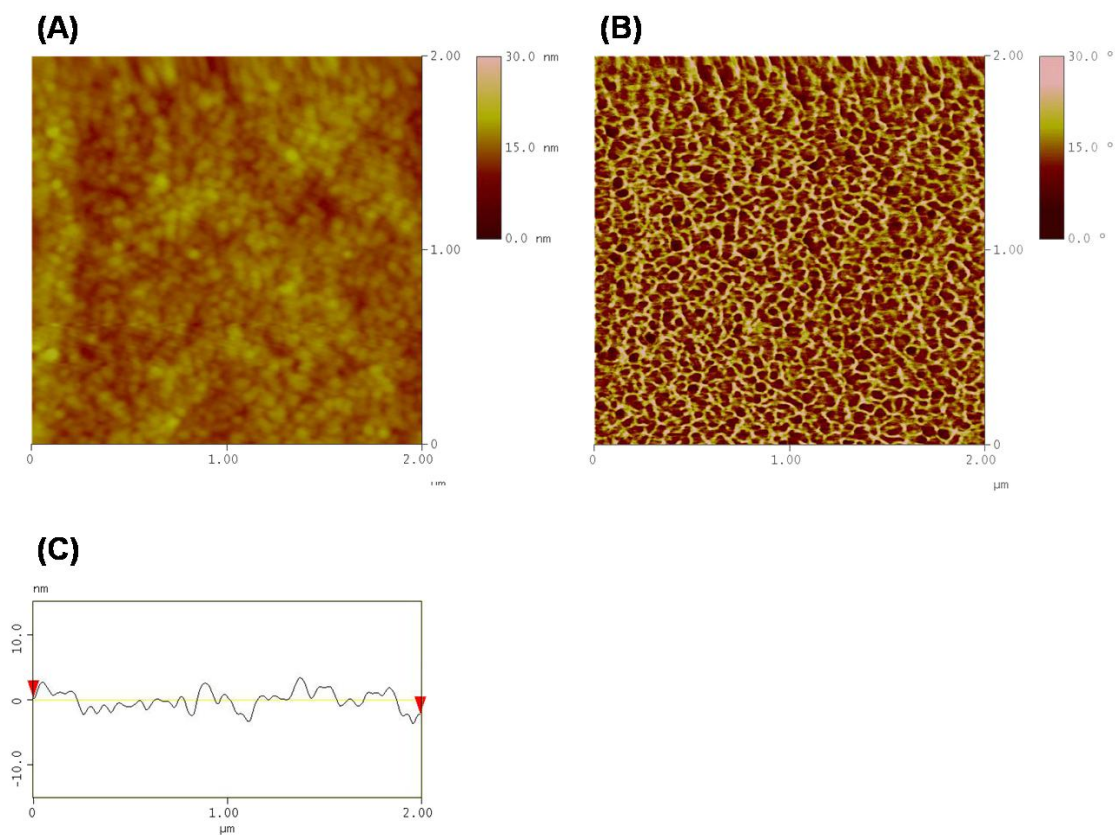
Figure 4.24. Tapping mode AFM images of thin film composite with PEG $_{2000}$ formed PES membrane by interfacial polymerization (NO. 6). (A) topography, (B) phase image, and (C) cross-section. Image size 2µm x 2µm. The root mean square roughness in (A) is 1.538 nm.
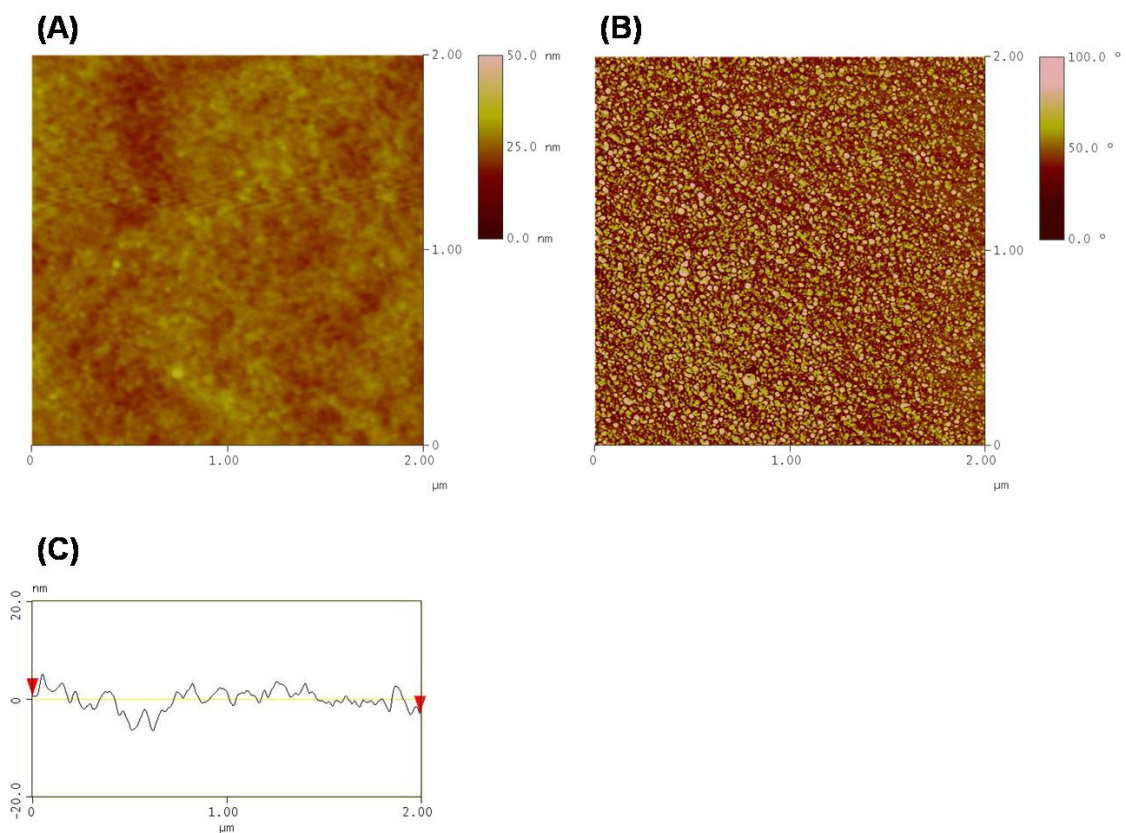
Figure 4.25. Tapping mode AFM images of thin film composite with chitosan formed PES membrane by interfacial polymerization (NO. 7). (A) topography, (B) phase image, and (C) cross-section. Image size 2μm x 2μm. The root mean square roughness in (A) is 2.044 nm.

**4.4.8. Protein Adsorption Test on Modified Membranes**

Static adsorption of β-lactoglobulin on the modified PES membrane surface was studied to compare the decrease the amount of adsorption on the modified PES membrane. As shown in Figure 4.26, the amount of β-lactoglobulin adsorbed on the PES membrane was reduced from 20% to 60 % by surface modification. Among the modified PES membranes, PEG grafted PES membrane using UV/Ozone showed lowest protein adsorption. Because this membrane showed lowest contact angle the hydrophobic interaction between protein and modified PES membrane might greatly decrease. However, chitosan grafted PES membrane using UV/Ozone showed highest protein adsorption in modified PES membranes even if the contact angle of this membrane showed the lowest value. But it still showed lower protein adsorption than the virgin PES membrane. Although it could reduce the hydrophobic interaction between protein and modified membrane, chitosan grafted PES membrane could increase the peptide bond between free amine groups in chitosan and hydroxyl groups in protein. Therefore, the protein adsorption increased in this chitosan grafted PES membrane. Also the protein adsorption could be more increased with more chitosan molecules grafted on PES membrane.
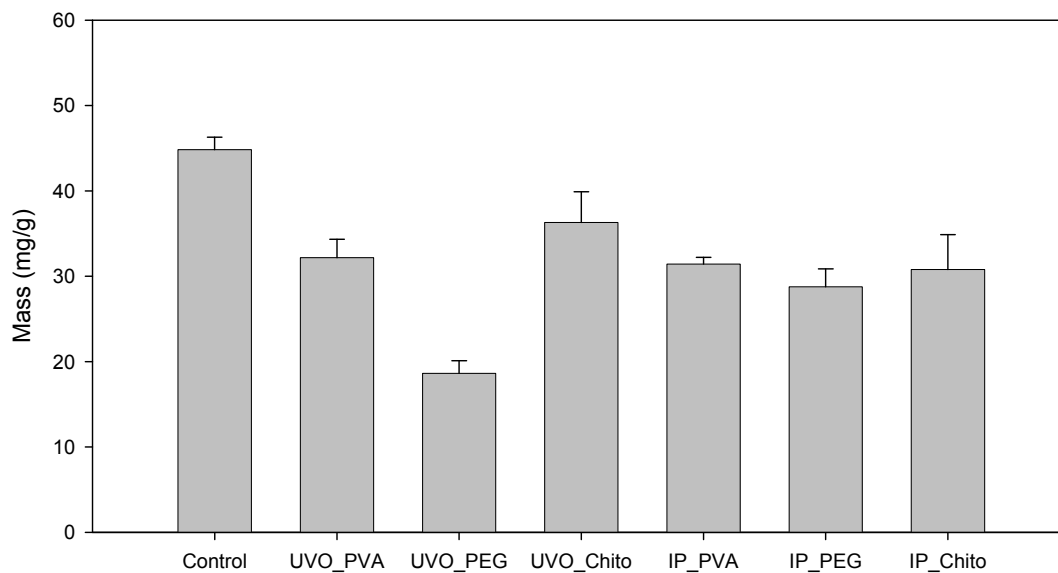
Figure 4.26. Mass of the β-lactoglobulin adsorbed on the unmodified and modified PES membranes by static adsorption experiment. The concentration of β-lactoglobulin was 2.5 mg/mL and the solution pH was 3.0.

4.5. Summary

Surface modification of PES membrane was investigated to improve the hydrophilicity and reduce the protein adsorption. Hydrophilic polymer grafting using UV/Ozone treatment and thin film composite by interfacial polymerization were used to improve the hydrophilicity of the commercial PES membrane. Modified PES membranes were characterized by contact angle, FTIR, XPS, and AFM. Contact angles of modified PES membranes were reduced by 20% to 50% of virgin PES membrane. FTIR spectrum and XPS spectrum supported that PES membrane was successfully modified by hydrophilic polymer grafting using UV/Ozone and thin film composite by interfacial polymerization. Tapping mode AFM was used to investigate the changes of surface topography, phase images, cross section, and root mean square roughness of modified PES membranes. Generally, the PES membranes modified by hydrophilic polymer grafting using UV/Ozone showed higher roughness (7.021 nm to 25.695 nm) than that of virgin PES membrane (2.067 nm). On the other hand, the PES membranes modified by interfacial polymerization showed lower roughness (from 1.187 nm to 2.044 nm) than that of virgin PES membrane. Although it is not homogeneous, the polyamide thin layers formed by interfacial polymerization have a relatively smooth surface.

Hydrophilic polymer grafted PES membranes using UV/Ozone shows generally lower contact angles and lower protein adsorption. These results indicated that the PES membrane with more hydrophilic surface could reduce the protein adsorption because it could reduce the hydrophobic interaction between protein and membrane.

CHAPTER V. CONCLUSION

The adsorption process of β-lactoglobulin on the polymeric membrane surface was investigated by static adsorption and dynamic adsorption experiments to understand fouling mechanism and optimize the process condition to minimize the membrane fouling. Since the major factor to cause the permanent membrane fouling is the irreversible adsorption of whey protein on the polymeric membrane, it is necessary to study the interaction of whey protein to the polymeric membrane surface at various conditions such as protein concentration, pH, and salt concentration. In this study, static and dynamic adsorption processes were investigated. In order to optimize the design of the system, it is important to establish the most appropriate the correlation of equilibrium data. Static adsorption results showed the adsorption properties of the equilibrium state. Dynamic adsorption experiments were studied using Quartz crystal microbalance with dissipation monitoring (QCM-D) system which can provide the unique and quantitative information of viscoelastic properties of the adsorbed protein layer as well as monitor the adsorption process in real time by simultaneously measuring of frequency shift and dissipation shift. From the dynamic adsorption results, most adsorption was occurred in the initial stage and minor adsorption and protein conformation were followed over time.

Both static adsorption and dynamic adsorption data showed same adsorption trends: the protein adsorption increased with protein concentration and at acidic and alkaline conditions. Based on these static and dynamic adsorption experiments, the major interactions to increase the protein adsorption were the hydrophobic interaction and electrostatic interactions. Especially, the hydrophobic interaction by dissociation of dimer

structure of β-lactoglobulin to monomer structure at acidic and alkaline conditions showed the greatly increasing of the amount of protein adsorption by the protein and membrane interaction which might form the strong and rigid protein layer on the polymeric membrane surface. The results of this study have clearly demonstrated that the β-lactoglobulin adsorption onto the polyethersulfone (PES) surface was mainly affected by the hydrophobic interaction between protein and PES membrane.

In order to reduce the protein adsorption on polymeric membrane, PES membrane was modified by two surface modification methods: hydrophilic polymer grafting using UV/Ozone and thin film composite by interfacial polymerization. These two modification methods are powerful techniques to improve the hydrophilicity of polymeric membrane. PVA, PEG, and chitosan were used as hydrophilic polymers to graft on PES membrane because of their excellent hydrophilic property. Surface properties of modified PES membranes were characterized by contact angle, FTIR, XPS, and AFM. And static adsorption experiment was investigated with modified membranes and compared to that of unmodified PES membrane. These results support that modified membranes have more hydrophilic surface and could reduce the amount of protein adsorption by 20% to 60%.

CHAPTER VI. FUTURE WORK

1. Based on this research the optimum processing conditions such as pH, salt

concentration, and protein concentration for the ultrafiltration system should be examined

to minimize membrane fouling.

2. Liquid whey filtration processing with modified PES membranes should be investigated

to compare the degree of membrane fouling.

APPENDICES

Standard Curve at pH 3.0

y=0.8583x + 0.0159

R^2=0.9995

Standard Curve at pH 5.2

y=0.8375x - 0.0025

R^2=0.9999

Standard Curve at pH 7.0

y=0.8133x - 0.0235

R^2=0.9995

Standard Curve at pH 9.0

y=0.8105x - 0.0021

R^2=0.9998
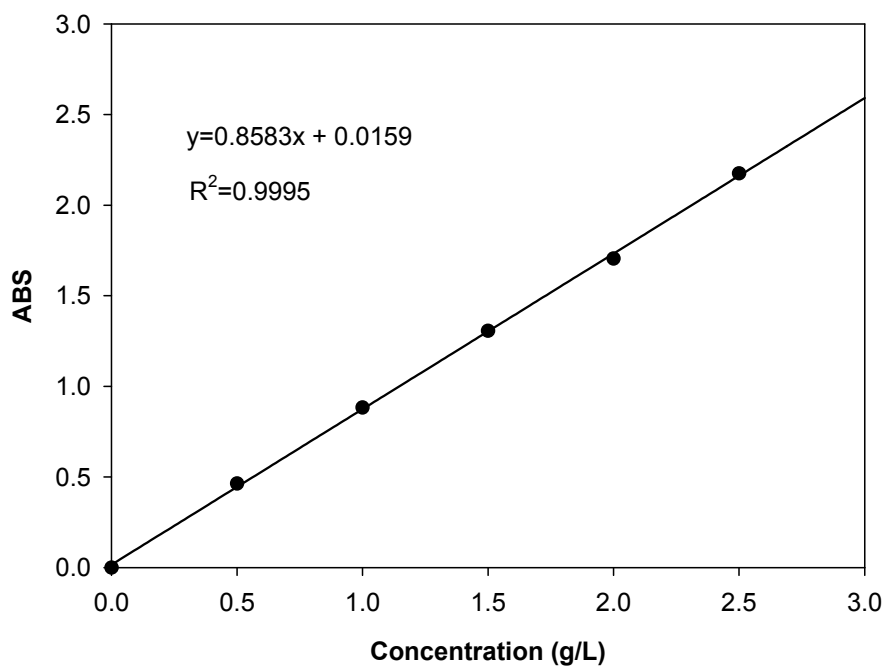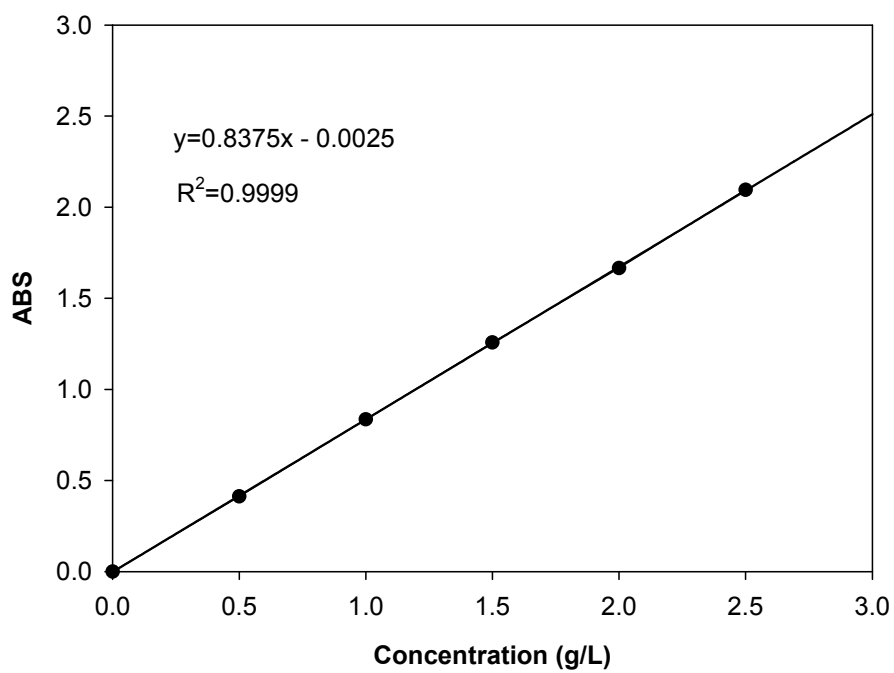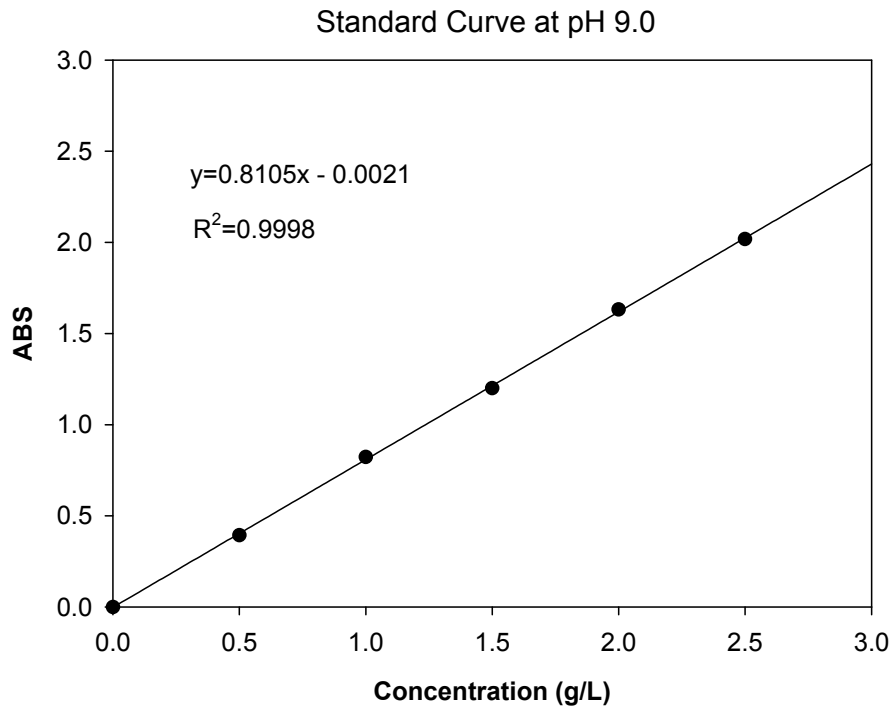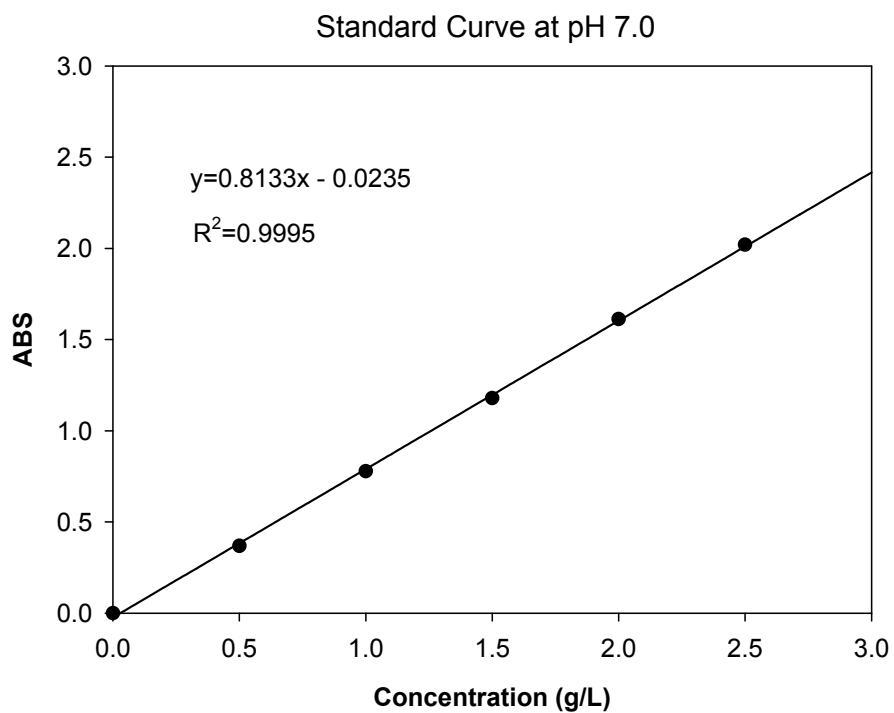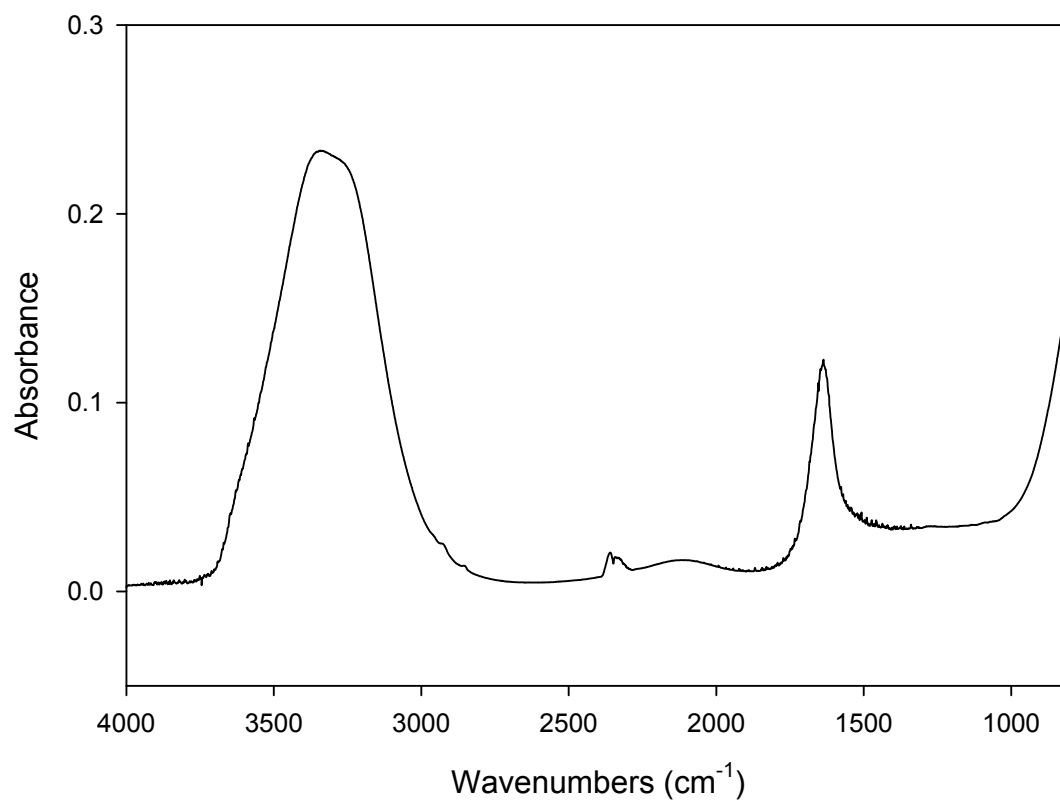
ATR-FTIR spectrum of 1% poly(vinyl alcohol)

XPS widescan spectra at taken off angle of 90 for unmodified and modified PES
membrane by hydrophilic polymer grafting using UV/Ozone.
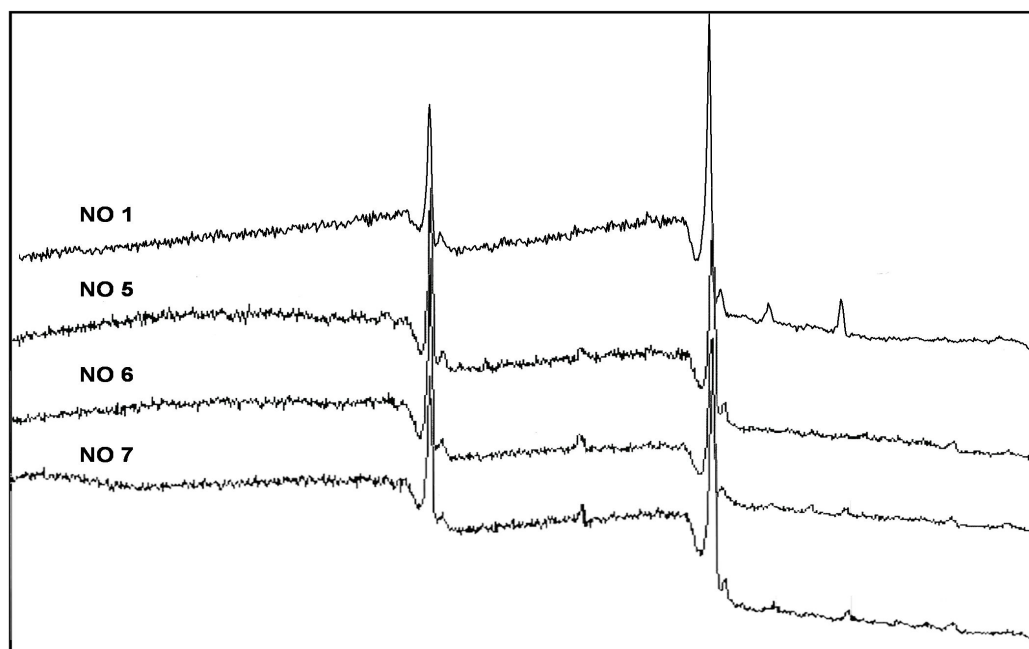
XPS widescan spectra at taken off angle of 90 for unmodified and modified PES membrane by interfacial polymerization.

REFERENCES

Adamson, A. W. 1982. *Adsorption of Gases and Vapors on Solids*. In Physical Chemistry of Surfaces: 4th ed., John Wiley & Sons, Inc., pp. 517-600.

Andrade, J. D. and Hlady, V. 1986. Protein Adsorption and Materials Biocompatibility: A Tutorial Review and Suggested Hypotheses. *Adv. Polym. Sci.* **79**: 1-63.

Atra, R., Vatai, G., Bekassy-Molnar, E., and Balint, A. 2005. Investigation of Ultra- and Nanofiltration for Utilization of Whey Protein and Lactose. *J. Food Engr.* **67**: 325-332.

Babu, P. R. and Gaikar, V. G. 2001. Membrane Characteristics as Determinant in Fouling of UF Membranes. *Sep. Purif. Technol.* **24**: 23-34.

Bartlett, M., Bird, M. R., and Howell, J. A. 1995. An Experimental Study for The Development of A Qualitative Membrane Cleaning Model. *J. Membr. Sci.* **105**: 147-157.

Beamson, G. and Briggs, D. 1992. *High Resolution of XPS of Organic Polymer;* Wiley; New York.

Belfer, S., Fainchtain, R., Purinson, Y., and Kedem, O. 2000. Surface Characterization by FTIR-ATR Spectroscopy of Polyethersulfone Membranes-Unmodified, Modified and Protein Fouled. *J. Membr. Sci.* **172**: 113-124.

Cayot, P. and Lorient, D. 1997. Structure-Function Relationships of Whey Proteins. In *Food Proteins and Their Applications*. Damodaran, S. and Paraf, A., Ed.; Marcel Dekker, Inc., New York, NY, pp. 225-256.

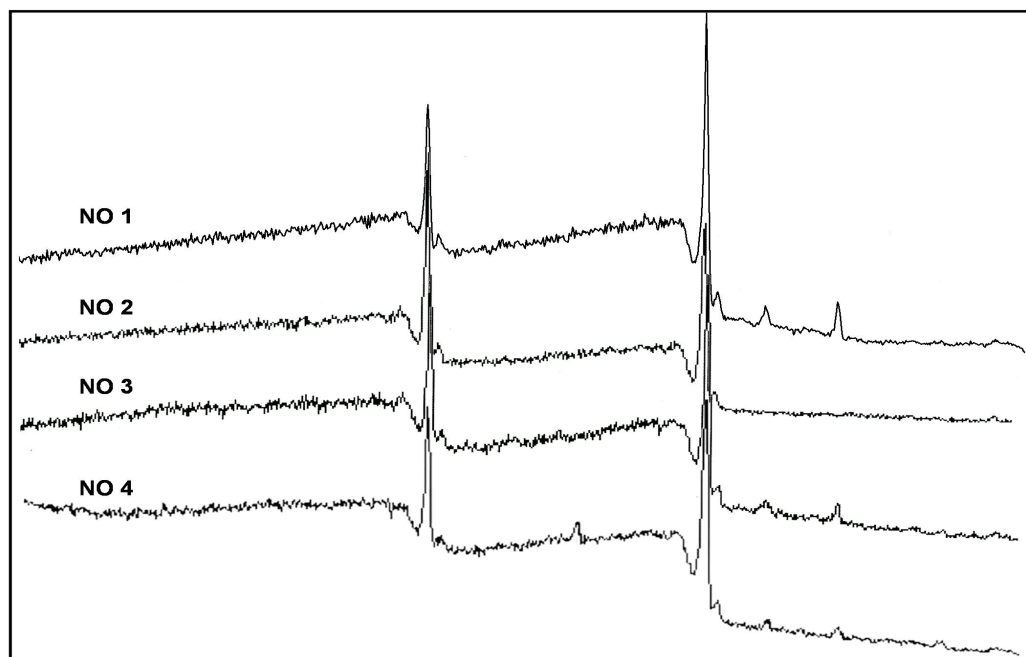Chan, R. and Chen, V. J. 2004. Characterization of Protein Fouling on Membranes: Opportunities and Challenges. *J. Membr. Sci.* **242**: 169-188.

Cheryan, M. 1998. *Ultrafiltration and Microfiltration Handbook;* Technomic Publishing Company, Inc.: Lancaster, PA.

Christiansena, K. F., Vegaruda, G., Langsruda, T., Elekjaerb, M. R., and Egelandsda, B. 2005. Hydrolyzed Whey Proteins as Emulsifiers and Stabilizers in High-Pressure Processes Dressings. *Food Hydrocolloids* **18**: 757-767.

Chu, L. Y., Wang, S., and Chen, W. M. 2005. Surface Modification of Ceramic-Supported Polyethersulfone Membranes by Interfacial Polymerization for Reduced Membrane Fouling. *Macromol. Chem. Phys.* **206**: 1934-1940.

Costa, A. R., de Pinho, M. N., and Elimelech, M. 2006. Mechanisms of Colloidal Natural Organic Matter Fouling in Ultrafiltration. *J. Membr. Sci.* **281**: 716–725.

Cussler, E. L. 1997. *Diffusion Mass Transfer in Fluid Systems*; 2nd ed.; Cambridge University Press; Cambridge, pp 308-330.

de la Fuente, M. A., Singh, H., and Hemar, Y. 2002. Recent Advances in The Characterization of Heat-Induced Aggregates and Intermediates of Whey Proteins. *Trends Food Sci. Technol.* **13**: 262-274.

Delaunaya, D., Rabiller-Baudrya, M., Paugama, L., Pihlajamäkib, A., and Nyström, M. 2006. Physico-Chemical Characterisations of A UF Membrane Used in Dairy Application to Estimate Chemical Efficiency of Cleaning. *Desalination* **200**: 189–191.

De Wit, J. N. 1998. Nutritional and Functional Characteristics of Whey Proteins in Food Products. *J. Dairy Sci.* **81**: 597-608.

Dong, H. and Bell, T. 1999. Ion Beam Surface Modification of Polymers, Towards Improving Tribological Porperties. *Surf. Coat. Technol.* **111**: 29–40.

Elofsson, U. M., Paulsson, M. A., Sellers, P., and Arnebrant, T. 1996. Adsorption During Heat Treatment Related To The Thermal Unfolding/Aggregation of β-Lactoglobulins A and B. *J. Coll. Int. Sci.* **183**: 408-415.

Euston, S. R., Hirst, R. L., and Hill, J. P. 1999. The Emulsifying Properties of β-Lactoglobulin Genetic Variants A, B, and C. *Colloids Surf., B*. **12**: 193-202.

Fennema, O. R. 1996. *Food Chemistry*; 3rd ed.; Marcel Dekker, Inc.: New York, NY, pp. 321-429.

Fontyn, M., van 't Riet, K, and Bijsterbosch, B. H. 1991. Surface Spectroscopic Studies of Pristine and Fouled Membranes Part 1. Method Development and Pristine Membrane Characterization. *Colloids Surf.* **54**: 331-347.

France, R. M. and Short, R. D. 1998. Plasma Treatment of Polymers: The Effects of Energy Transfer from An Argon Plasma on The Surface Chemistry of Polystyrene, and Polypropylene. A High-Energy Resolution X-ray Photoelectron Spectroscopy Study. *Langmuir* **14**: 4827-4835.

Freger, V. 2003. Nanoscale Heterogeneity of Polyamide Membranes formed by Interfacial Polymerization. *Langmuir* **19**: 4791-4797.

Gerenser, L. J. 1987. X-Ray Photoemission Study of Plasma Modified Polyethylene Surfaces. *J. Adhes. Sci. Technol.* **1**: 303-318.

Göken, M. and Kempf, M. 1999. Microstructural Properties of Superalloys Investigated by Nanoindentations in An Atomic Force Microscope. *Acta Mater.* **47**: 1043-1052.

Hamza, A., Pham, V. A., Matsuura, T., and Santerre, J. P. 1997. Development of Membranes with Low Surface Energy to Reduce The Fouling in Ultrafiltration Applications. *J. Membr. Sci.* **131**: 217-227.

Haynes, C. A. and Norde, W. 1994. Globular Proteins at Solid/Liquid Interfaces. *Colloids Surf., B* **2**: 517-566.

Hester, J. F., Banerjee, P., and Mayes, A. M. 1999. Preparation of Protein-Resistant Surface on Poly(vinylidene fluoride) Membranes Via Surface Segregation. *Macromolecules* **32**: 1643-1650.

Higuchi, A., Hashiba, H., Hayashi, R., Yoon, B. O., Sakurai, M., and Hara, M. 2004. Serum Protein Adsorption and Platelet Adhesion on Aspartic-Acid-Immobilized Polysulfone Membranes. *J. Biomater. Sci. Polymer Edn.* **15**: 1051-1063.

Hoffmann, M. A. M. and van Mill, P. J. J. M. 1999. Heat-Induced Aggregation of β-Lactoglobulin as A Function of pH. *J. Agric. Food Chem.* **47**: 1898-1905.

Hollander, A. and Behnish, J. 1998. Vacuum-Ultraviolet Photolysis of Polymers. *J. Surf. Coat. Technol.* **98**: 855-858.

Höök, F., Kasemo, B., Nylander, T., Fant, C., Sott, K., and Elwing, H. 2001. Variations in Couples Water, Viscoelastic Properties, and Film Thickness of a Mefp-1 Protein Film during Adsorption and Cross-Linking: A Quartz Crystal Microbalance with Dissipation Monitoring, Ellipsometry, and Surface Plasmon Resonance Study. *Anal. Chem.* **73**: 5796-5804.

Inchinose, N. and Kawabushi, S. 1996. Excimer Laser-Induced Surface Reaction of Fluoropolymers with Liquid Water. *Macromolecules* **29**: 4155-4157.

Jalili, N. and Laxminarayana, K. 2004. A Review of Atomic Force Microscopy Imaging Systems: Application to Molecular Metrology and Biological Sciences. *Mechatronics* **14**: 907–945.

Jim, K. J., Fane, A. G., Fell, C. J. D., and Joy, D. C. 1992. Fouling Mechanisms of Membranes During Protein Ultrafiltration. *J. Membr. Sci.* **68**: 79-91.

Jonsson, G., Prádanos, P., and Hernández, A. 1996. Fouling Phenomena in Microporous Membranes. Flux Decline Kinetics and Structural Modifications. *J. Membr. Sci.* **112**: 171-183.

Kelly, S. T. and Zydney, A. L. 1995. Mechanisms for BSA Fouling During Microfiltration, *J. Membr. Sci.* **107**: 115-127.

Kemperman, A. J. B., Rolevink, H. H. M., Bargeman, D., van den Boomgaard, Th., and Strathmann, H. 1998. Stabilization of Supported Liquid Membranes by Interfacial Polymerization Top Layers. *J. Membr. Sci.* **138**: 43-55.

Kilduff, J. E., Mattaraj, S., Pieracci, J. P., and Belfort, G. 2000. Photochemical Modification of Poly(ether sulfone) and Sulfonated Poly(sulfone) Nanofiltration Membranes for Control of Fouling by Natural Organic Matter. *Desalination* **132**: 133-142.

Kim, K. S., Lee, K. H., Cho, K., and Park, C. E. 2002. Surface Modification of Polysulfone Ultrafiltration Membrane by Oxygen Plasma Treatment. *J. Membr. Sci.* **199**: 135-145.

Kobayashi, T., Kobayashi, T., Hosaka, Y., and Fujii, N. 2002. Ultrasound-Enhanced Membrane-Cleaning Processes Applied Water Treatments: Influence of Sonic Frequency on Filtration Treatments. *Ultrasonics* **41**: 185-190.

Korikov, A.P., Kosaraju, P.B., and Sirkar, K.K. 2006. Interfacially Polymerized Hydrophilic Microporous Thin Film Composite Membranes on Porous Polypropylene Hollow Fibers and Flat Films. *J. Membr. Sci.* **279**: 588–600.

Langmuir, I. 1918. The Adsorption of Gases on Plane Surfaces of Glass, Mica and Platinum. *J. Am. Chem. Soc*. **40**: 1361-1403.

Li, J., Sanderson, R. D., and Jacobs, E.P. 2002. Ultrasonic Cleaning of Nylon Microfiltration Membranes Fouled by Kraft Paper Mill Effluent. *J. Membr. Sci.* **205**: 247-257.

Liikanen, R., Yli-Kuivila, J., and Laukkanen, R. 2002. Efficiency of Various Chemical Cleanings for Nanofiltration Membrane Fouled by Conventionally-Treated Surface Water. *J. Membr. Sci.* **195**: 265–276.

Madaeni, S. S., Mohamamdi, T., and Moghadam, M. K. 2001. Chemical Cleaning of Reverse Osmosis Membranes. *Desalination* **134**: 77-82.

Mansur, H. S., Oréfice, R. L., and Mansur, A. A. P. 2004. Characterization of Poly(vinyl alcohol)/Poly(ethylene glycol) Hydrogels and PVA-Derived Hybrids by Small-Angle X-Ray Scattering and FTIR Spectroscopy. *Polymer* **45**: 7193-7202.

Marshall, A. D., Munro, P. A., and Trägårdh, G. 1993. The Effect of Protein Fouling in Microfiltration and Ultrafiltration on Permeate Flux, Protein Retention and Selectivity: A Literature Review. *Desalination* **91**: 65-108.

Marx, K. A. 2003. Quartz Crystal Microbalance: A Useful Tool for Studying Thin Polymer Films and Complex Biomolecular Systems at The Solution-Surface Interface. *Biomacromolecules* **2003**: 1099-1120.

Masel, R. I. 1996. *Principles of Adsorption and Reaction on Solid Surfaces;* 1st ed.; John Wiley & Sons, Inc.: New York, NY, pp. 108-234.

Maubois, J. L. and Ollivier, G. 1997. Extraction of Milk Proteins. In *Food Proteins and Their Applications*, eds., Damodaran, S. and Paraf, A. New York: Marcel Dekker, Inc., pp. 579-595.

Mcdonogh, R. M., Bauser, H., Stroh, N., and Chmiel, H. 1990. Concentration Polarisation and Adsorption Effects in Cross-Ultrafiltration of Proteins, *Desalination* **79**: 217-231.

McKenzie, H. A. and Sawyer, W. H. 1967. Effect of pH on β-Lactoglobulins. *Nature* **214**: 1101-1104.

Murray, B. S. and Deshaires, C. 2000. Monitoring Protein Fouling of Metal Surfaces via a Quartz Crystal Microbalance. *J. Coll. Int. Sci.* **227**: 32-41.

Musale, D. A. and Kulkarni, S. S. 1996. Fouling Reduction in Poly(acrylonitrile-co-acrylamide) Ultrafiltration Membrnaes. *J. Membr. Sci.* **111**: 49-56.

Muthukumaran, S., Kentish, S., Lalchandani, S, Ashokkumar, M., Mawson, R., Stevens, G. W., and Grieser, F. 2005. The Optimisation of Ultrasonic Cleaning Procedures for Dairy Fouled Ultrafiltration Membranes. *Ultrason. Sonochem.* **12**: 29–35.

Muthukumarana, S., Yanga, K., Seuren, A., S. Kentish, S., Ashokkumarb, M., Stevens, G. W., and Grieser, F. 2004. The Use of Ultrasonic Cleaning for Ultrafiltration Membranes in the Dairy Industry. *Sep. Purif. Technol.* **39**: 99–107.

Norde, W. 1992. The Behavior of Proteins at Interfaces with Special Attention to the Role of the Structure Stability of the Protein Molecule. *Clin. Mater.* **11**: 85-91.

Norde, W. 2003. *Colloids and interfaces in life sciences*. Marcel Dekker, Inc.: New York, NY, pp. 263-284.

Nystrom, M., Pihlajamaki, A., and Ehsani, N. 1994. Characterization of Ultrafiltration Membranes by Simultaneous Streaming Potential and Flux Measurements, *J. Membr. Sci.* **87**: 245-256.

O'Sullivan, C. K. and Guilbault, G. G. 1999. Commercial Quartz Crystal Microbalances -Theory and Applications. *Biosens. Bioelectron.* **14**: 663-670.

Pearce, R. J. 1992. Whey protein recovery and whey protein fractionation. In: Zadow, ed. *Whey and Lactose Processing.* Amsterdam: Elsevier Applied Science, pp. 271-316.

Peppas, N. A. and Wright, S. L. 1996. Solute Diffusion in Poly(vinyl alcohol)/Poly(acrylic acid) Interpenetrating Networks. *Macromolecules* **29**: 8798-8804.

Petersen, R. J. 1993. Composite Reverse Osmosis and Nanofiltration Membranes. *J. Membr. Sci.* **83**; 81-150.

Pieracci, J., Crivello, J. V., and Belfort, G. 2002. Increasing membrane permeability of UV-modified poly(ether sulfone) ultrafiltration membranes. *J. Membr. Sci.* **202**: 1–16.

Pujar, N. S. and Zydney, A. L. 1997. Charge Regulation and Electrostatic Interactions for a Spherical Particle in a Cylindrical Pore. *J. Colloid Interface Sci.* **192**: 338–349.

Rajagopalan, M., Ramamoorthy, M., and Doraiswamy R. M. 2004. Cellulose Acetate and Polyethersulfone Blend Uultrafiltration Membranes. Part I: Preparation and Characterizations. *Polym. Adv. Technol.* **15**: 149-157.

Rattray, W. and Jelen, P. 1996. Thermal Stability of Skim Milk with Protein Content Standardized by the Addition of Ultrafiltration Permeates. *Int. Dairy Journal* **6**: 157-170.

Reddy, A. V. R., Mohan, D. J., Bhattacharya, A., Shah, V. J., Ghosh, P. K. 2003. Surface Modification of Ultrafiltration Membranes by Preadsorption of a Negatively Charged Polymer: I. Permeation of Water Soluble Polymers and Inorganic Salt Solutions and Fouling Resistance Properties. *J. Membr. Sci.* **214**: 211-221.

Ribeiro, M. H. L., Lourenço, P. A. S., Monteiro, J. P., and Ferreira-Dias, S. 2001. Kinetics of Selective Adsorption of Impurities from A Crude Vegetable Oil in Hexane to Activated Earths and Carbons. *Eur. Food Res. Technol.* **213**: 132–138.

Ricq, L., Narcom, S., Reggiani, J. C., and Pagetti, J. 1999. Streaming Potential and Protein Transmission Ultrafiltration of Single Proteins and Proteins in Mixture: B-lactoglobulin and Lysozyme, *J. Membr. Sci.* **156**: 81-96.

Rivaton, A., and Gardette, J. L. 1999. Photodegradation of Polyethersulfone and Polysulfone. *Polym. Degrad. Stab.* **66**: 385-403.

Rodahl, M., Höök, F., Fredriksson, C., Keller, C. A., Krozer, A., Brzezinski, P., Voinova, M., and Kasemo, B. 1997. Simultaneous Frequency and Dissipation Factor QCM Measurements of Biomolecular Adsorption and Cell Adhesion. *Faraday Discuss* **107**: 229-246.

Sadana, A., 1992. Protein Adsorption and Inactivation on Surfaces. Influence of Heterogeneities. *Chem. Rev.* **92**: 1799-1818.

Sadhwani, J. J. and Veza, J. M. 2001. Cleaning Tests for Seawater Reverse Osmosis Membranes. *Desalination* **139**: 177-182.

Sauerbrey, G. Z. 1959. Use of A Quartz Vibrator for Weighing Thin Films on A Microbalance. *Z. Physik* **155**: 206−210.

Shukla, S., Bajpai, A. K., and Kulkarni, R. A. 2005. Preparation, Characterization, and Water-Sorption Study of Polyvinyl Alcohol Based Hydrogels with Grafted Hydrophilic and Hydrophobic Segments. *J. Appl. Polym. Sci.* **95**: 1129-1142.

Simon, A., Gondrexon, N., Taha, S., Cabon, J., and Dorange, G. 2000. Low-Frequency Ultrasound to Improve Dead-End Ultrafiltration Performance. *Sep. Sci. Technol.* **35**: 2619-2637.

Smithers, G. W., Ballard, F. J., Copeland, A. D., De Silva, K. J., Dionysius, D. A., Francis, G. L., Goddard, C., Grieve, P. A., McIntosh, G. H., Mitchell, I. R., Pearce, R. J., and Regester, G. O. 1996. New Opportunities from the Isolation and Utilization of Whey Proteins. *J. Dairy Sci.* **79**: 1454-1459.

Song, Y. Q., Sheng, J., Wei, M., Yuan, X. B. 2000. Surface Modification of Polysulfone Membranes by Low-Temperature Plasma-Graft Poly(ethylene glycol) onto Polysulfone Membranes. *J. Apply. Polym. Sci.* **78**: 979-985.

Song, Y., Sun, P., Henry, L. L., and Sun, B. 2005. Mechanisms of Structure and Performance Controlled Thin Film Composite Membrane Formation via Interfacial Polymerization Process. *J. Membr. Sci.* **251**: 67-79.

Sun, S., Yew, Y., Huang, X., and Meng, D. 2003. Protein Adsorption on Blood-Contact Membranes: Review. *J. Membr. Sci.* **222**: 3-18.

Taniguchi, M., Pieracci, J., Samsonoff, W. A., and Belfort, G. 2003. UV-Assisted Graft Polymerization of Synthetic Membranes: Mechanistic Stuides. *Chem. Mater.* **15**: 3805-3812.

Thom, V., Jankova, K., Ulbricht, M., Kops, J., and Jonsson, G. 1998. Synthesis of Photoreactive a-4-Azidobenzoyl-x-Methoxypoly(ethylene glycol)s and Their End-on Photo-Grafting onto Polysulfone Ultrafiltration Membranes. *Macromol. Chem. Phys.* **199**: 2723-2729.

Timasheff, S. N. and Towned, R. 1964. Structure of the β-Lactoglobulin Tetramer. *Nature* **203**: 517-519.

Trägårdh, G. 1989. Membrane Cleaning. *Desalination* **71**: 325-335.

Ulbricht, M. and Riedel, M. 1998. Ultrafiltraion Membrane Surface with Grafted Polymer 'Tentacles': Proparation, Characterization and Application for Covalent Protein Binding. *Biomaterials* **19**: 1229-1237.

Verheul, M., Pedersen, J. S., Roefs, S. P. F. M., and de Fruif, K. G. 1999. Association Behavior of Native β-Lactoglobulin. *Biopolymers* **49**: 11-20.

Visser, J. and Jeurnink, T. J. M. 1997. Fouling of Heat Exchangers in the Dairy Industry. *Exp. Therm. Fluid Sci.* **14**: 407-424.

Voinova, M. V., Rodahl, M., Jonson, M., and Kaseme, B. 1999. Viscoelastic Acoustic Response of Layered Polymer Films at Fluid-Solid Interfaces: Continuum Mechanics Approach. *Physica Scripta* **59**: 391-396.

Walstra, P., Geurts, T. J., Noomen, A., Jellema, A., and van Boekel, M. A. J. S. 1999. *Dairy Technology*. Marcel Dekker, Inc.: New York, NY, pp. 27-105.

Wang, R., Zhang, Y., Ma, G., and Su, Z. 2006. Modification of Poly(Glycidyl Methacrylate-Divinylbenzene) Porous Microspheres with Polyethylene Glycol and Their Adsorption Property of Protein. *Colloids Surf., B* **51**: 93-99.

Wang, Y. Q., Wang, T., Su, Y. L., Peng, F. B., Wu, H., and Jiang, Z. Y. 2006. Protein-Adsorption-Resistance and Permeation Property of Polyethersulfone and Soybean Phosphatidylcholine Blend Ultrafiltration Membranes. *J. Membr. Sci.* **270**: 108-114.

Wavhal, D. S. and Fisher, E. R. 2002. Hydrophilic Modification of Polyethersulfone Membranes by Low Temperature Plasma-Induced Graft Polymerization. *J. Membr. Sci.* **209**: 255-269.

Wavhal, D. S. and Fisher, E. R. 2003. Membrane Surface Modification by Plasma-Induced Polymerization of Acrylamide for Improved Surface Properties and Reduced Protein Fouling. *Langmuir* **19**: 79-85.

Wei, Y. M., Xu, Z. L., Qusay, F. A., and Wu, K. 2005. Polyvinyl Alcohol/Polysulfone (PVA/PSF) Hollow Fiber Composite Membranes for Pervaporation Separation of Ethanol/Water Solution. *J. Apply. Polym. Sci.* **98**: 247-254.

Werner, C., König, U., Augsburg, A., Arnhold, C., Körber, H., Zimmermann, R., and Jacobasch, H. J. 1999. Electrokinetic Surface Characterization of Biomedical Polymers-A Survey. *Colloids Surf., A* **159**: 519-529.

Yang, M. C. and Lin, W. C. 2003. Protein Adsorption and Platelet Adhesion of Polysulfone Membrane Immobilized with Chitosan and Heparin Conjugate. *Poly. Adv. Technol.* **14**: 103-113.

Zeng, X. and Ruckenstein, E. Cross-Linked Macroporous Chitosan Anion-Exchange Membranes for Protein Separations. *J. Membr. Sci.* **148**: 195-205.

Zhang, Y., Xiao, C., Liu, E., Du, Q., Wang, X., and Yu, H. 2006. Investigations on The Structures and Performances of a Polypiperazine Amide/Polysulfone Composite Membrane. *Desalination* **191**: 291-295.

Zhao, J., Wang, Z., Wang, J., and Wang, S. 2006. Influence of Heat-Treatment on CO_2 Separation Performance of Novel Fixed Carrier Composite Membranes Prepared by Interfacial Polymerization. *J. Membr. Sci.* **283**: 346-356.

Zhou, C., Friedt, J. M., Angelova, A., Choi, K. H., Laureyn, W., Frederiz, F., Francis, L. A., Campitelli, A., Engelborghs, Y., and Borghs, G. 2004. Huamn Immunoglobulin Adsorption Investigated by Means of Quartz Crystal Microbalance Dissipation, Atomic Force Microscopy, Surface Acoustic Wave, and Surface Plasmon Resonance Techniques. *Langmuir* **20**: 5870-5878.

Zydney, A. L. 1998. Protein Separations Using Membrane Filtration: New Opportunities for Whey Fractionation. *Int. Dairy Journal* **8**: 243-250.

CURRICULUM VITAE

JUN TAE KIM

EDUCATION BACGROUND

09/2003-05/2007   Ph.D. in Food Science

Rutgers, The State University of New Jersey

03/1999-02/2001   M.S. in Graduate School of Biotechnology

Korea University

03/1992-02/1999   B.S. in Food Science and Biotechnology

Korea University

(1994-1997: Military Army Service in Korea)

WORKING EXPERIENCE

09/2003-05/2007   Participant in National High School Student Lunch Program

01/2003-07/2003   Research Assistant in Fusionbt Co. Ltd. in Korea

03/2001-12/2002   Research Assistant in BioCoats Co. Ltd. in Korea

09/2003-08/2006   Graduate Assistantship at Rutgers University

09/2000-02/2001   Teaching Assistantship at Korea University

03/1999-09/2000   Research Assistantship at Korea University

PUBLICATION AND PRESENTATION

Jun Tae Kim, Norbert Weber, Gye Hwa Shin, Qingrong Huang, and Sean X. Liu "The Study of β-lactoglobulin Adsorption on Polyethersulfone Thin Film Surface Using Quartz Crystal Microbalance with Dissipation Monitoring" *JFS* (Accepted in Jan. 2007)

Kwon T. Hwang, Jun T. Kim, Soon T. Jung, Gun S. Cho, Hyun J. Park "Properties of Chitosan-Based Biopolymer Films with Various Degrees of Deacetylation and Molecular Weights" *J. Apply. Polym. Sci.*, 89, 3476-3484 (2003)

Jun T. Kim, Dong S. Cha, Gee D. Lee, Tae W. Park, Dong K. Kwon, Hyun J. Park "Process Optimization of Sweet Potato Pulp-Based Biodegradable Plastics Using Response Surface Methodology" *J. Apply. Polym. Sci.*, **83**, 423-434 (2002)